TEMPLE UNIVERSITY GRADUATE BOARD

Title of Dissertation: A PROACTIVE APPROACH TO TRAIN CONTROL

Author: DAVID F. THURSTON

Read and Approved by: ………………………………………………………

                           ………………………………………………………

                           ………………………………………………………

                           ………………………………………………………

                           ………………………………………………………

Date submitted to Graduate Board: ………………………………………………..

Accepted by the Graduate Board of Temple University in partial fulfillment of the requirements for the degree of **Doctor of Philosophy**

Date ………………………………   ………………………………………………………….
                                        (Dean of the Graduate School)

A PROACTIVE APPROACH TO
TRAIN CONTROL

A Dissertation
Submitted to
The Temple University Graduate Board

In Partial Fulfillment
of the Requirements for the Degree
DOCTOR OF PHILOSOPHY

By
David F. Thurston
May, 2012

Examining Committee Members:

Dr. Iyad Obied, Committee Chair, Electrical and Computer Engineering
Dr. Saroj Biswas, Electrical and Computer Engineering
Dr. Li Bai, Electrical and Computer Engineering
Dr. Christopher Barkan, Railroad Engineering Department – University of Illinois
Dr. Vallorie Peridier, Mechanical Engineering

ABSTRACT

A PROACTIVE APPROACH TO TRAIN CONTROL

By David F. Thurston

Doctor of Philosophy

Temple University, 2011

Major Advisor: Dr. Iyad Obeid

The main objective in optimizing train control is to eliminate the waste associated with classical design where train separation is determined through the use of "worst case" assumptions to calculate Safe Braking Distances that are invariant to the system. In fact, the worst case approach has been in place since the beginning of train control systems.

Worst case takes the most conservative approach to the determination of train stopping distance, which is the basis for design and capacity of all train control systems. This leads to stopping distances that could be far more than actually required under the circumstances at the time the train is attempting to brake.

A new train control system is proposed that utilizes information about the train and the conditions ahead to optimize and minimize the Safe Braking Distance. Two methods are proposed to reduce safe braking distance while maintaining an appropriate level of safety for the system. The first introduces a statistical method that quantifies a braking distance with various hazards levels and picks a level that meets the safety

criteria of the system. The second method uses train mounted sensors to determine the

adhesion level of the wheel and rail to determine the appropriate braking rate for the train

under known circumstances.

Combining these methods provides significant decreases in Safe Braking

Distances for trains. A new train control system is utilized to take advantage of these

features to increase overall system capacity.

ACKNOWLEDGMENTS

There are several people and organizations that made this work possible. In attempting to acknowledge all of them, I'm sure that I will leave some out, but this represents my best attempt to capture them all.

First of all, I cannot start without thanking Dr. Henry Senduala for guiding me in the beginning of my time at Temple. He was my original advisor as a graduate student and helped introduce me to the University and its requirements. I wish him the happiest retirement. Right behind him was Dr. Sarjo Biswas, whose support through course work and the Graduate School was always beneficial. His association and help (especially in Engineering Math!) will always be remembered. Of course a big part of this work involves probability and I would be remiss to not mention Dr. Li Bai, who helped thought his course work and support. I would also like to thanks Dr. Chris Barkan, Director of the Railroad Engineering Program at the University of Illinois. Dr. Barkan was an avid supporter of my work and stands as a leader in the field of railway education in the U.S. To round out the PhD Committee, I thank Dr. Iyad Obeid, who took on an old but determined grad student and did more to shape this paper than anyone else. His review and guidance offered me a great deal of confidence in finishing the research. I cannot thank him enough for helping to make my dream a reality.

There was a wealth of support from the rail industry as well. First and foremost would be the data and access to information on the LRT operation of the RiverLINE in Southern New Jersey. Al Fazio, then General Manager and a long time friend provided the go ahead to obtain the data, and, Bill Roberts, Arve Berthelsen and Foster Temeko

were instrumental in helping to acquire the files, drawings and plans of the LRV used in the baseline. In addition to the operating personnel, Safetran Systems (Having acquired Quantum electronics) provided the license agreement to use the event recorder software to be able to analyze the data received. I wish to particularly acknowledge Mr. Doug Minto of Safetran (now call Invensys) for his help in acquiring the license that made the analysis possible.

Within my own firm of Parsons, Train Performance Calculator software was made available that was used in determining stopping distance and the creation of comparable graphs of differing deceleration rates. Carl Wood of Parsons was invaluable in teaching me the TPC and in making unique enhancements to the TPC that we are using in our day to day applications for our customers now.

The laboratory used to illustrate the ability to use spectroscopy for a contaminant sensor was provided by Emily Olsheski, at her lab in Houston, TX. The experiments were very informative and her help on chemical analysis and advice in the research was very welcomed.

I cannot finish without mentioning my family. This goes beyond the typical support one would find in an adventure such as this, but included very tangible implications of its success. My daughters Christina and Leanne always offered support and their continuation into graduate school inspired me all the more. My youngest Greg, who is now a freshman in the engineering program at the University of West Virginia might not see the support, but there is no better way to learn that to teach. I will miss our homework sessions. To my oldest son David, I cannot have reached this stage without his help. At the time of my preliminary exam, he was a senior in the Electrical

Engineering program at the University of Pittsburgh. Clearly, his help (and I hope that I helped him as well!) in studying the core curriculum portion of the preliminary exam was in no small part the reason I passed.

No one could even consider starting an endeavor such as this without the support and encouragement of the core of our family – my wife Cathy. After nearly 8 years of study nights, weekends in the basement writing papers and doing homework, this has finally come to an end. Nothing would have been possible without her, and now it is time to move forward with the next step in our lives.

David F. Thurston

DEDICATION

To Cathy

TABLE OF CONTENTS

LIST OF TABLES

LIST OF FIGURES

CHAPTER 1

1   INTRODUCTION

1.1   General Background

During the last few years, both freight railroads and mass transit operations have enjoyed continuing increases in traffic even though the route mileage of freight carriers in the U.S. has declined precipitously as shown in figure 1. The increase in traffic is largely attributed to the passing of the Staggers Act in the 1970's that deregulated the industry [1]. Deregulation has also allowed railroads to abandon or sell less profitable lines, while mergers have consolidated several main line tracks. All of this has caused an accelerated effect of traffic growth on the lines that still exist [2].

Class 1 Freight Railroads Traffic vs. Track Miles
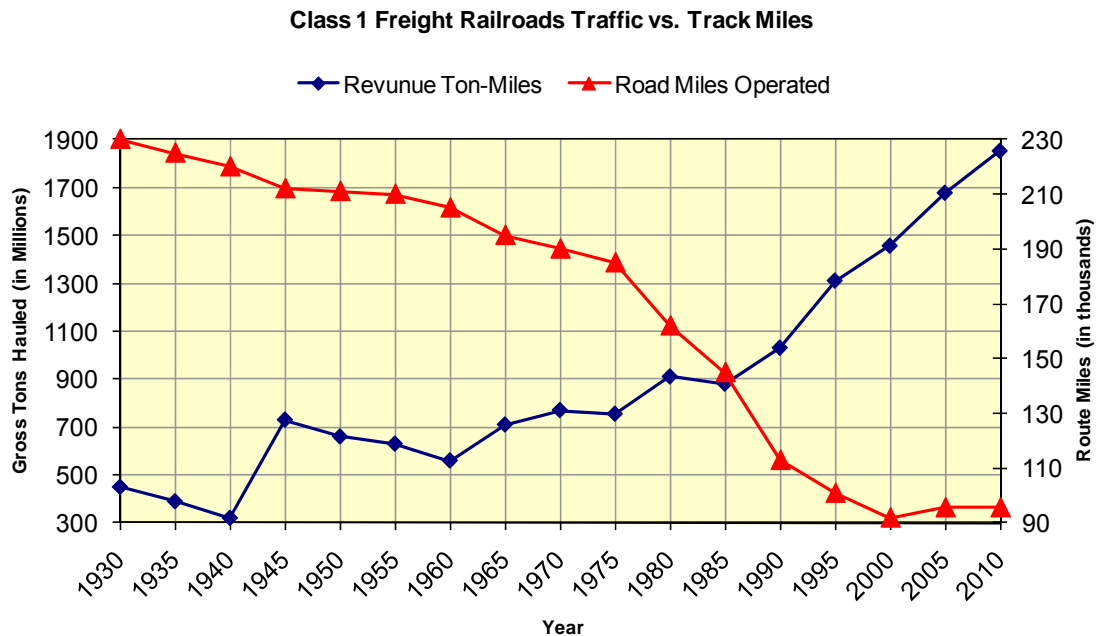
Figure 1, U.S. Mainline Freight Railroad Traffic Growth vs. Trackage.

The Railroads inherent efficiency has recently caused great interest with the cost of crude oil jumping to over $150 a barrel in 2008. The same conditions have caused a great revival for mass transit. As Figure 2 shows, mass transit ridership has significantly increased over the last decade due largely to the number of new Light Rail Transit (LRT) and Commuter Rail projects that have been built [3]. By mid 2008, the gasoline price spike drove ridership to record highs throughout the nation. The recession that followed has lowered transit ridership, however as the economy in the United States and the world recovers, these levels should start to increase along the same trend.   Freight traffic has more than recovered losses in the same period.
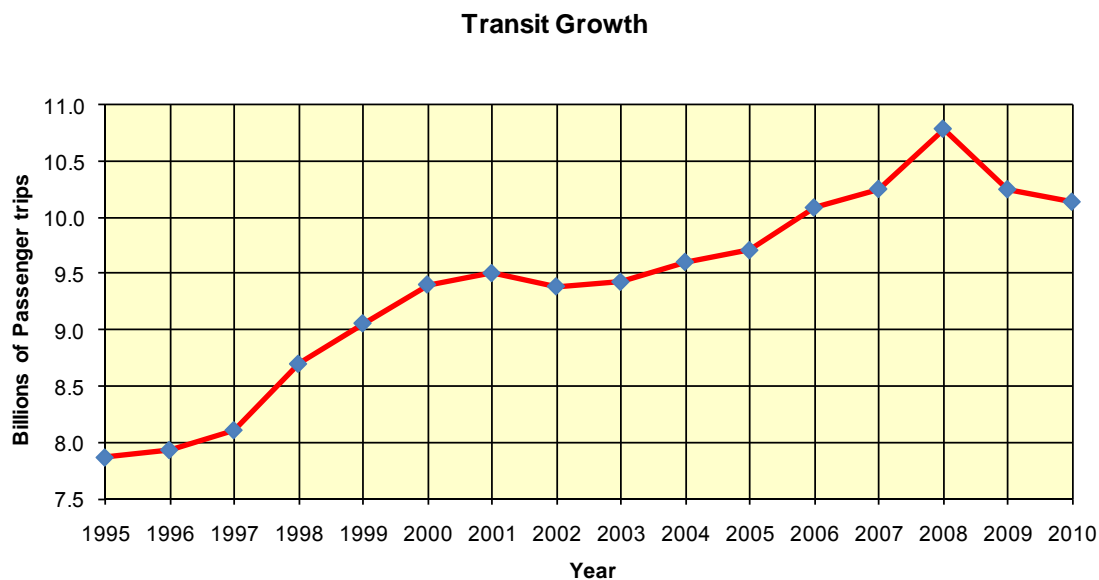
Transit Growth

Figure 2, U.S. Mass Transit Ridership Growth.

The demand fueling the growth in the rail industry has caused railroads and transit agencies to either create or increase capacity throughout the United States. Growth drives capital planning for new rail lines, but where existing lines are already in place, additional track is not always possible. In these areas, other solutions need to be used to

increase capacity. Many of the capacity constraints can be addressed with modification in the alignment by eliminating curve speeds and other physical constraints to train operation. However many of these changes are limited by cost or the physical nature of the line. One common method to increase capacity is upgrading the train control system.

Rail and Mass Transit systems rely on signal systems of various types to provide safety in their operations. These operations require the separation of trains as they operate along the track. The amount of separation is pre-determined in the design of the train vehicles, the specific type of train signaling or "train control", and the operating rules of the property. The proper design and use of these three factors determine the overall capacity of the system in terms of headway (the time between a train leaving a point and the next train arriving at the same point) and throughput (the number of trains per hour or the number of passengers per hour per direction).

1.2   Optimization of Train Control

There is an old axiom in the railroad and transit industry that says that if it were not for the train control system, it would be possible to run a lot more trains. The fact of the matter is that train control systems are *designed* to space trains apart at a distance at least equal to the Safe Braking Distance (SBD) for the train. SBD is based on a series of events that provides enough distance for ***any*** train to stop, and is sometimes called the "guaranteed" braking distance.

To guarantee sufficient stopping distance for *any* train, design engineers have always used the worst case scenario for calculating SBD. Over time, these same design engineers have become more conservative with respect to the SBD model components.

As a result, the actual "performance" braking of the train (what distance the train can actually stop under good conditions) versus the SBD provided for in the train control system (all of the worst case components of the SBD calculation added together) has created an ever widening capacity gap. As the gap between stopping distances for SBD and for performance braking increases, the overall system capacity is lowered. Since train control systems are required to use the SBD rate, train spacing is enforced at a distance (SBD) which is far in excess of what the train could stop under typically common conditions (dry rail, low winds, fully operative brakes, etc.).

An example of this effect is shown in Figure 3 below. This shows a typical SBD stopping curve plotted as a function of speed over distance. The two signals shown along the distance axis are spaced to provide sufficient distance to allow the train to stop. A typical performance stopping curve is also plotted that shows how the train could actually stop under normal conditions. The difference in performance and SBD distances translates to lost capacity of the system from the fact that under the typical conditions trains are stopped far shorter that is necessary for safety, and spaced farther apart that actually required. Longer SBD means longer distance between signals causing larger distances for following train movements. This equates to fewer trains being able to move over the territory within a given time frame.
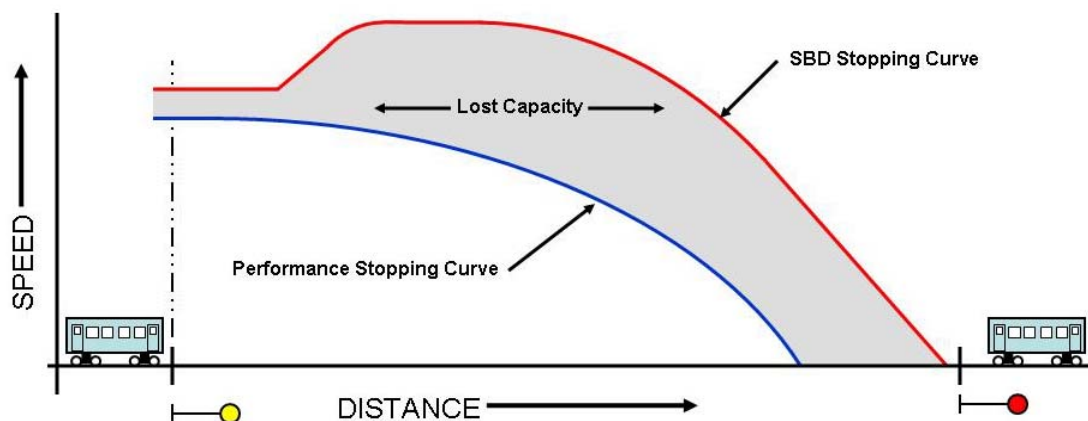
Figure 3, Lost Capacity in Conservative SBD Criteria.

This is further illustrated in figure 4. This shows a plot of typical values required for braking distance using SBD and performance braking as the underlying distance (plus a train length) for determining a theoretical minimum headway in Trains per Hour (TPH)[1]. Details of the calculation can be found in Appendix C.
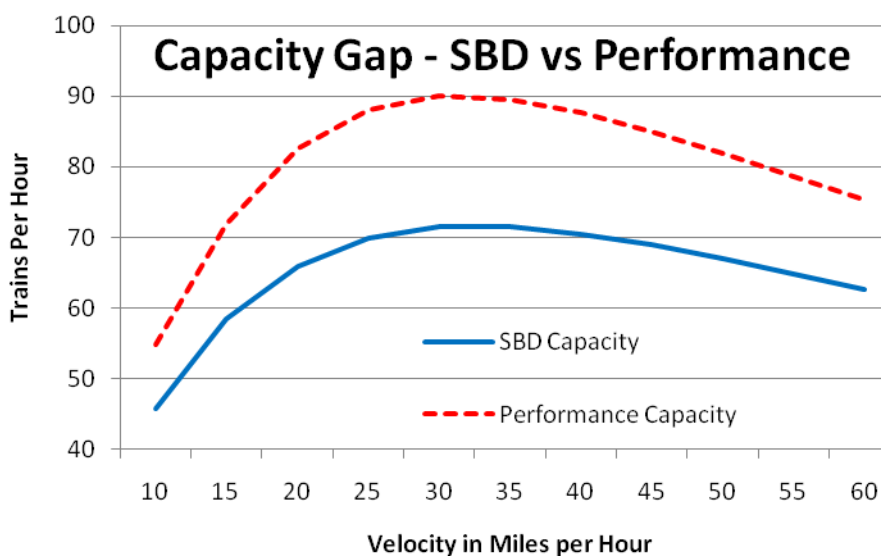
Figure 4, Comparison of Capacities between full SBD and Performance Braking.

___

[1] It should be noted that the number of trains per hour in this Figure are not practical or sustainable numbers, but are shown to illustrate the relative margins between the two scenarios.

Performance Braking differs from SBD for a number of reasons. These include the fact that performance does not take into account several of the factors found in SBD. It is, in effect, how the train is expected to "perform" under normal operation. In addition, the actual braking rate used for performance braking assumes a much higher achievable deceleration. As with SBD, Performance Braking is uniquely defined for each type of train and property it is applied to.

Over the last few years, several issues have affected the application of the SBD models used in modern day train control. These have increased the capacity gap at a time where transit ridership has reached all time highs. These include:

- Fear of litigation should trains stop beyond the provided distance,

- Inclusion of parts not previously considered such as runaway acceleration for processor based propulsion equipment,

- Terminal designs that lack sufficient tail track distance, and

- Attempting to enforce end of track at terminal operations.

It is interesting to note that all of these issues rely on SBD for the critical distance the train needs to stop. This is true regardless of the train control system used. In fact, it has been suggested that when properly designed, several of the train control systems offered today can provide virtually the same capacity [4] [5] [6]. Therefore if SBD is optimized, the maximum capacity can be achieved.

There is a historic precedent in the design approach and implementation of the spacing that is enforced by the signal system. This involves the use of a fixed "worst case" criteria to calculate the safe margin required for stopping distance of trains.

1.3   Design Impact on Capacity

The classical approach to the calculation of train stopping distance is critical to the design of train control systems. This distance represents the guaranteed distance required to stop the train under all circumstances as shown in Figure 5 below. If this distance is overstated, trains are spaced further apart than necessary. Given the same conditions for operation, larger spacing between trains increases headway and decreases overall capacity. This is true for all currently available train control technology, and constitutes one of the most important and significant factors in safety and capacity.
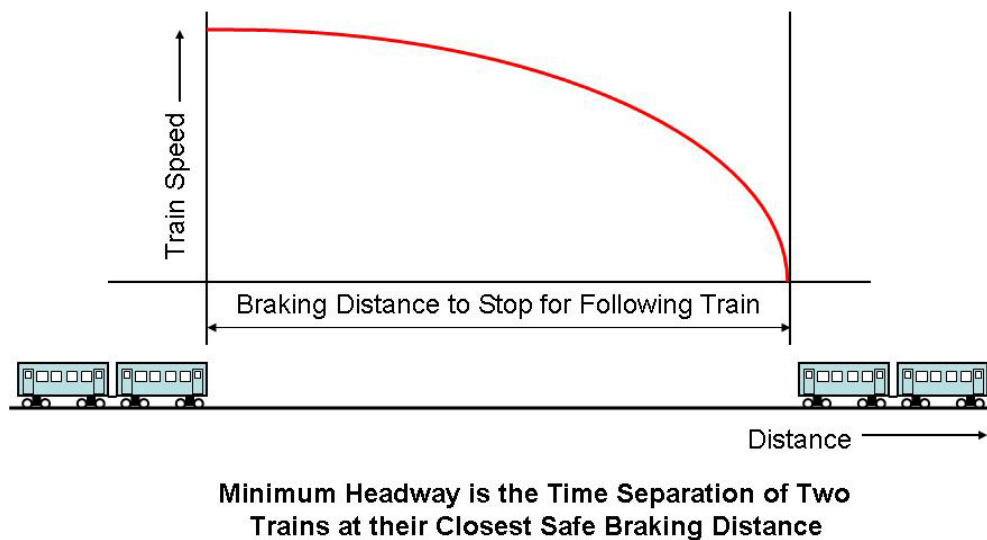
Figure 5, The Braking Distance Headway Relationship

Once the SBD is determined, it can be applied to the signal system design by creating "signal blocks". In its simplest form, each signal block provides sufficient

distance to stop the train traveling at the maximum authorized speed, and only one train will be allowed to occupy each block. SBD is the calculation that provides this distance.

Signals located along the track inform passing trains as to the occupancy of the blocks ahead. As such, a signal that protects an occupied block displays a signal that indicates stop, and do not pass. The signal before this would indicate to the train to approach the next signal prepared to stop [7]. This requirement differentiates train signals from highway traffic signals that rely strictly on timing for their sequencing. This railroad signal progression of a moving train is illustrated in Figure 6 below showing a train traveling though signal blocks.
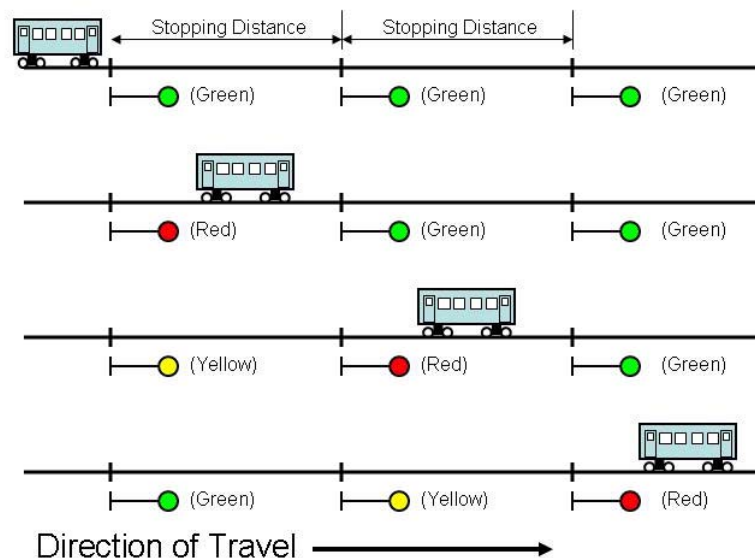
Figure 6, A Typical Sequence showing train occupancy and signals aspects.

Traditional signal systems use track circuits to detect block occupancy that was first patented in 1872 by William Robinson [8]. Track circuits utilize the rails as part of an electrical circuit. Since train wheels and axles are connected electrically, they short

(or "shunt") the electrical current flowing in the rails starving the end of the track circuit from current. This lack of current is the basis of train occupancy detection with track circuits.

More advanced train control systems do not utilize track circuits for train location detection. These systems involve other means such as global positioning satellites, or track mounted transponders that are interrogated by passing trains that indicate their location. In North America, this type of system is referred to as Positive Train Control (PTC) for railroad applications and Communications Based Train Control (CBTC) for transit operations. Regardless of the train control technology used, the methods of determining SBD remains the same.

Train control systems use a Safe Braking Distance (SBD) to determine the appropriate length to separate trains to avoid collisions. The same properties that allow trains to propel themselves with great efficiency also prevent them from stopping suddenly. Although a direct calculation of SBD in often impossible, it is possible to create a mathematical model of SBD. Validation can be performed both empirically and through software algorithms [9]. Calculating SBD can be divided into several parts of a model to represent the process used to stop at train. This model is composed of several distinct parts that address characteristics of the train, the train control system, and other external influences. The model has been described by others in the past [10], but these parts were represented in a detailed discussion in the IEEE Guideline for Safe Braking Distance [11] and are shown in Figure 7 below.
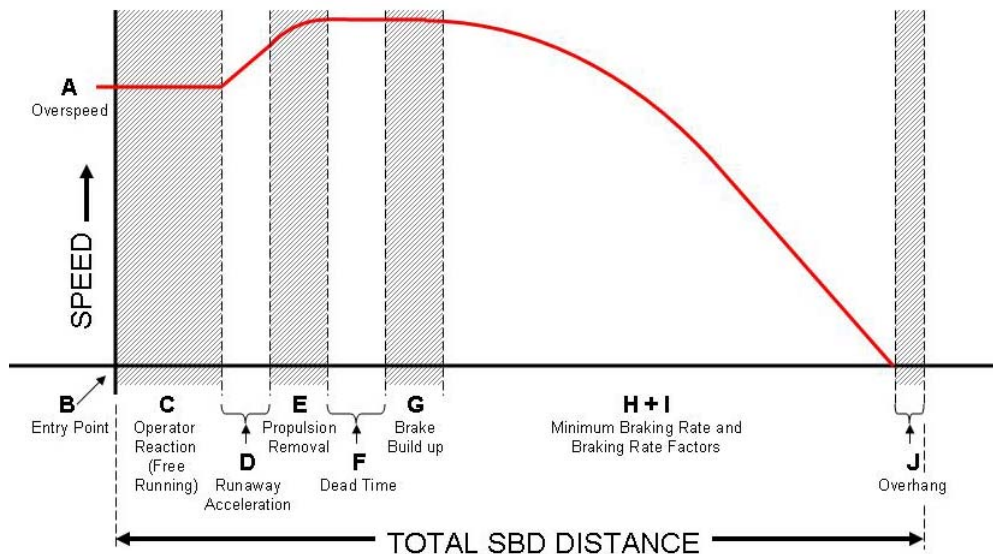
Figure 7, The IEEE SBD Model Labeled with all Parts

Each part is given a letter and name in an effort to standardize the industry

approach to specifying signal system details as described below:

   A: **Entering Speed -**Although not an actual distance, A represents the

   entering speed of the train when an action to stop the train occurs. The

   most common measuring device for speed is a tachometer attached to an

   axle of the train. As the wheel turns, the tachometer generates a series of

   pulses whose frequency is proportional to the speed of the train.   In many

   cases, an "overspeed" value is added to compensate for variations due to

   calibration errors, instrument accuracy, and spinning or sliding of the

   wheel.

   B: **Entry Point -** This is actually a reference point along the track where the

   action to stop the train is to occur.

C: **Operator Reaction (Free Running) -** Once the train passes the entry point B, there is an allowance in the SBD for reaction time of both the train operator and the equipment that comprises the train control system. While the operator reaction time allows the operator the opportunity to apply the train brake in an appropriate manner, equipment reaction time allows for system latency. If no action is taken by the operator at the end of this time period, a "penalty brake application" is made by the train control system to stop the train.

D: **Runaway Acceleration -** Train control systems are designed to be fail-safe. That is, when there is a failure of the system, it will fail to a known state that presents no hazards. Propulsion systems are not generally designed to be fail-safe, and as such represent a potential hazard of forcing a train to accelerate at the maximum rate at any time. The worst case scenario that produces the longest distance to stop for "runaway acceleration" has the train accelerating at its maximum rate during the end of the Free Running section of the SBD model (part C).

E, F, and G: **Control -** Once the train control system recognizes that the train is in an over-speed condition or any other reason to enforce a penalty brake application, propulsion power is removed and the train brake is applied. However, these are not instantaneous events. These portions of the SBD model provide for these real world conditions that start at the same point in time, but effect the SBD at different distances.

H and I: **Braking -** These parameters are the actual full braking rate of the train with the H portion the distance traveled while decelerating under normal conditions, and the I portion the distance traveled for additional safety factors such as low wheel to rail friction rates (called adhesion) and trains with degraded braking capacity.

J: Vehicle Overhang - Vehicle Overhang is the distance from the point on the vehicle that is detected by the train control system to the forward most point of the vehicle. In train control systems that rely on track circuits, this distance is measured directly from the train's front coupler to the centerline of the lead axle. In Communications Based Train Control where train detection relies on inertial navigation updated by track mounted transponders, this portion represents the uncertainty of the detection as the vehicle moves farther from the last refresh point.

In the traditional approach, each part is viewed as an independent event.   As such, parts are assembled serially (the exception is the timing of part E, F, and G where a single event starts all three at the same time).

The distance to stop is calculated from the entering speed, and each part's contribution to the distance traveled based on duration of time or a rate of acceleration/deceleration.

1.4   Additional Factors Effecting Capacity

The overall impact of SBD on a train control and system capacity is described above; however, there are several other key factors that determine the ultimate system capacity of a rail line. Among the most influential of these are: vehicles, stations, and alignment. In the analysis of system capacity, all of these require optimization of design to achieve the highest throughput, and are influenced by SBD.

1.4.1   Vehicle Considerations for Capacity

Vehicle design, operation and maintenance play a critical role in determining overall system capacity. These factors are outside the control of the train control designer; however, proper systems integration and modeling techniques must include their effect on the ability of the train control system to provide adequate stopping distance under any condition.

One classic issue concerns the various types of train brakes. Vehicle manufactures typically utilize a variety of braking systems to meet contract specifications for vehicle performance such as dynamic or regenerative brakes where the traction motors powering the train are turned into generators to resist motion. However, braking rates used in SBD calculations are required to utilize only "vital" braking systems. Vital implies a fail-safe, closed loop operation that is available to the operator under all conditions. Dynamic or regenerative brakes are not generally considered vital since there are several single points of failure that can render this braking mode inoperative.

This is also true for track brakes[2] and similar braking systems that are not designed as "stand-off" (this is where a loss of control or system fault always results in a brake application). True "vitality" implies a system that is designed in a closed loop and fails in a safe predictable manner for any scenario. Since we do not live in a perfect world, vitality can be provided through fault tree and hazard identification that eliminates any single point failures that result in the practical elimination of unsafe conditions. At the end of the analysis, all probability of unsafe failures must meet or exceed the system safety criteria to be acceptable. Reliability is not a substitute for safety.

Another issue involves the operating rules of the system that for practical reasons allows normal train operation with a percentage of train brakes "cut-out" (either on a per car or per truck or wheel assembly basis). For example on railroad applications, the Federal Railroad Administration limits normal operation of trains with less that 85% of all brakes that are operative [12]. Therefore, railroad SBD must take into consideration the fact that up to 15% of the nominal braking force is not working.

Doorway design plays a direct factor in determining capacity. The number of doors and the width of the doors determine the flow rate for passenger getting on and off the train. A greater number of doors or wider doors will create a lower rate of "friction" as passengers interact at station stops[3]. The friction rate is directly related to the length of time the train is stopped at stations (typically called dwell time). Longer dwells mean longer trip times, and reduced system capacity. In a comparison made on a heavy rail

---

[2] Track brakes are common in Light Rail systems where a shoe is pushed down onto the top of the rail from the truck assembly to provide significant braking force.

[3] This data is from an unpublished report on a major mass transit system analyzing car door configurations.

transit system, the operation of vehicles with two side doors compared to three side doors revealed that on-time performance increased from 89.1% to 95.7% [5]. This highlights the fact that restrictions caused by smaller or fewer doors can have a significant impact on train operation and system capacity.

1.4.2   Station Considerations for Capacity

System capacity is also affected by station design, due to the effects of inadequate platform width and length. Heavy rail transit, where overcrowding can be a serious peak hour issue, have volumes of passengers sufficient to create lengthy queuing and excessive friction between flows of passengers. This situation could be amplified by small platforms creating crush loading of passengers unable or unwilling to allow passengers off of the train. The subsequent increase in dwell results in lost capacity for the system.

Another consideration in capacity for Commuter Rail and Light Rail Transit is low level platforms. The extra time associated with higher friction rates and the longer and less convenient path for passengers utilizing the steps to reach the low platform creates lengthy dwells. The extra time involved in station stops are directly added to the headway resulting in decreased capacity.

1.4.3   Track Considerations for Capacity

One of the largest issues in design that impacts capacity and safety is the civil alignment. "Civil alignment" includes the grades, curves and location of track switches. In general, any situation that forces a train to reduce speed decreases capacity. The

slowing train creates congestion in its "wake" as it will not clear occupied blocks as fast

as a faster train. Speed reductions in civil alignments result from curves, steep grades

(trains may have insufficient power to maintain their speed), and bridges, among others.

Mitigating these issues is beyond the scope of train control systems, but these problems

can create permanent constraints to capacity.

End terminals and intermediate junctions where trains are routed from one track

to another via switches are fixed locations along the track. Terminals are typically located

at the end of revenue operations to berth trains into a station platform, change the

direction of operation, and allow the train to proceed back to the other end of the line.

Operation of a terminal normally includes pairs of switches to route trains into any

terminal platform track from the inbound track, and from any terminal platform track to

the outbound track. An example is shown below in Figure 8.
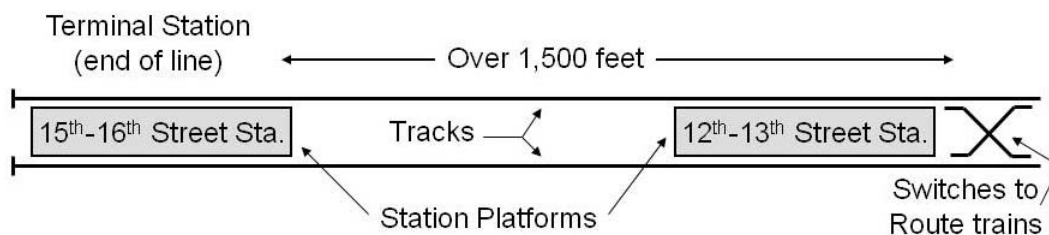
Figure 8, Terminal Layout to Illustrate Capacity Issue.

Terminal layout and civil design play an important role in overall system

capacity. Civil restrictions often decide where switches are located, however maximum

terminal capacity is achieved generally when switches are located very close to end of the

terminal station platforms. This is illustrated in the following example of an actual transit

line terminal shown in figure 9, below. In terminal stations such as this, trains entering

off of the line from the right are routed to an unoccupied platform track (the default

would generally be the straight move). While that trains dwells at the station and

prepares for its return journey in the opposite direction, a train on the other platform track

has the opportunity to leave. While our first train is still in the terminal, the following

train arrives and is routed to the unoccupied track in the terminal where it dwells and

prepares for its journey in the opposite direction. Once in the terminal, the first train can

then be routed back out onto the line. This alternating process is continued over and over

again during peak periods to provide the highest throughput. Since the train waiting to

leave on the lower track must allow the inbound train to be clear of the switches before a

new route can be made, the distance traveled between the switches and the platform adds

to the time it takes for the train to leave the terminal.

In this example, the first crossover encountered by a train leaving 15th -16th

Station on the upper track is beyond the 12th-13th Station. Trains reversing into or out of

the terminal at 15th – 16th Station must negotiate a switch that is over 1,500 feet – and one

station stop – away.
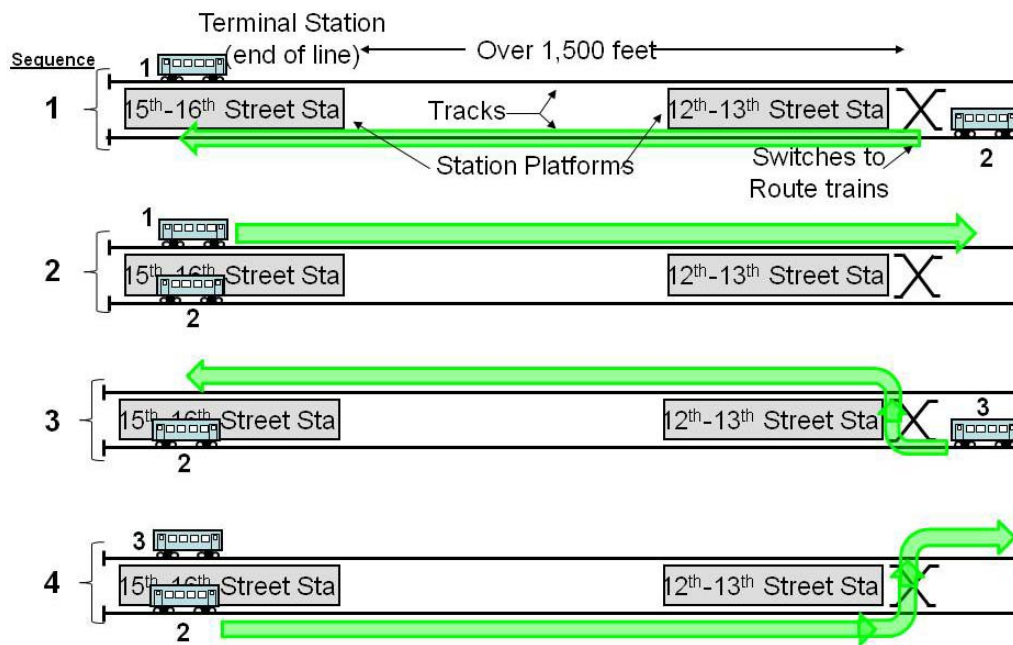
Figure 9, Typical Terminal Operational Sequence

Capacity is significantly reduced in this example due to:

- The extra time taken to run outbound trains before they are past the switches at 12th-13th Street Station, and

- The extra time taken for inbound trains approaching the terminal to traverse the switches.

SBD also factors into terminal design. Ideal terminals include "tail" tracks that extend beyond the end of platform to allow a train to stop safely while entering the terminal station at a practical speed. In Figure 10 below, a typical two track terminal is shown with speed-distance charts above the track model with trains entering the terminal from right to left. Three curves are shown in the speed-distance chart. The first represents normal train performance of a train entering the terminal and stopping at the

platform with no interference from the train control system (this is the single dashed

line). This is the ideal situation for capacity and represents the fastest approach and

shortest clearing times for the switches controlling movement in to the terminal. The

other curves represent the enforcement curves of a train control system that would be

imposed on a train operating in this area. The solid line shows where and how a train

would be allowed to travel in the situation where there are no tail tracks. It can easily be

seen that normal train performance would be severely impacted by slowing the train well

before the train enters the platform. The double dashed line represents the same

enforcement speeds, but with a tail track added to the terminal. In this case, the normal

train performance is not effected (the normal performance curve is always below this

enforcement curve) and provides optimum travel times at the terminal.
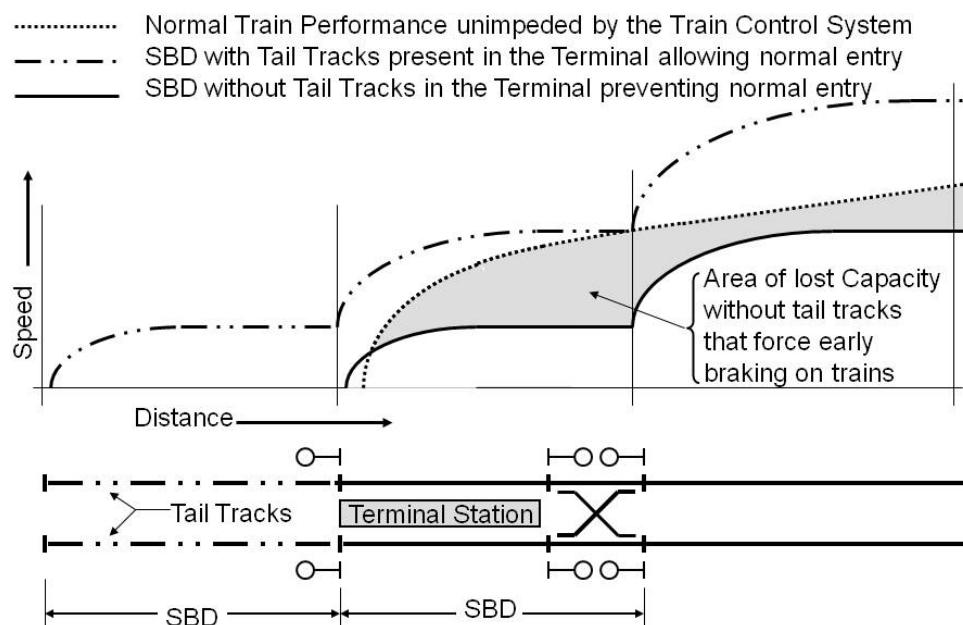
Figure 10, Capacity Loss due to Tail Tracks.

The grey area between the SBD curve without tail tracks and the normal performance curve represents the capacity lost due to the train control enforcement of the train's speed. Since the train is operating at a lower speed, it takes more time to travel the distance into the platform area. This lower operating speed is reflected back into following trains and overall system capacity is reduced.

1.5   Signaling Details

Railroad train control has roots in the earliest railways in England [8]. The safe separation of trains at that time concerned opposing movement, rather that following movements of trains. As new forms of higher density operations were required, train braking became the most important factor in capacity. This continues today in all forms of train control, and how SBD is utilized by these systems is determined by the technology employed. Signaling types vary, but can be generally classified into the following categories [13], and [14]:

- Manual Block (Time Table and Train Order) – A dispatcher is used to control operations via paper and voice communications only. This system is based on rules rather than any electronic enforcement. Its roots come from the beginning of train control when the telegraph was used to transmit information between operators at stations to determine the occupancy of the track. This system is rarely used today, and it exhibits very low capacity.

- Track Warrant Control (TWC, DTC[4] or Form D[5]) – Track Warrant has replaced Manual Block on low density freight operations. It is a rules based systems that has the same limited capacity, and requires only voice radio coverage for dispatcher to train communications.   .

- Automatic Block Signals (fixed wayside signals located along the right-of-way) – By far the most common form of signaling on freight railroads, consists solely of a series of lights mounted on poles at the entrance to track sections called blocks to inform the train operator of occupancy ahead. Capacity is dictated by the length of the block, which is equal to the calculated SBD for the speed limit assigned to the track.

---

[4] DTC or Direct Train Control is an operational method used by Western railroads in the General Code of Operating Rules (GCOR).
[5] Form "D" is similar to DTC, but is the operational method used by Eastern railroads in the Northeast Rules Advisory Committee (NORAC) rule book.
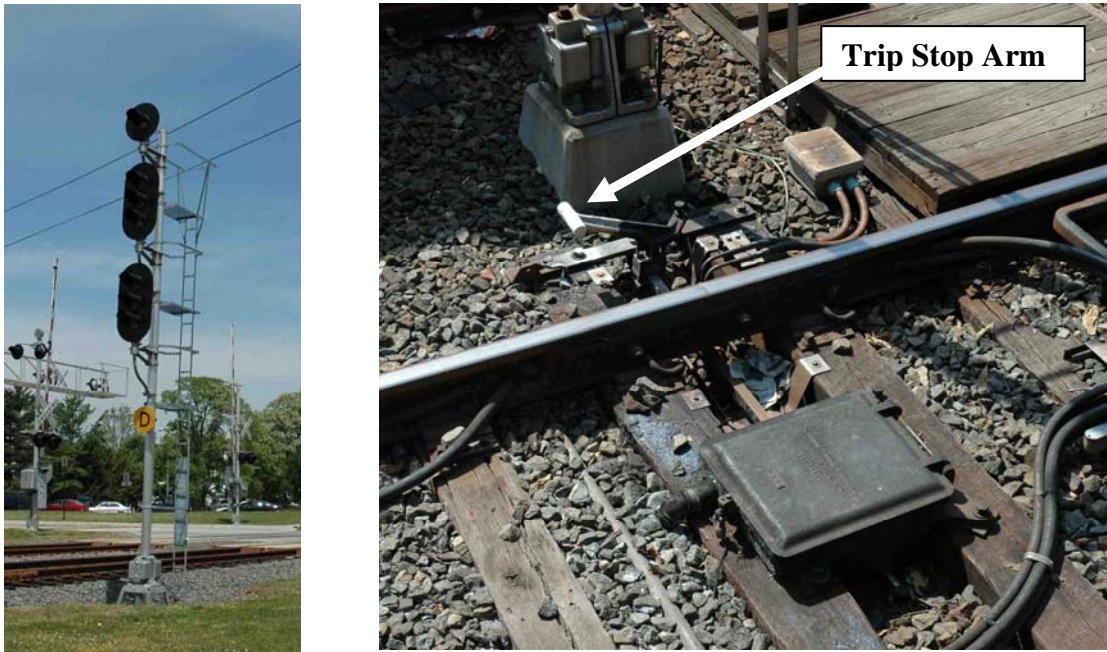
Trip Stop Arm

Figure 11, A Fixed Wayside Signal (left), and a Mechanical Trip Stop (right).

- Trip Stop – This is a form of enforced train control generally used for

  heavy rail transit and some Light Rail systems. Operation requires a

  "double red overlap" that "trips" the train into an emergency brake

  application when passing a red (stop) signal equipped with a tripping

  device. The tripping device can be either mechanical (a "trip arm" is

  extended up to actuate a valve on the air brake system) or magnetic (the

  trip arm is replaced with a magnetic circuit), and when activated causes an

  emergency brake application on the train. Since the enforcement is done

  at the red signal, an additional block is required between trains for safety,

  hence the "double" red. Signal aspects are dependent on SBD. This type

of system can provide for intermittent enforcement of train speeds as it is only effective as the train passes over the trip stop.

- Inductor based Automatic Train Stop – This is similar to trip stop, but uses a magnetic circuit between devices on the train and on the track to enforce the wayside signal. The enforcement is done at the signal *approaching* the red signal and no overlap is required. Trains passing signals displaying less than their most permissive aspect[6] are automatically stopped by a penalty brake application unless the engineman applies a brake manually. This was primarily a railroad technology rather that a transit one and it is in extremely limited use today. This technology is also intermittent as it is effective only when the train passes over the Inductor. Recent legislation concerning the requirement for Positive Train Control (see below) allows for the replacement of inductive train stop on the general system of railroads in the United States.

---

[6] Aspects are the actual color or position of the signal. In this case, the most permissive signal forces the engineman into action before the danger is encountered at the red signal, and therefore the second red signal (the overlap) is not required.

Figure 12, An inductive Train Stop

- Cab Signals (With and without enforcement) – Just as the title implies, the signal information in this technology is transferred to the cab of the train for the operator to see. In conventional cab signals, energy is applied to the rails that is decoded by the on board equipment and interpreted as signals or speed commands. Penalties are enforced when the train is overspeed for any given situation. Railroads use power frequency (PF) track circuits while most transit systems use audio frequencies (AF). Cab signals provide for continuous enforcement of speed as the codes are transmitted to the train at all times.
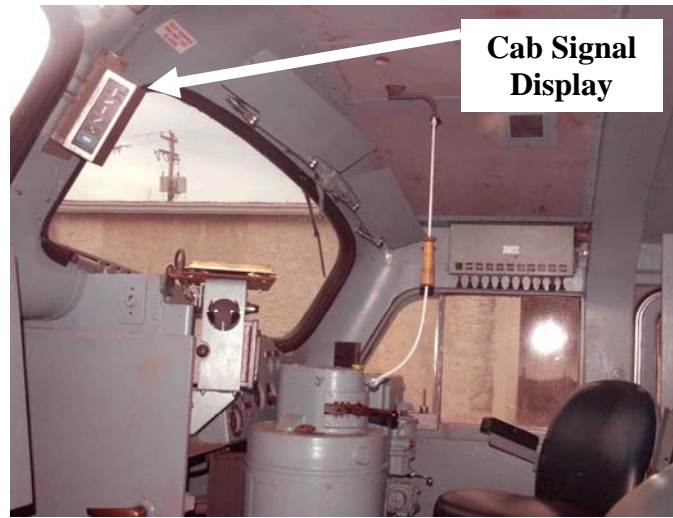
Figure 13, Locomotive Cab equipped with Cab Signals

- Profile Based Systems – Profiling is the ability for the train to calculate its

  brake initiation point to a known target. Modern train control includes a

  "profiling" feature derived from location determination on board the train.

  Profiling means that the train knows the distance to any fixed point along

  the railroad that the train needs stop. Since the train also knows its current

  speed, it can calculate a more accurate SBD. This allows trains to

  continue to operate at speed until it is necessary for the train to begin

  braking to the stop. In any case, SBD is still constrained by the worst case

  model.

  In this type of train control, the information passed to the train is a

  distance to go, rather than a speed command. The on board equipment

  determines the actual point where braking is required. In this way, trains

  need not reduce speed until required by the actual SBD at their actual

speed as opposed to a fixed block length based on the maximum

authorized speed (MAS). This is also a continuous enforcement system.

- CBTC - (Communications Based Train Control) – This form of train

   control relies on trains knowing where they are, and transmitting that

   information to a wayside control computer. The computer determines

   movement authority (an actual location along the right-of-way), and

   transmits it to the train so that the train can proceed to its authority limit.

   In addition, there are CBTC systems that work on other principals, but the

   common factor is that there is no reliance on track circuits for train

   detection. PTC (Positive Train Control) is another type of CBTC train

   control system where the location determination is generally accomplished

   through the Global Positioning System (GPS). Where CBTC is normally

   a transit application, PTC is a railroad application. Both types are a

   continuous enforcement system as changes in track occupancy are

   immediately reflected in the information supplied to the train. In summary,

   train control systems vary by application and technology. Their

   implementation varies as well.

Table 1 below summarizes some of the unique features of the train control types

described above.

Train Control Type	Pros	Cons	Usage
Manual Block	Inexpensive	Low Capacity and Safety	Being Phased out
Track Warrant	Inexpensive	Low Capacity and Safety	Low Density Lines
Block Signals	Low Technology	No Enforcement	Commonly Used on Railroads
Trip Stop	Simple Enforcement, Low Tech	Intermitent, Expensive	Commonly Used on Transit
Inductive Train Stop	Simple Enforcement, Low Tech	Intermitent	Being Phased out
Cab Signals	Continuous Enforcement, Many Vendors	Cost, Limited Number of Speed Commands	High Speed, Dense Operation
Profile Based Systems	High Capacity	Requires an Onboard Database	New Starts, Capacity Upgrades
CBTC	High Capacity	Requires an Onboard Database	New Starts, Capacity Upgrades

Table 1, A Comparison of Train Control Types

1.6   Additional Considerations

It is easy to see that there is an effect on system performance that depends on the train control system chosen. Although SBD is calculated from the same basic principles for any train control system; how the system conveys information to the train and how it is enforced determines its effect on overall system capacity. Figure 14 below illustrates a simulation of this fact for a complex transit system, where three different train control schemes were applied to the same conditions of alignment, trains, passenger loading, train length and SBD parameters while decreasing the operating headway in approximately eight second increments [4].   In effect, as more and more trains are injected into the system (decreasing the headway), passenger trip time remains fairly stable until congestion forces a dramatic increase. The "knee" of these curves illustrates the clear capacity limit of the system[7]. Adding more trains (shorter headway), increases trip time to unacceptable levels beyond the one minute, fifty two second headway for both AF Cab Signals and CBTC.

---

[7] Clear capacity of the system implies that all trains will be allowed to operate at the maximum design speed with no interference from trains ahead from encroaching on their SBD wake. The system has more capacity, but only at the expense of run time between stations and terminals.

Since trip times are fairly constant before the system's clear capacity is reached, calculating the overall capacity in Passengers per Hour per Direction (pphpd) is trivial. If eight (8) car trains are used, with a crush load of 250 passengers, each train carried 2,000 passengers. Headway times are easily converted to trains per hour (tph) by dividing the headway time by 60 minutes. The result is multiplied by the number of passengers per train to determine the pphpd. This is also plotted in the figure below. A shorter headway is possible only if the SBD allows the trains to bunch closer together. By optimizing the SBD calculation, it is possible to shorten headways resulting in more capacity.
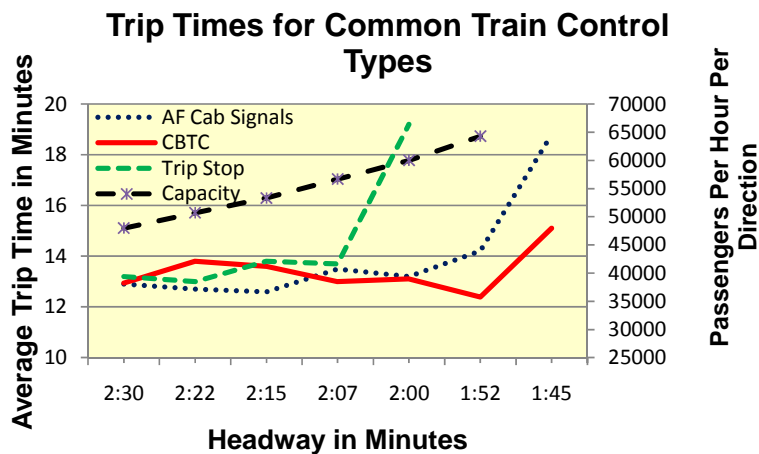
Figure 14, Simulated Trip Times per Headway

From the figure above, it is apparent that the more modern train control systems represented by AF Cab Signals and CBTC offer nearly identical capacity as expressed in run times. Since corresponding changes in the common SBD model for these systems

causes similar changes in run times, this confirms that SBD is the overriding capacity

factor in the design of these systems [4], [5], [6].

The overall maximum operating speed has a dramatic impact on capacity as well.

For example, Amtrak's Northeast Corridor (NEC) between New York Penn Station and

Newark, New Jersey was designed to provide the maximum capacity. The maximum

design speed for the area of interest was 90 mph. However, the maximum capacity was

provided at a lower speed. The design of the train control system (cab signals) included a

special 60 mph speed command that provided the highest capacity at the lowest run time.

The chart below illustrates this example showing the capacities at the available speeds the

signal system enforced when block spacing is optimized for 90, 80, 60 and 45 mph

speeds (the available speed commands in the system) [15]. This is based on CE-205, a

standard adopted by Amtrak for safe Braking Distance. There is a tradeoff between

speed and the SBD needed to operate the train safely at that speed. As seen in Figure 15,

increased speeds lower the run time but also lower the system's capacity. Even though

the trains are clearing faster at the higher speeds, the increase in SBD grows faster

effectively lowering throughput.

Capacity Based in CE-205 Braking
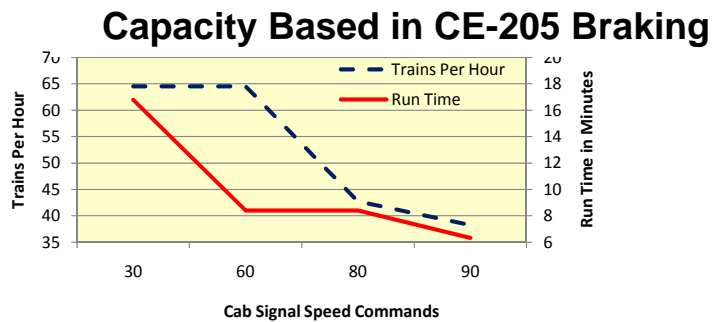
Figure 15, Capacity Analysis for Speed Commands of Amtrak's Cab Signal System

When the same analysis is performed with blocks optimized for higher speeds, the capacity of the line decreases to 47 trains per hour. Note that capacity in this case is a theoretical number defined under ideal conditions to compare designs and is not a practical number of trains that can actually operate.

The computing power available today has allowed for more accurate calculations of SBD. This is especially true when the effects of grades and curves are factored in. As an example, in traditional railroad designs that calculated SBD over grades encountered along the track, the entire mass of the train was assumed to be concentrated at one point. This implied that calculating the effect of grades on SBD (and therefore the spacing between signals) for trains was considered for only the front of the train. The "point mass" methodology yields shorter stopping distance when the beginning of the block is at a point of where the grade changes. This is shown in Figure 16, below.
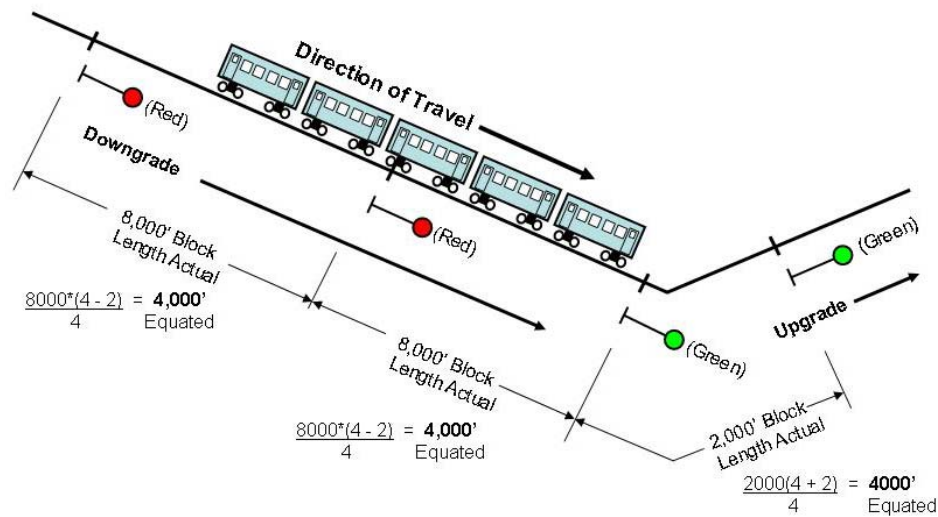
Figure 16, An example of equated distance calculation for an extreme case

In the figure above, the train traveling from left to right is situated entirely on a

downgrade of 2 percent[8]. The traditional method for calculating the effect of the grade

uses the formula[9]:

$$\frac{D(4 \pm G)}{4} = D_e \qquad (1)$$

Where: D = the measured or actual distance,

G = the grade, and

D_e = Equated Distance

The actual distances between signals provides for sufficient equated distances for

signal spacing along the railroad. The equated distance is the value used in evaluating

SBD by determining the equivalent distance provided to the train in a given block with

respect to the grades encountered. In cases of descending grades, the equated distance is

---

[8] Grades of railways are defined as the number of feet of vertical change over a horizontal distance of 100 feet. This is expressed as a percentage. For example, a -2% grade represents a track alignment descending at a rate of 2 feet for every 100 feet of horizontal distance [16].
[9] For convenience, this formula is derived in the Appendix.

less than that for level track. This indicates that longer actual distance between signals is required to provide the same effect on level track.

However, for the signal block in advance of the train[10] in the Figure 16 above, the point mass calculation has taken the entire train to be on the upgrade trackage when it is clearly not. This implies that this signal block effectively provides for a distance that is *50% more* that the same actual distance on level track when in fact the train on the downgrade requires more distance to stop.   This illustrates how errors can be introduced with this method.

The examples of grade compensation and simple capacity analysis have been used for a number of years within the industry. Computer modeling of SBD is a common approach used today. This takes the form of a Train Performance Calculator (TPC)[11] that operates on either a run time basis where transit times and performance are predetermined and used additively to simulate rail and transit systems too complex for previous methods, or a time step basis where the train resistance equations are parameterized and run at sufficient time intervals to simulate train performance.

The introduction of TPC based calculations for SBD increases the accuracy through for a number of reasons. This methodology uses the actual conditions encountered by a train. Many complex parameters can be introduced into the calculation to determine the braking of a train. These include employing the "laws of physics"

---

[10] If you can see the aspect (the lights) of a signal, you are "to the rear" of that signal. "In Advance" of the signal implies you are beyond the signal and occupying the block it governs.
[11] Train Performance Calculators (TPCs) are a mathematical model of train operation. They use the parameters of force within the equations of motion to determine the deceleration and stopping distance of trains. The appendix has a detailed description of a typical TPC software package.

approach that eliminates the point mass error described above by distributing the train's

mass over its entire length [4]. In addition, it is possible to determine the attained speed

of trains and adjust the entering speed calculated rather that the maximum speed allowed

at every occurrence. It is also possible to run several models with various parameter

changes to optimize operating procedures or to correctly model train performance. The

appendix contains a user manual of a TPC that is commercially available that describes

operations of this type of software.

TPCs generally use train resistance models to calculate speed, time and distance

that a train travels along the track. These models utilize various parameters and are

calibrated through observation and iteration. One of the most commonly used models is

the Davis equation shown below [16].

$$R_u = 0.6 + \frac{20}{w} + 0.01V + \frac{KV^2}{wn} \qquad\qquad (2)$$

Where: R_u = Train Resistance in pounds/ton,

w = Weight on each axle,

n = Number of Axles,

V = Velocity

K = Resistance to Drag

Other models introduce parameters such as angular momentum of the wheels, and

wind resistance based on the type of train under study. Many factors influence capacity

of a rail system, and a few are mentioned above. SBD is a key criterion in the design and

ultimate capacity of any train control system. Taking a proactive approach to

determining the minimum required SBD will yield optimized capacity.

CHAPTER 2

2   A NEW APPROACH TO OPTIMIZE TRAIN CONTROL

2.1   Basic Concepts

Advanced train control systems utilize profiling techniques that use a Distance-to-go concept for calculation SBD from a specific target location back to the position of the train to determine the point at which the brakes need to be applied to stop short of the target. These systems offer the best capacity for a given situation but still use the traditional worst case SBD model to space trains.

A system that is constantly evaluating several time variant components to achieve safe but decreased stopping distances is proposed and shown in Figure 17. Of particular interest are issues such as runaway acceleration and the achievable rate of deceleration once braking starts. This is calculated through statistical means as opposed to worst case scenarios. This method is presented in two parts. The first part addresses the parts A through G of the IEEE SBD model. This is an exercise in establishing the likelihood of these events occurring. The second part addresses advanced knowledge of adhesion to calculate the actual achievable deceleration rate of the train. When these parts are combined into a single optimized SBD calculation, increased capacity will result. Additional details of the second part are provided as follows:

Real time knowledge of the available adhesion rate, and therefore the available braking effort, would allow for continuous optimization of stopping distances. It is

proposed to utilize an array of on board sensors to determine surface conditions of the

wheel and rail as well as other parameters to determine the adhesion rate. With this

information flowing from all trains into a network of controllers, a closed system would

be created that transmits real time adhesion conditions to trains *before* they encounter

them. This allows each train to proactively adjust SBD for the actual operating

conditions. Figure 17 shows the concept graphically where trains adjust their SBD

according to the parameters that are transmitted to it in four steps.
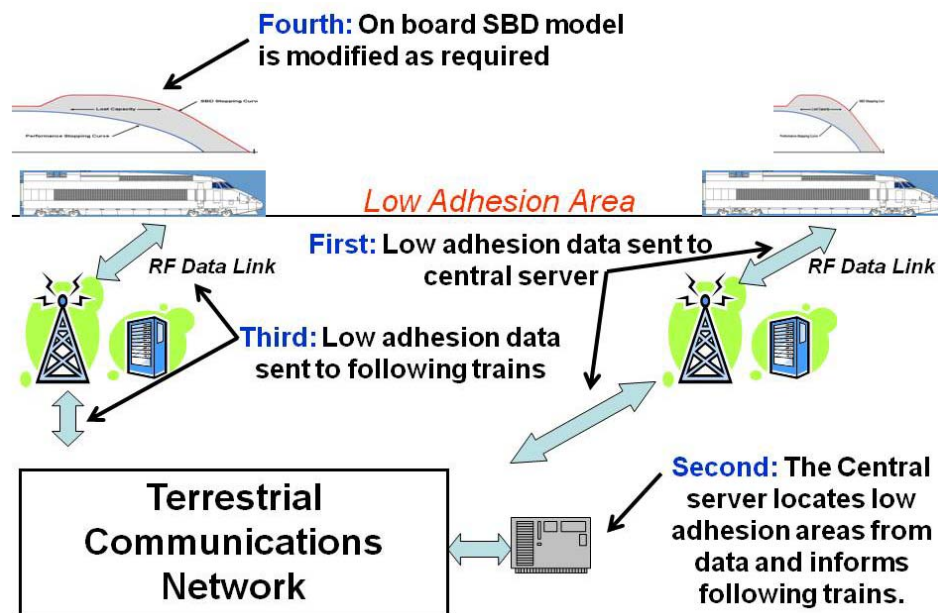
Figure 17, Proposed Train Control System

An example of the dynamic nature of the system's approach to calculating SBD is

shown in Figure 18. Note that the affect of the low adhesion area is presented to the

train's calculation of SBD at a point where the SBD begins to intrude on the area of low

adhesion rather than when the train is actually at this area. The effect of the low adhesion

is adjusted proportionally over the length of the train as it enters and exits the low adhesion area.

This example also shows the typical effect of an ascending grade. Note that the ascending grade effect on the SBD calculation overlaps the area where SBD is recovering from a low adhesion condition. The current SBD calculation is used to determine where the grade begins to influence future SBD values. Since the grade remains constant throughout the remaining portion of the example, the new SBD calculation becomes a constant once the entire train is on the +2% grade.
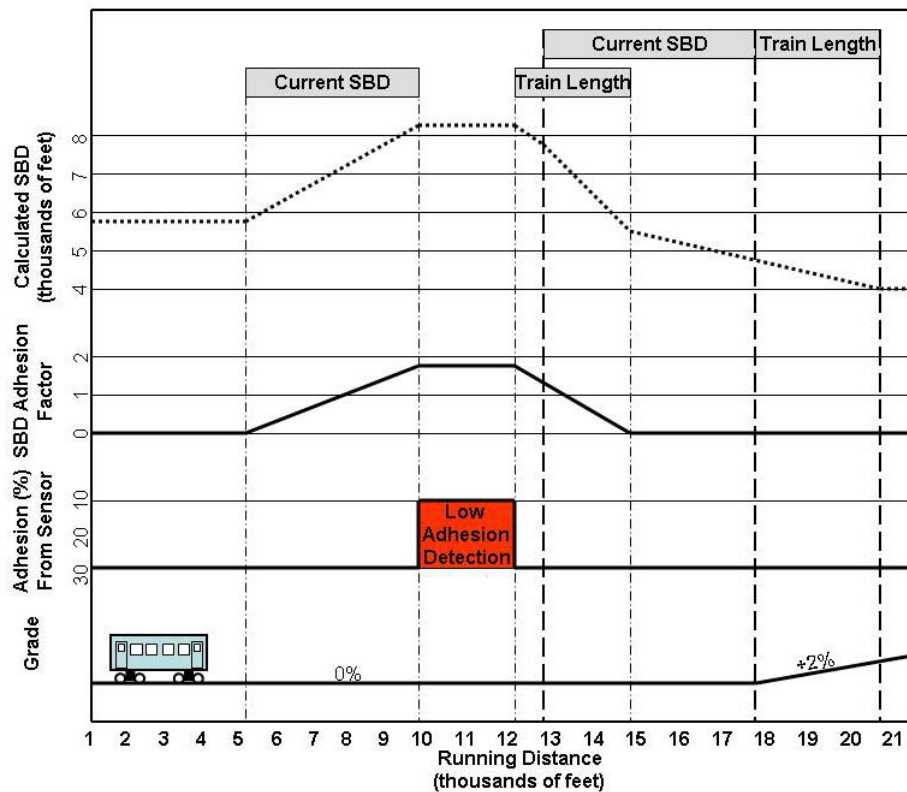
Figure 18, Detected Adhesion affect on SBD

Using this methodology of proactively determining the current operating environment from the trains ahead, the SBD calculation would always reflect the minimum required and not the worst case. This maximizes capacity at all times.

Although there have been attempts to measure the condition of a rail adjacent to the operating rail line as a precursor to real time adhesion conditions, the controls placed in effect either lowered the maximum authorized speed or provided crew advisories for these conditions. In both cases, a manual intervention is made that has potentially little effect on the safety case for the system [17].

The proposed solution creates a global model as shown in Figure 18 that tracks local issues within a database and broadcasts information to trains so that the proper SBD calculation can be made. This calculation may be performed on board the train as the train travels to its current movement authority, or the calculation may be made by equipment along the right-of-way (or where the trains are dispatched from). The first scenario minimizes the required bandwidth of the data communications system between the trains and the field, while the later scenario minimizes the amount of equipment on board the train. In either case, the safety critical nature of this information can be maintained by requiring confirmation from multiple trains of the adhesion condition and a handshake of messages confirming the delivery of the information before more conservative SBD distances can be used.

2.2   Conventional SBD Background

Growth in the rail and transit industries has spurred development of advanced technologies in train control and other disciplines related to train operation with the intent to increase capacity. There has not been a corresponding increase in peer reviewed academic literature and text books to go along with this development. In fact, the industry has recognized that there is a shortfall in new engineering talent entering the rail and transit field [18].

Train Control systems have been in use for over 100 years. They remain the primary safety system for rail and transit operation today. The development of train control has varied between rail (represented by the general system of railroads for the United States) and transit (represented by subway, light rail and street car systems). In the United States, this is largely due to the differences in requirements of these modes as well as the regulatory environment. Although transit train control systems are not regulated by the Federal government, railroad systems are. The Federal Railroad Administration (FRA) has promulgated several rules contained in the Code of Federal Regulations that describe requirements and the need to establish SBD parameters [19], [12]. These documents also form the basis for how these systems interact with brake and propulsion systems on locomotives. The Federal Transit Administration (FTA) has elected to allow the individual states to regulate transit systems. As a result, there is little if any consensus in the U.S. on this issue.

Train Control is a wide ranging discipline that covers may different modes of transport as well as several engineering activities. For example, Halinaty, Firth and Chiu

outline the basic requirements of a Communications Based Train Control (CBTC) system only as an introduction to the difficulties in commissioning such a system [20]. CBTC is fortunate to have common an IEEE Standard for many features desired [21], but other types of conventional signaling systems are only briefly described in the Institution of Railway Signal Engineers[12] (IRSE) publications [8], much older references [22], or historical works such as McEvoy's description of interlocking function [23].

Capacity in rail and transit systems has been detailed in previous papers by this author, where the real driver for capacity within a train control system is SBD [4]. Criteria for determining SBD has been a discussion point for suppliers, consultants and system integrators for some time. Increases in system capacity mean higher efficiency and better service delivery. However, work in standardization of SBD parameters and procedures have been generally confined to work from the IEEE [11], [24]. The first effort was not in fact ever published by the IEEE, but it is available within the industry. The second was published in 2009. Previous efforts to define SBD models are included in the IEEE standard 1474 [21], which parallels the previous work [11] and [24], but does not go beyond Communications Based Train Control (CBTC).

Safety is of the first importance in determining SBD. Should SBD not represent the true length of track required for stopping, serious accidents will be the result. The NTSB report on the New York City Transit accident on the Williamsburg Bridge in 1996 clearly indicates this fact [25]. During the accident investigation, it was found that there

---

[12] The Institution of Railway Signal Engineers is a professional organization based in the United Kingdom that is devoted to the advancement of signal and communications engineering. There literature is almost exclusively based on European technology.

was insufficient braking distance provided for signal blocks approaching and on the bridge. The result was a following train colliding with a train stopped on the bridge with one fatality and sixty nine injuries.

Conventional means for calculation SBD are shown in Vincze and Tarnai for the new European Railway Train Control System (ERTMS) [26] and in several standards similar to Australian Rail Track Corporation, LTD (ARTC) in Australia [27]. There are however new approaches that include new technologies such as pointed out by Zhuan for Electronically Controlled Pneumatic (ECP) brakes [28]. Conventional freight train brakes use a reduction in air pressure in a brake pipe that runs the length of the train to initiate a brake application on the cars. When a brake application is made on the locomotive, it can take up to several seconds for the reduction to become effective at the rear of the train causing excessive reaction time for the braking to occur. ECP brakes operate using an electrical signal that call for braking of the entire train with no delay. This reduces the equipment reaction time and provides for shorter stopping distances.

2.3   Existing Methods to Calculate SBD

Traditional methods for the evaluation of train control systems and SBD have centered on worst case criteria for every possible circumstance. Examples from all over the world of this conservative methodology are described in Vincze and Tarnai in Europe [26], ARTC in Australia [27], and Bureika and Mikaliunas in Russia [29]. This method ensured that the resultant analysis would be safe, but not efficient in terms of providing the optimum capacity. In addition, European methodology for safety determination

promulgated by CENELEC (the European standards organization for electronic equipment) specifies Safety Integrity Levels (SIL) that are solely based on systems development as opposed to a probability of unsafe events. Short provided a discussion on the use and misuse of SIL levels for the Institution of Railway Signal Engineers that detailed this methodology [30].

New approaches have been described where the overall probability of a hazardous event as presented by the Federal Transit Administration [31] is used to reduce SBD as well as other design parameters by North, Fazio and Shashidhara [32] , [33] and [34], and Rodriguez, Ho, and Burt [35]. These discussions centered on a global approach to risk and provided a reduction in SBD. However, this approach is difficult to quantify. Similar approaches were found in the validation analysis of safety critical software by Malvezzi, Bonnet, Cork, Karbstein and Presciani [36]. A unique approach developed by an IEEE Standards working group several years ago detailed an approach that breaks down the risk elements into those items typically used in SBD analysis [24]. This unpublished work is updated and applied with the new IEEE SBD Guideline [11] in a following chapter as a means to optimize the calculation of specific portions of the new model. The remaining portions are the subject of the rest of this research. Maintenance of safety is always the first importance in a train control systems. With the introduction of probability into the SBD calculation, a means to determine what the acceptable level of safety needs to be addressed. Once the safety requirement is known, a statistical analysis of SBD can be compared so that safety objectives are met.

Other methods of validation of SBD were discovered as well. Patra created a software algorithm to determine the safety level of SBD calculations [9]. Unfortunately, the analysis was checked against the worst case model. In this case, reductions in SBD from the worst case are generally not achieved.

2.4   PTC "Predictive" Enforcement

Recent legislation enacted by the United States Congress has mandated the installation of Positive Train Control (PTC) on virtually all Class 1[13] mainline and Passenger railroads. PTC is a train control system generally based on the Global Positioning System (GPS) where trains determine their own location. This information is sent via data radio to wayside controllers that determine the appropriate movement authority for the train.

PTC type systems are being developed throughout the world with similar architecture. In Australia; Barney, Haley and Nikandros detailed a simulation methodology to determine SBD of heavy haul freight trains [37]. However all of their methodologies were based on traditional worst case scenarios. In the U.S., PTC is currently being developed for deployment before the mandated 2015 time limit. The braking algorithm being progressed involves specific inputs such as speed, train weight and alignment. This is called "Adaptive Braking" in that it calculates a different solution based on the data on hand [38]. Reports on this development such as those from Ede, Polivka, Brosseau, Tse, and Reinschmidt detail purely reactive methodology [39]. No

---

[13] A Class I railroad is defined as having annual revenues of at least $250M

real proactive approach to adhesion is under consideration even though it is a major component in the calculation.

2.5   Tribology

Tribology deals with the motion between surfaces along with the study of friction and lubrication. The same advantage that steel wheel on steel rail offers in efficiency for trains over other wheeled modes of transport also prevents them from stopping quickly. This topic is relevant to SBD and the capacity issue since the largest factor in the calculation of SBD is the maximum deceleration rate of the train once the brakes are fully applied.

In rail and transit applications, friction between the rail and wheel is the called adhesion. Higher levels of adhesion provide higher levels of deceleration and acceleration due to the fact that greater friction between the wheel and the rail allow higher forces to be applied without wheel slip.   Wheel slip is to be avoided since it reduces braking effectiveness and causes abnormal wheel wear. In traditional calculations of SBD, picking an appropriate adhesion to apply to SBD calculation is the key to safety.

Rail vehicle wheel slip issue has been effectively modeled by Cocci, Presciani, Rindi and Volterrani [41] and Armstrong [42], but there are few solutions to situations where low adhesion is encountered. Vassic, Franklin and Kapoor investigated some wayside instrumentation techniques, but concentrated on chemical rail treatments and their effect on wheel slip [43]. Similar approaches can be found throughout the industry

as reported by Metro North Railroad [44], [45] and the Southeastern Pennsylvania Transportation Authority [46] where high pressure water treatments temporarily increased adhesion during the peak fall leaf seasons in the United States.

Despite these approaches, low adhesion areas remain a concern of rail operators. The capacity in rail systems was noted by McDonald in systems that issued manual advisories to crews approaching these conditions [17]. Conventional SBD calculations assume a poor adhesion to satisfy the worst case, however knowledge of adhesion conditions ahead of the train could ensure an optimized calculation to minimize SBD.

Kalker's work on the contact rolling resistance of elastic bodies has been one of the major studies in this field [47]. It was the first to describe this interaction and mechanics of this interface and remains the leading approach after almost 40 years since first published. This understanding of the relationship of smooth rolling bodies and the available friction between them is the basis of lubrication theory.

More recent studies sponsored by the Federal Railroad Administration indicate that contaminants typically found on the rail are directly related to the level of adhesion [67]. Therefore knowing what contaminants are present and their concentrations can lead to a way to measure the available adhesion.

2.6   Sensor Technology

Since adhesion plays an important role in the calculation of SBD, it is important to establish a methodology to detect current levels of adhesion directly from a train traveling along the track. Currently, adhesion measurements are limited to measurement

of the tractive or braking forces applied to the wheel prior to the detection of wheel slip.

Wheel slip is typically measured through the use of tachometer attached to two

independent axles where the two rotational speeds are compared. Any difference in the

signals indicates slip. In another method, Yu, Mei, and Wilson used an FFT of a signal

from a single axle to detect discrete changes in speed to detect wheel slip [48]. A similar

approach was used by Park, Kim, and Yamazaki to form a feedback loop in traction

power control circuits to correct for wheel slip [49].

The above methods are reactive in that they recognize conditions after the

occurrence of slip. This method can be used only to determine the conditions at the

location of the train. For SBD to be optimized for adhesion, it is necessary to have

knowledge of the conditions before the train encounters them since adhesion can change

throughout the entire stopping distance of the train. Adhesion is best during dry

conditions on level track. Different compounds being present on the rail or wheel tend to

decrease adhesion. By detecting these compounds or anomalies on the rail or wheel

surface, a better estimate of adhesion and therefore the maximum braking effort can be

made.

Similar detection of surface contaminants in other industries proved insightful to

the rail and transit application. Hamilton found that the Fourier Transform of reflective

absorption from infrared spectroscopy identified soiled surfaces in pharmaceutical

facilities [50]. Liquids typically cause a decrease in available adhesion for rail vehicles.

Similar to Hamilton's work, Harig, Braun, Dyer, Howle, and Truscott found liquids on

surfaces scanned by similar methods [51].

Among several methods used to detect surface contaminants, Raman scatter from lasers provides significant promise [52].   Both Chyba et al. [53] and Sedlacek and Ray [54] utilized this technique to identify surface contaminants using LISA[14].   These methods all employ properties useful in detecting rail surface qualities that effect adhesion and SBD.   In the proposed train control scheme, adhesion conditions are transmitted from one train to trains behind to describe what conditions will be experienced. Using spectral sensors mounted on trains is a novel way to detect contaminants that change adhesion and allow for accurate estimation of stopping distance.

Results from the LISA tests and others indicated that the spectrometers were able to not only detect the materials but the amount and thickness of the materials present [55], [56], and [57]. In the case of military applications, only very small amounts of material are needed to be detected to trigger alarms mounted on highway trucks traveling along a highway [58], [59]. This is a similar environment found on rail cars (dust, vibration, shock, etc.) where rail contaminant sensors would be mounted to estimate the impact on adhesion. In addition, sampling times were sufficiently high to not cause miss detection due to speed or vibration.

2.7   Filters and Estimators

The contaminants found on the rail can be grouped into categories for classification. These channels of identified materials are essentially signatures that

[14] LISA stands for "Laser Interrogation of Surface Agents".

provide a way to observe the current level of adhesion based on experience. The nature of the solution required multiple inputs from the spectral sensors that described separate channels of detected contaminants, and output a single response that described the current adhesion conditions.   Although a form of this had been done in a laboratory setting by Malvezzi, Allotta and Rindi [40], and others [49], [61], and [62]; real time adhesion measurements were isolated to wheel slip that had already occurred. Estimators were researched for adaptation to the needs of adhesion that included recursive mean, least squares (RLS), and other approaches. Of particular interest was the Multiple Input Single Output (MISO) work performed by Han, Sheng, Ding and Shi that derived a model for a general case [63]. They derived a state space model that consisted of several inputs and associated transfer functions that operated on a single output. A similar approach could be used in establishing a system to estimate adhesion on a train.

Chen found that the RLS was enhanced with localized groups of data that narrowed the field of available data [64], however in the case of contaminant estimation, it was more useful to view the filtering as an intermittent event (specific discrete events that indicate adhesion rather that a continuous measurement) that was supplemented by the resulting estimators when direct measurements are not avaialble.   Kaplanoğlu, Şafak and Varol utilized somewhat arbitrary transfer function in a MISO model as a starting point for the estimation of liquid levels to use as feedback to control a chemical process [65]. This approach is especially useful to simplify the approach to estimating the characteristics of rail contaminants that might be found through a spectrometer, and a similar approach is the bases for estimating adhesion in the proposed train control system.

The most useful tool found in dealing with adaptive filters was the UNIT add-on for Matlab developed by Wills, Ninness and Gibson [66]. Matlab generally does not perform MISO or MIMO adaptive filtering "right out of the box", and this toolbox allows such an analysis with the latitude of using several algorithms within the process. The algorithms were each reviewed and applied to optimize their use [67], [83].

It was then possible to construct a model of the entire MISO adaptive filter with appropriate noise functions added in to analyze the sensitivity and overall usefulness of the approach. This noise included the spectral and quantization noise observed by Flaherty [68], Kearsley, Barnard, Gadhyan, Lin, Tong, Wang, and Zhong [69], and Zhang, Zhao3, Yuan and Huang [70].

2.8   Summary

Train control systems are becoming more complex with time, but in virtually every case the methodology used in the determining basic train separation (SBD) has remained unchanged. If a rail system is thought of as a closed system of trains operating over a specified alignment, sensor data of the wheel and rail conditions can be accumulated to provide these conditions to following trains. With this knowledge, SBD and capacity can be adjusted for conditions in real time providing optimum capacity for current conditions.

A major determinant of SBD is adhesion. Adhesion is a measure of the friction between the rail and wheel. It is expressed as a factor derived from the coefficient of friction [16]. Once the train begins to decelerate, adhesion limits the amount of braking

force that can be applied through the wheels without slipping. The slipping action

decreases the braking effort, and the stopping distance increases.

Adhesion has been calculated over a wide range of conditions such as wet or

lubricated rail. These variations correspond to a large distribution of SBD requirements.

Worst case scenarios force Train Control Designers to use longer distances that are

appropriate for low adhesion conditions that are much too conservative for clean or dry

rail conditions. This conservative approach to design can also occur in tunnels where the

likelihood of unfavorable rail conditions is remote.

The resultant deceleration of the train is typically expressed in miles per hour per

second (mphps). Transit vehicle stopping tests on dry rail can yield deceleration rates as

high as 5.0 mphps, while typical deceleration rates for train control design are typically in

the range of 1.0 mphps. As seen in the figure below, this range in deceleration yields

drastic differences in stopping distance.
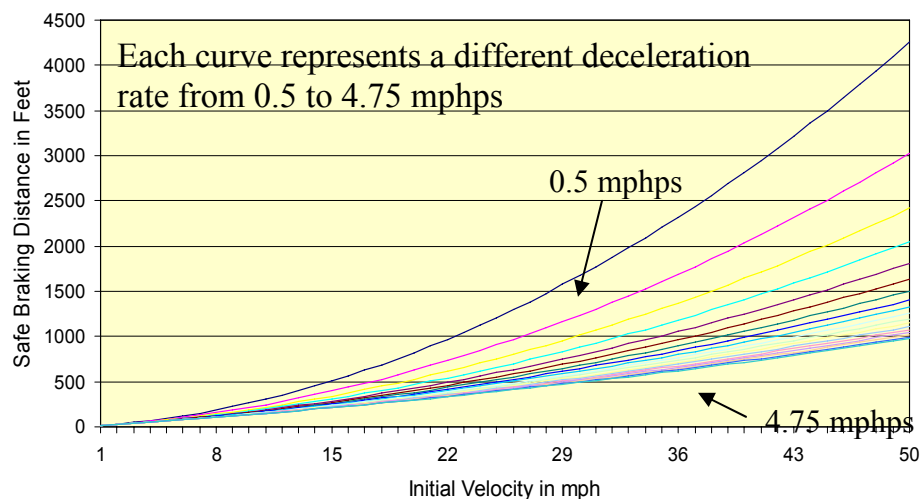
Figure 19, Stopping distances with varying deceleration rates

Sensor technology has been developed that can provide data on conditions of the contact surfaces of the wheel and rail. Armed with this information, train control engineers will be able to adjust SBD on a train, location and condition basis.

To optimize the capacity of the line, the train control system must be designed with the minimum SBD that is practical. The worst case approach takes into account many scenarios that are unlikely to occur at the same time. In the past, probabilistic methods for calculating SBD have met with mixed results. Over twenty years ago, an initial IEEE recommended practice utilizing this method was nearly completed, but never finalized [24].   More recently in 1997, variations were developed that applied to a specific system on specific vehicles that provided improved performance. However, a probabilistic approach to SBD has not been widely accepted. As part of a train control optimization, it is proposed to utilize this method within the framework of a new system that optimizes SBD through statistical and measured means. Combined with a priori knowledge of adhesion conditions and the operating parameters in effect, the minimum SBD can be determined that still maintains appropriately safe conditions.

Taking a probabilistic approach is not meant to compromise safety in any way. There is a tradeoff between safety and operations that must be defined in order to optimize the system and still provide the level of safety that is required. By optimizing the SBD calculation that provides the distance to safely stop the train, we also remove some level of safety associated with the longer distance. This research has found that very slight reductions in the level of safety provided (in the form of the probability of a

train exceeding the SBD) can yield significant reductions in SBD while maintaining the safety of operations actually required.

The link between SBD and system capacity had been established through the analysis of train operation and computer modeling. In the following sections, a proposed solution and methodology for implementation will be described in greater detail.

The remaining research concentrates on two areas. The first looks at parameters related to the train actually doing the SBD calculation. This data is collected locally on the train and therefore is not transmitted over the data radio network. The second area looks at conditions to be encountered by the train that will affect the stopping calculation that is transmitted from trains ahead. The optimized SBD calculation is based on a series of results that combine values for each part of the SBD model's contribution to SBD with its associated probability. The final SBD used by the train provides a safety level that meets the designated criteria for the system. Examples of this criteria are also discussed. In order to compare these results with a known baseline, the traditional methods will be used in an example that will be carried on into the proposed system to give a head to head comparison of any reduction in SBD.

CHAPTER 3

3   CONVENTIONAL ANALYSIS FOR SBD BASELINE

3.1   Traditional "Worst Case"

As previously mentioned, the traditional methodology for determining SBD

involves examining the "worst case" or most conservative view of each and every

parameter involved in determining the overall distance. In fact, this distance is often

referred to as the "guaranteed" braking distance [11] as if to imply that no vehicle would

ever take more than this distance to come to rest. Experience shows that regardless of the

distance provided by this method, conditions exist whereby vehicles will always exceed

this distance (think of traveling in your car over patches of ice where practical limits do

not apply). This issue is particularly evident in the fall when tree leaves drop onto rails

and interact with the rail/wheel contact area to form a slick surface [44], [49]. However,

train control systems are not generally designed to protect against extreme conditions

such as this that are both very rare and are mitigated through operational procedures.

3.2   A Sample braking distance baseline

An example used for illustrative purposed consists of a typical transit system

utilizing Automatic Train Protection (ATP). The term ATP implies that the train control

system will enforce penalty brake applications when the train exceeds the SBD curve

created by the SBD model parameters.   Human factors are an important part of SBD

analysis, and include consideration of reaction to changes in conditions as well as alarms.

Traditional methodology assumes that the operator takes no action to prevent hazards from occurring, and is referred to as a "hands off" approach.

For uniformity, the nomenclature in the IEEE 1698 Guideline will be used as a basis in determining a calculated SBD baseline [11]. This baseline will be used to show any benefits from the proposed modifications to this methodology. Each part of the SBD model (A thru J) will be discussed to determine the effect on the overall distance. These parts were described in a previous section, and are repeated for clarity in the figure below. The figure also includes the calculated distances that each component adds to the overall distance.
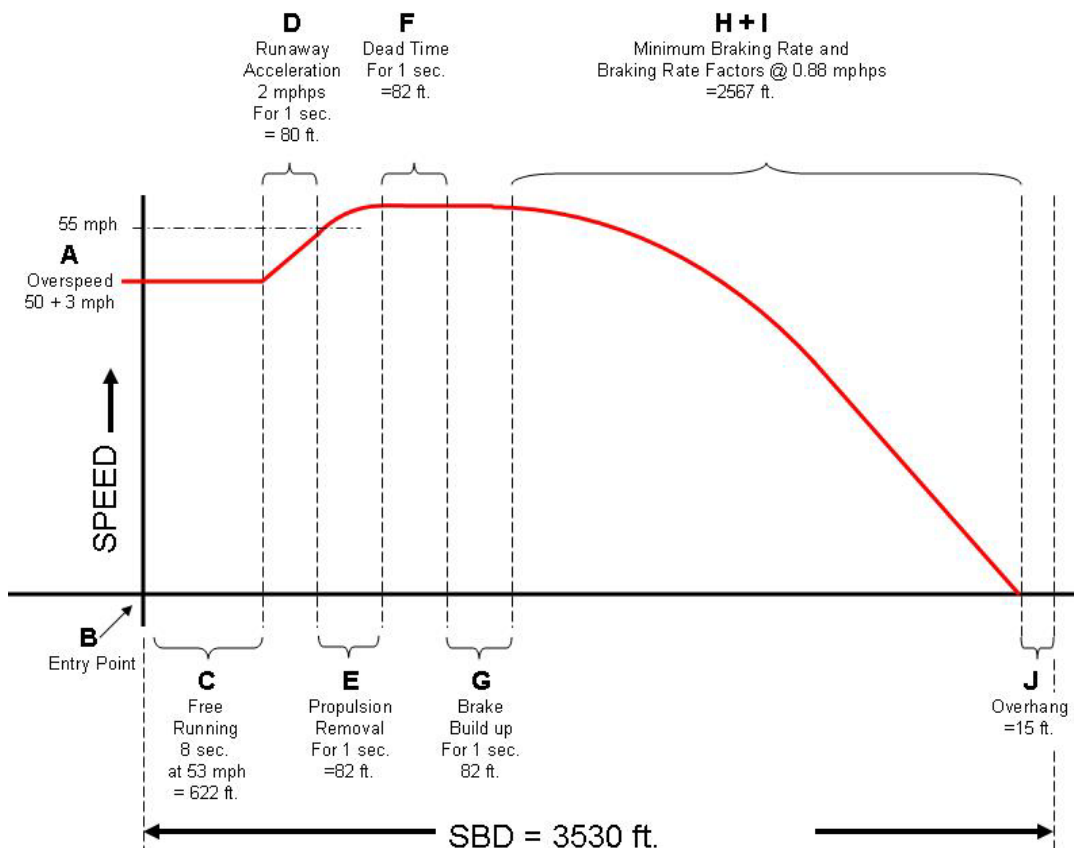
Figure 20, Example of a traditional approach to a SBD model with values

The effect of grades and curves are ignored at this time for ease of calculation. Information on the application of these features can be found in Section 1.3.   The following is the detailed discussion of the individual parts as applied to a baseline from the conventional approach to SBD calculation.

- **A – Maximum Entry Speed**

This is the actual speed of the train as it enters the braking zone. Speed is typically measured by digital encoders mounted on the end of an axle as shown in the Figure 21, below. The output of the device generates a square wave at a frequency proportional to speed. However, this device requires calibration to maintain accuracy from wheel wear. Measurement error due to calibration is accepted to be within 3 mph, and therefore the Entry Speed is taken as 3 mph over the maximum authorized speed at this point. For this analysis, arbitrary 50 mph plus 3 mph (worst case for calibration error) entering speed will be used.
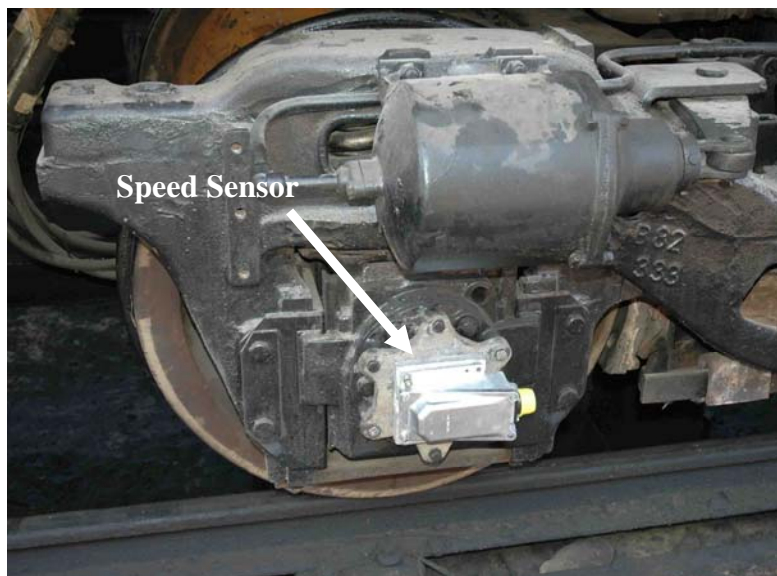
Figure 21, An example of a speed measuring tachometer at the end of the axle.

- **B – Entry Point**

The entry point is the location where the action of braking is initiated. It is merely a fixed point along the right-of-way.

- **C – Distance Traveled During Operator Reaction Time**

Operator Reaction time is a period allotted for the vehicle to initiate a braking mode. It includes time for the operator to react to an alarm or change in status or a change in movement authority.   In addition, Reaction Time includes a portion for on board equipment to detect, process, and act on a need to stop or slow the train. This is typically eight (8) seconds for railroad applications, although the interpretation of the governing regulations varies [19].

At 53 mph, the distance traveled is given by the equation;

$$D_C = V_A * 1.466 * t_R \qquad \textbf{(3)}$$

Where D_C = Reaction Distance component of SBD,

V_A = Maximum Entry Speed,

t_R = Reaction Time, and

1.466 = is the conversion between mph and fps.

For this example, the distance for eight (8) seconds at 53 mph is 621.86 feet.

- **D – Runaway Acceleration**

Runaway Acceleration can have a great influence on total SBD. Runaway occurs when the propulsion system fails and calls for unrestricted acceleration. To conform to the logic of the worst case scenario, this period of the SBD curve is calculated with an empty train to achieve the highest acceleration possible. It is in

effect immediately following the end of the reaction period to have the most significant effect on the total SBD. The increase in speed is normally detected by the train control system as an overspeed condition and immediately initiates a power removal and brake command. Power removal does take a finite amount of time, and Runaway Acceleration ends when the propulsion control is removed.

For this example, Runaway Acceleration is in effect for one second. The maximum acceleration available will be taken at 2.0 mphps. To simplify the calculation, jerk rate limiting is not considered, and the acceleration is assumed to be uniform throughout the period. Therefore, the speed at the end of the Runaway Acceleration period is 55 mph, and integrating over the one second period yields a distance traveled of D_D = 79.2 ft.

- **E – Propulsion Removal**

The next three parts of the SBD model are all related in that they all start at the same point in time (Propulsion Removal, Dead Time, and Brake Build Up). For the purposes of this analysis, each portion is examined as an independent event. The first portion is Propulsion Removal. For the SBD model, this is the distance the vehicle has traveled from the propulsion control removal until the tractive force generated by the vehicle is zero. This generally lasts a short period of time and is taken as one second in this SBD model. For ease of calculation, the drop in acceleration is assumed to be linear. Therefore the calculated distance for the portion is D_E = 81.4 ft., and the exiting speed is 56 mph.

- **F – Dead Time**

Dead Time is the distance traveled by the train from when the tractive effort of the vehicle has dropped to zero, until the brake system has begun its effectiveness. On some SBD models, the Brake Build Up (see part G, below) begins before the end of the Propulsion Removal portion whereby the Dead Time portion is eliminated. For this SBD model, the assumption is made that the Dead Time is one second long while and the train coasts.

Again, for ease of calculation, the 56 mph speed is maintained for the short duration of this portion yielding a distance of $D_F = 82.1$ ft. calculated using formula **(2)** as in the Reaction Time portion.

- **G – Brake Build Up**

The Brake Build Up portion is the distance traveled from when the braking system on the vehicle begins its effectiveness (typically 10% of the braking effort called for) until the full braking rate is achieved. This, combined with the previous two portions of the SBD model, provides a good mathematical representation of an enforced stop by a train control system.

For the calculation of distance traveled, a constant deceleration is assumed. The rate used is 50% of the final full braking rate of the next portions of the SBD model, and it has a duration of one second. This provides an exit speed of 55.5 mph and a distance traveled of $D_G = 81.8$ ft.

- **H – Minimum Brake Rate**

Once the full braking rate is achieved, the vehicle continues to slow at a constant rate of deceleration. The actual rate used is a combination of two primary parts. The first is the Minimum Brake Rate. This is a rate that can be determined through empirical methods of actual field testing with vehicles loaded with material to simulate a fully loaded (or worst case) condition. The other part consists of additional distance added to compensate for other factors that can affect the overall braking rate. For the purposes of the example SBD model, these two rates are combined into a single deceleration rate to determine the distance traveled during full braking.

- **I – Braking Rate Safety Factors**

The second portion of full braking takes into account all of the unique features of the operation it is applied to. In some cases this is rules based, and in some cases this is equipment based.

In the case of rules, the operator may be instructed to handle the train under strict procedures in an effort to stop. This is particularly true for long or heavy freight trains where a severe brake reduction at the wrong time can cause excessive slack action[15] or even derailment. Split brake applications are commonly used to stretch the slack out of a train before the primary brake

---

[15] The term "slack" refers to the free space between coupled cars of a train. "Slack action" can occur in long or heavy trains where this extra distance can collapse or expand the length of a train causing high coupler stresses to occur in hard braking or acceleration.

application to stop the train occurs. The effect in this case is to lower the overall

deceleration rate in the portion of the braking model.

Another rules based constraint is the amount if inoperative brakes allowed

before train operation is restricted. The limit of inoperative brakes for a railroad

train to move imposed by Federal Regulation is at 15% [12]. If the operating

rules allow for normal operation with these brakes inoperative, then the SBD

model must allow for the extra distance required to stop the train with only 85%

of the braking power of the train available.

For the calculation of distance traveled during this portion of the example

SBD model, a constant deceleration is assumed. The rate used in this example

corresponds to a popular braking rate used by several Commuter Rail properties

in the United States and is 0.88 mphps. Using the formula for deceleration:

$$D_{IH} = V_{IH}^2 * 0.8333 \qquad \qquad \textbf{(4)}$$

Where: D_{IH} = Brake rate component of SBD, and

V_{IH} = Velocity at the beginning of the braking period.

The distance for part H and I of this SBD model is 2,567 ft.

- **J – Vehicle Overhang**

Vehicle Overhang is the distance from the point on the vehicle that is

detected by the train control system to the forward most point of the vehicle. In

train control systems using track circuits[16], this distance is measured directly from

the train's front coupler face to the centerline of the lead axle where the wheels

will effectively be detected with track circuits. In Communications Based Train

Control where train detection relies on inertial navigation updated by track

mounted transponders, this portion represents the uncertainty of the detection as

the vehicle moves farther from the last refresh point. For the calculation of

vehicle overhang during this portion of the SBD model, 15 ft. is used.

The total SBD calculated is then the sum of all the above described parts

of the SBD example as shown above is:

$$D = D_C + D_D + D_E + D_F + D_G + D_{IH} + D_J \qquad \textbf{(5)}$$

Therefore

$$D = 622 + 80 + 82 + 82 + 82 + 2567 + 15 = 3{,}530\, ft. \qquad \textbf{(6)}$$

This becomes the distance that is provided in a conventional signal system to stop

a train on track where the maximum authorized speed is 50 mph. This is also the basic

distance used to space wayside signals under the same scenario. The nature of the SBD

assumes that this will be sufficient to stop the train short of any detected obstruction in

front of the train. However it does not indicate to what level the safety the distance has

achieved. Historically, this has been all that was required in terms of providing safety.

The proposed train control system quantifies the level of safety and can be compared to

---

[16] Track circuits utilize the rails as part of an electrical circuit to detect trains. The first axle shorts the rails together diverting current from a detection device. In this case the train is detected when the first axle is in the track circuit, not the actual front of the train.

the conventional method above by looking at the difference in the provided distances.

The first step is to determine what is actually required in terms of safety and the SBD

number.

CHAPTER 4

4 HOW SAFE IS SAFE?

4.1 Introduction

The traditional method for calculating SBD assumes worst case for each and every portion of the model used. Safety is assumed within the calculation with this methodology as field testing may not be able to replicate all of the poor adhesion conditions that will be found in regular service. Even though the SBD calculation is meant to provide a guaranteed distance for a train to stop, there will always be a finite probability that the train will exceed that distance when stopping. The result would be a collision and possible injuries or fatalities.

So what is safe? How can we quantify safety in terms of SBD? These questions form the basis of a statistical analysis that can be used to identify the level of safety required for a system. The safety level can be expressed in a variety of ways. Similar to reliability, mean time to a fatality or hours of operation between hazardous events can describe a safety level that could be used. For the LRT example used in the baseline, it is possible to describe the level of safety as a probability of a train exceeding the provided SBD. This could also be extended to say that when it is required to stop short of an obstruction or train, provides a finite probability of exceeding the provided distance that will cause a fatality from the resulting impact.

4.2   A statistical approach to braking distance

Employing a statistical approach to the SBD model provides a methodology for determining train stopping distance based on known hazards that may reduce SBD as compared to worst case scenarios. This is accomplished by matching the probability of exceeding the calculated SBD with the probability that is targeted for a safe system. In order to determine what is appropriate for a safe system, the probability of a hazardous event (in this case, stopping a vehicle beyond the provided distance) needs to be determined.

The traditional approach to SBD determination is founded in experience. As shown in the LRT example, the model parameters all represent either the longest distance achievable for the individual model part or a deceleration rate so conservative as to provide excessive distances to stop. However, it is possible to quantify by a statistical analysis the probability of a train exceeding the provided distance, and to compare that distance with commonly accepted metrics for safety. Two such metrics include the European Comité Européen de Normalisation Électrotechnique (CENELEC) standard EN 50126 [71], and a 1976 report to Congress that described the features of Automatic Train Control [72].

For the CENTELEC standard, risk is expressed in specific steps called Safety Integrity Levels (SIL), with SIL 0 requiring the lowest requirement for safety to a maximum of SIL 4. The tolerable hazard rate for each level is expressed as hazardous events per hour of system operation. Typical values used for safety critical functions in SIL 4 are less that 10^{-8}.

The only reference for American systems in terms of hazard level can be found in a 1976 report to Congress on Automatic Train Control systems in transit [72]. Within this report, data indicated that the current level of safety was adequate for rail mass transit systems in the United States, and that the current hazard rate, expressed as hazard per number of passengers carried, was an injury rate of one per one million, while the fatality rate was one per twenty billion.

The fatality rate above can be used to determine the minimum level of safety required once it is expressed in terms of a probability of exceeding a specific SBD.   In the LRT example used previously, the following parameters are used to characterize a typical Light Rail Transit system:

- 19 hours of daily train operation

- Continuous operating headway of 15 minutes

- Average loading of 150 passengers per train

An operating headway of 15 minutes provides for four trains per hour per direction. 19 hours of operation at this headway equates to 152 trains per day with 150 passengers each, or for both directions: 8,322,000 passengers per year.

Approximating the number of trains and their associated ridership over a yearly period and the given minimum fatality rate (20 billion passengers) creates the following formula for determining Mean Years to Fatality as:

$$MYTF = \frac{R_f}{r} = \frac{2x10^{10}}{8.322x10^6} = 2403 \qquad \textbf{(6)}$$

Where: MYTF = Mean Years to Fatality,

R_F = Fatality Rate per passengers,

r = Numbers of Riders per Year.

Since the likelihood of exceeding any provided SBD is only relevant when the train is attempting to stop short of a potential hazard, the number of these brake applications considered can be approximated for any specific line or operation. In the typical case presented, it is assumed that the line is 15 miles in length, with a station stop each mile. Therefore each of the 152 trains is required to make 15 brake applications that are considered safety critical. For the purposes of this example, we will assume that each brake application is required to prevent a serious accident. Since this is not always the case, this represents an upper bound of the calculation[17]. The formula shown below calculates the number of critical brake applications one year.

$$BA = (\#\_of\_trains) * (\#\_of\_critical\_brake\_applications) * (Days/year)$$

With the parameters listed above, this formula indicates that there are 832,200 critical brake applications per year for the LRT system used as a base case..

The probability of a train stopping beyond the provided distance can be calculated as a function of the probability of the provided SBD (the MYTF) and the number of times the train needs to stop (the BA) given as a probability of a fatality for each brake application. Therefore the overall probability for the system to reach the level of safety required implies that the probability of exceeding a stopping distance must be equal to or

---

[17] For the LRT application in the example, station stops are associated with either the end of double track representing a risk of head on collision from opposing trains or an enforced stop at a near side highway grade crossing. Near side crossings require a stop so that warning flashing light signals and gates for motor vehicle and pedestrian traffic are not blocked for extended times while the train is in the station. In this light, it is reasonable to assume that each stop must be made to prevent possible fatalities.

less than the probability shown in Equation 7 as expressed in the probability of a fatality for each critical brake application.

$$F_x(x) = P = \{X(\xi) \le x\} = \frac{1}{BA * MYTF} \tag{7}$$

Where:　　　　BA = Yearly Brake Applications, and

　　　　　　　MYTF = Mean Years to Fatality (as calculated above).

For the example used in the traditional SBD case, the calculated probability of exceeding SBD for the level of safety consistent with the level of the Report to Congress is calculated in Equation 8 below. This represents the minimum acceptable level of safety in terms of the probability of overrunning the distance provided to stop.

$$F_x(x) = P = \{X(\xi) \le x\} = \frac{1}{832,200 * 2403} = 5.0x10^{-10} \tag{8}$$

For this example, this answers the question "how safe does the system have to be?" The conventional approach provides a SBD that is based on a string of worst case events in stopping a train. As such, it provides a probability of exceeding the provided SBD that represents the upper bound of what this calculation represents. In the next two chapters, techniques are discussed that allow a reduction SBD as compared to the conventional calculation, while also providing a probability of exceeding the provided SBD that meets the requirements of Equation 8.

CHAPTER 5

5   STATISTICAL APPROACH FOR NON BRAKING PORTION OF SBD

5.1   Methodology

Looking back on the IEEE SBD model developed for the LRT example, it becomes apparent that there are two groups of parameters, each driven from a different source. The first group is concerned with human and equipment reaction to changes and is the subject of this chapter. The contribution to SBD for this group is contained on the following train in the proposed train control system, and requires only a posteriori knowledge of the train and equipment type.

The second group deals with the actual braking of the train and is the subject of the next chapter. This group deals with a priori knowledge of the conditions ahead for the train that is supplied over the digital radio link in the proposed train control system. This information is used to calculate the distance required for the train to brake under these conditions.

Each portion of the IEEE model will be examined in detail and associated with a contribution of distance and probability. As appropriate, these values will be combined into a series of results that provide a distance and likelihood of stopping the train. The distance associated with the probability that matches or exceeds the requirement for safety (the value expressed in Equation 8) represents the minimum distance needed for SBD.

5.2   Application of the SBD model in the Statistical approach

The fundamental hazard associated with the train control system is overrunning the provided SBD. This applies to fixed block wayside systems that have permanent facilities along the wayside as well as moving block train control that calculates SBD continuously on board the train. The overall calculation of the probability of exceeding a specific distance can be applied to the IEEE SBD model so that a direct comparison can be made to the LRT baseline example previously calculated using conventional methods.

Each portion of the IEEE SBD model represents an event that describes the response of the train's systems to stopping [11]. Some are initial values, while others are characteristics of the equipment. For example, Part D is called Runaway Acceleration. This component assumes a worst case failure of the propulsion system that drives the train into maximum acceleration. Part C is called Free Running and represents the reaction time of the on board equipment (it takes time to recognize a changed condition) and the train operator (it takes time for the operator to respond to the new conditions. Although each part contributes to the SBD calculation in some way, each portion of the model can be viewed as an independent event. The likelihood of Runaway Acceleration occurring is a function of the propulsion system, while the reaction of the train control equipment or the operator is not. Similarly, Parts E, F and G are functions only of the braking system and are not linked to the other drivers of SBD model parts.   In summary, although all of the model parts are linked in a serial way to describe the SBD model, the effect on the SBD calculation from each are not linked in any way.

When the probability of exceeding a distance is calculated for each portion of the model, the distances for each calculation can be added while the probability for each portion is multiplied. Every combination of the model portions summed and multiplied as described here creates a different distance and associated probability of overrunning.

Since traditional methods for calculating SBD are not based on statistical methods but are indeed statistical in nature, traditional methods overstate the required stopping distances by virtue of their "worst case" designs, and form an upper bound of the statistical model. It is unlikely that this would change over time unless human factors (rest, work rules, etc.) change. Therefore the analysis holds for all time.

Each portion of the SBD model (A through J) is discussed below in the statistical sense, including the affect of each part on distance and its probability of occurrence.

- **A – Maximum Entry Speed**

This is the actual speed of the vehicle as it enters the braking zone. The calibration error referred to in the traditional method can be represented as a Cumulative Distribution Function (CDF) based on empirical data. For this, and other portions of the statistical model, information was gathered from event data recorders found on Light Rail Vehicles (LRV's) on an operating transit system.

Train speed data was taken from the event recorder and entered into a spreadsheet that grouped the data into equally spaced ranges. Each run from the data was correlated to the railroad's actual location, and Maximum Authorized Speeds (MAS) was overlaid onto the data. Where there was enough distance for

the train to adjust its speed approaching new speed limits, the entry speed was

noted and recorded in a spreadsheet. This data was collected into a histogram that

showed the distribution of values for the operating speeds. An example is shown

below.
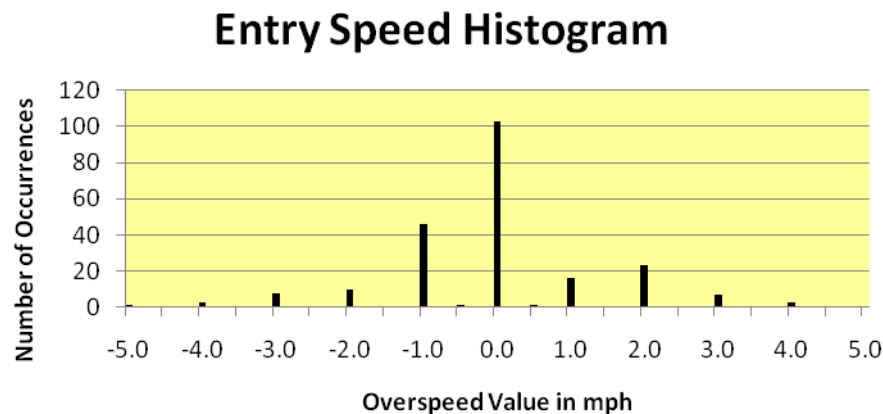
Figure 22, The LRV Entry Speeds represented in a Histogram.

The Histogram of data represents a form of a Cumulative Distribution

Function (CDF) of the occurrence of each overspeed value encountered in the

data, and was converted to a true CDF shown below. The occurrences were

divided by the total number of samples to calculate the probability for each set.

The CDF was simplified by grouping the occurrences into three values of

overspeed that approximated the data.

The 50 mph plus 3 mph used in the conventional example was replaced

with the CDF for entry speeds. This gives up to three different results for the

Statistical SBD analysis, each with a unique distance (based on the speed) and

probability (based on its occurrence). The results provide a solution for each part

of the CDF of entry speed. Each result will consist of a sum of distances traveled and a corresponding product of probabilities of each component of the SBD model.

The figure shows a step function plot with "Probability" on the y-axis (0.0 to 1.0) and "Overspeed in mph" on the x-axis (-2 to 4). Beside it is the equation:

$$F_x(x) = P(X(\xi) \le x) = \begin{cases} 1 & x \ge 1 \\ 0.95 & 0 \le x \le 1 \\ 0.75 & -1 \le x \le 1 \\ 0 & x < -1 \end{cases}$$
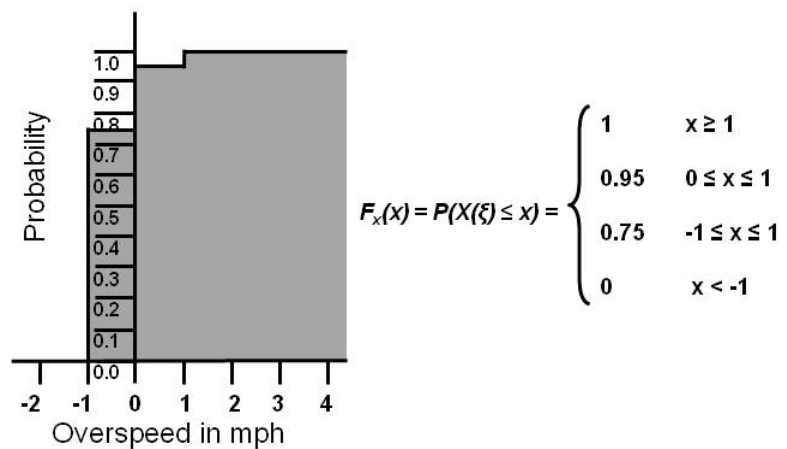
Figure 23, The CDF used for Entry Speed

It is important to note that the type of train control plays a role in determining this CDF. For example, where speed and train separation are enforced with trip stop technology, attainable[18] speed is used in the design that allows much higher entry speeds. This has the affect of creating a much broader range of values to consider in the CDF. This example uses a fixed block cab signal system with continuous speed control that enforces the entry speed to be less than the Maximum Authorized Speed (MAS) plus 3 mph.

---

[18] Attainable speed is generally determined to be the speed achieved at maximum acceleration from the last signal or enforced speed restriction.

- **B – Entry Point**

Just as in the example of the traditional calculation of SBD, the entry

point is the location where the action of braking is initiated. It is merely a fixed

point along the right-of-way and acts as a reference point for the calculation.

- **C – Distance Traveled During Operator Reaction Time**

From the conventional model, Reaction Time was a period allotted for the

vehicle to initiate a braking mode. However the time for the operator to react to a

change or an alarm varies with each operator and the circumstances that are in

effect. Even the Reaction Time for on board equipment to process and act on

changes can vary based on processor loop times[19]. In the LRT example used as

the baseline, the only constant is the time provided by the train control system for

these events to occur. The only mitigating factor for the entire reaction time

period is the case where regulations require a specific time period for this event.

This currently applies only to the general systems of railroads under the

jurisdiction of the Federal Railroad Administration where reaction time for cab

signals may not exceed eight (8) seconds as specified in CFR 49 § 236.563 [19].

For a statistical approach to reaction time, results from human reaction

studies [73] and [74] were used to start a calculation for reaction time. These

studies indicated that human reaction to stimulus, such as a cab signal command

downgrade is 0.24 seconds. Added to this was additional time to reach for the

---

[19] Microprocessors in safety related Train Control applications typically run an executive program in a continuous loop. The time to execute a specific function depends on where the processing is for that function in the loop, and where the loop is in its current execution.

LRV controller handle and place it into the correct braking mode. Randomized

possessor loop times and equipment cab signal recognition time[20] completed the

timing sequence. A histogram of the summed values was created that contained

the number of occurrences within each tenth of a second. Overall, this makes for

a fairly normal distribution of events within the 3 second range, which is

consistent with industry practice.   A sample is shown in the Figure 24 below.
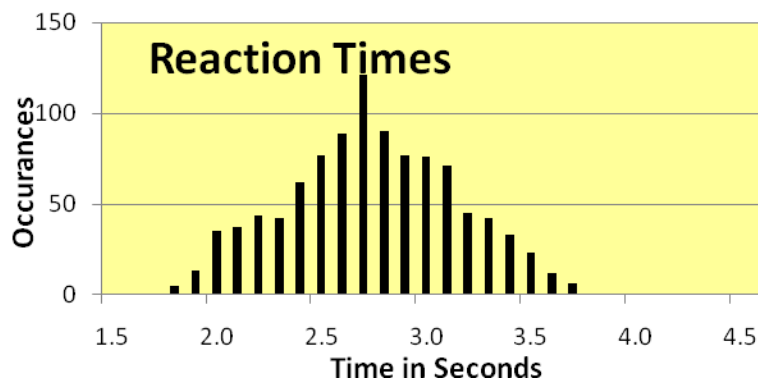
Figure 24, A Typical Histogram of Reaction Times

The CDF from this data is shown below. As in the entry speed CDF, the result

shown here is simplified to ease the overall calculation of SBD. This includes placing a

cutoff of reaction times below three seconds as per industry practice. This accounts for

the high likelihood of three seconds with corresponding additions of events between three

and four seconds.

---

[20] Equipment recognition for cab signal equipment requires at least three consecutive cycles of code to prove safety and allow a change in speed command to be recognized.

$$F_x(x) = P(X(\xi) \leq x) = \begin{cases} 1 & x \geq 4 \\ 0.9 & 3.5 \leq x \leq 4 \\ 0.6 & 3 \leq x \leq 3.5 \\ 0 & x < 3 \end{cases}$$
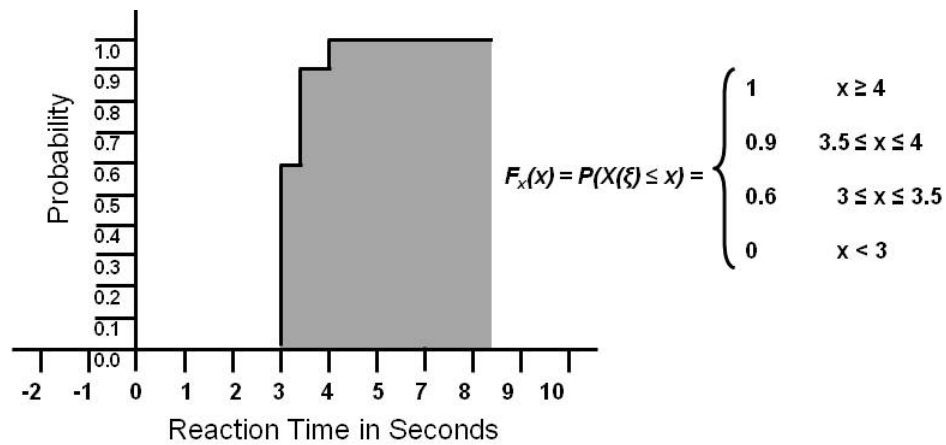
Figure 25, CDF of Operator Reaction Times

The probabilities of these Reaction Times represent a component to solutions of the total SBD calculation. As such, each level of probability has an associated distance consumed during the reaction time and a probability of occurrence that is added to the overall SBD calculation.

- **D – Runaway Acceleration**

As mentioned in the LRT example of the conventional SBD calculation, Runaway Acceleration can have a dramatic influence on the results. Fortunately, this is a relatively rare event. In fact for the LRT system used for the baseline, there has never been a recorded case of Runaway Acceleration in over five years of operation.

To determine the probability of occurrence for this event, a Failure Modes and Effect Analysis (FMEA) was conducted on the vehicle propulsion system. This consists of a series of evaluations of system components and their interaction to determine the severity of a failure and likelihood of occurrence. The FMEA

was a top down evaluation of propulsion system components. The subject Light

Rail Vehicle uses an AC induction motor driven by a Variable Voltage-Variable

Frequency (VVVF) inverter made up of microprocessor controlled IGBT devices.

Failure of the IGBT within the inverter will cause only degradation in output

power (failure to create an AC waveform for the induction motors in either a short

or open). Therefore the only failures of interest are contained in the control

portion of the device.

For the purpose of SBD calculations, the only states of interest are either

full acceleration or no acceleration, and this is reflected in the CDF. This

particular LRV achieves a maximum acceleration of two mphps over a range of

speeds. For the analysis, the acceleration rate was assumed to be constant over

the entire speed range of the vehicle.   These failure types and their associated

probabilities are shown in the CDF below.

$$F_x(x) = P(X(\xi) \le x) = \begin{cases} 1 & x \ge 0 \\ 10^{-7} & 2 \le x < 0 \\ 0 & x < 2 \end{cases}$$
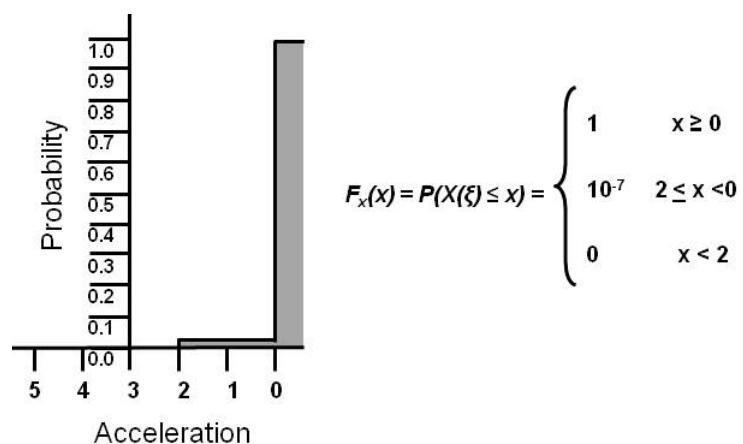
Figure 26, The CDF of Runaway Acceleration

The probabilities of the runaway acceleration represent another component to solutions of the total SBD. The distances run during this period and probabilities of occurrence were added to the SBD calculations in the same way as the other portions.

- **E – Propulsion Removal**

As in the conventional SBD calculation, the next three parts of the SBD model all start at the same point in time (Propulsion Removal, Dead Time, and Brake Build Up). In the LRT example used in the baseline analysis, these three portions are highly predictable and invariant. Therefore they do not introduce any opportunity for statistical analysis. The values used in the conventional SBD calculation for these parts remain the same except for the actual speed used at their initiation. The first portion is Propulsion Removal. For the SBD model, this is the distance the vehicle has traveled from the propulsion control removal until the tractive force generated by the vehicle is zero. This is taken as one second in this SBD model. For ease of calculation, the drop in acceleration if any is assumed to be linear. These results are added to the SBD calculation as before.

- **F – Dead Time**

Dead Time is the distance traveled by the train from when the tractive effort of the vehicle has dropped to zero, until the brake system has begun its effectiveness. For this SBD model, the assumption is made that the Dead Time is one second long while and the train coasts. The resultant distances are again added to the statistical SBD calculation.

- **G – Brake Build Up**

The Brake Build Up portion is the distance traveled from when the braking system on the vehicle begins its effectiveness (typically 10% of the braking effort called for) until the full braking rate is achieved as in the conventional SDB calculation.

For the calculation of distance traveled, a constant deceleration is assumed. The rate used is 50% of the final full braking rate of the next portions of the SBD model, and has duration of one second. As in the previous parts of the SBD model, the resultant distances are input into the SBD calculations.

- **H and I – Brake Rate (minimum and Safety Factors)**

Once the full braking rate is achieved, the vehicle continues to slow at a constant rate of deceleration. The Part H or minimum rate is that achieved under ideal conditions of adhesion, while the Part I or Safety Factor rate takes into consideration conditions such as low adhesion or brake inefficiencies.

For the calculation of distance traveled during this portion of the SBD model, a constant deceleration is assumed for now. The proposed train control system that will optimize this Brake Rate factor is described in the next chapter.

- **J – Vehicle Overhang**

Vehicle Overhang for the cab signal example used here is a fixed distance from the point on the vehicle that is detected by the train control system to the forward most point of the vehicle. If this had been a Communications Based Train Control (CBTC) system, the value would have included a statistically based

positional uncertainty. This value, added to the actual overhang is based on the

ability of the train control system to know exactly where the train is at any given

time. The further away from any navigation update point, the greater the

uncertainty distance.

For the calculation of vehicle overhang during this portion of the SBD

model, the same 15 ft. is used to make a direct comparison between the

conventional example and the statistical calculation of SBD.

5.3   Preliminary Results

Below is a brief combination of the results of all of the other parameters from the

calculation above. The final results will combine all of the calculations together with the

proposed calculation of the braking rate, and is presented in the final chapter.

All of the SBD model parts and their associated probabilities calculated in the

statistical analysis are listed and sorted in table 2. The table lists in each row on the left

side under the Parameters heading the probability of occurrence of each part of the

analysis ($P(V_i)$) for Overspeed (with the actual speed in effect), Reaction, Runaway and

brake Rate. For the purpose of this preliminary analysis, the Brake Rate used was 0.88

mphps with a probability of one. This represents the same value used in the base case

(see chapter 6 for techniques to optimize this distance).

The next column is the combined probability (P) for the entire row. Since each

event is independent from each other, this is the product of all of the individual

probabilities of the model parts and represents the likelihood of the train stopping at the

distances calculated from the parameters. As such, a probability equal to or greater that the value listed is the probability of a train exceeding the associated stopping distance, and is comparable to the required level of safety as expressed as the probability determined in Equation 8 from Chapter 4.

The next columns are the distances contributed to the total SBD by each part of the model (D_i) with the last column the total calculated SBD for the row. The results are sorted from highest to lowest probability of overrunning the stopping distance. To meet the required safety level, the probability must equal or exceed the value in Equation 8 (5 x 10^{-10}). This is highlighted in red in the last row of the table, and requires only 3,019 feet.

| | Parameters | | | | Probability | Distance | | | | | | | |
| | Overspeed | | Reaction | Runaway | Brake Rate | | | | | | | | | |
scenario	$P(V_A)$	V_A	$P(V_C)$	$P(V_{D-E-F-G})$	$P(V_{H+I})$	$P = (X(\xi) ? x)$	D_C	D_D	D_E	D_F	D_G	D_{H+I}	D_J	D_{SBD}
9	7.500E-01	49	6.000E-01	1.000E+00	1.000E+00	4.500E-01	215.502	71.9	71.9	71.9	71.5	1965.06	15	2,483
6	7.500E-01	49	3.000E-01	1.000E+00	1.000E+00	2.250E-01	251.419	71.9	71.9	71.9	71.5	1965.06	15	2,519
8	2.000E-01	50	6.000E-01	1.000E+00	1.000E+00	1.200E-01	219.9	73.3	73.3	73.3	73	2046.83	15	2,575
3	7.500E-01	49	1.000E-01	1.000E+00	1.000E+00	7.500E-02	287.336	71.9	71.9	71.9	71.5	1965.06	15	2,555
5	2.000E-01	50	3.000E-01	1.000E+00	1.000E+00	6.000E-02	256.55	73.3	73.3	73.3	73	2046.83	15	2,611
7	5.000E-02	51	6.000E-01	1.000E+00	1.000E+00	3.000E-02	224.298	74.8	74.8	74.8	74.5	2130.26	15	2,668
2	2.000E-01	50	1.000E-01	1.000E+00	1.000E+00	2.000E-02	293.2	73.3	73.3	73.3	73	2046.83	15	2,648
4	5.000E-02	51	3.000E-01	1.000E+00	1.000E+00	1.500E-02	261.681	74.8	74.8	74.8	74.5	2130.26	15	2,706
1	5.000E-02	51	1.000E-01	1.000E+00	1.000E+00	5.000E-03	299.064	74.8	74.8	74.8	74.5	2130.26	15	2,743
18	7.500E-01	49	6.000E-01	1.000E-07	1.000E+00	4.500E-08	215.502	73.3	77	76.3	75.9	2215.36	15	2,748
15	7.500E-01	49	3.000E-01	1.000E-07	1.000E+00	2.250E-08	251.419	73.3	77	76.3	75.9	2215.36	15	2,784
17	2.000E-01	50	6.000E-01	1.000E-07	1.000E+00	1.200E-08	219.9	74.8	78.5	77.7	77.4	2302.13	15	2,845
12	7.500E-01	49	1.000E-01	1.000E-07	1.000E+00	7.500E-09	287.336	73.3	77	76.3	75.9	2215.36	15	2,820
14	2.000E-01	50	3.000E-01	1.000E-07	1.000E+00	6.000E-09	256.55	74.8	78.5	77.7	77.4	2302.13	15	2,882
16	5.000E-02	51	6.000E-01	1.000E-07	1.000E+00	3.000E-09	224.298	76.3	79.9	79.2	78.9	2390.56	15	2,944
11	2.000E-01	50	1.000E-01	1.000E-07	1.000E+00	2.000E-09	293.2	74.8	78.5	77.7	77.4	2302.13	15	2,919
13	5.000E-02	51	3.000E-01	1.000E-07	1.000E+00	1.500E-09	261.681	76.3	79.9	79.2	78.9	2390.56	15	2,982
10	5.000E-02	51	1.000E-01	1.000E-07	1.000E+00	5.000E-10	299.064	76.3	79.9	79.2	78.9	2390.56	15	3,019

Table 2, Preliminary listing of calculated SBD values and their probabilities

Note that the conventional method resulted in a SBD of 3530'. This represents a level of safety that is well beyond the requirement. The statistical approach provides a 14.5% decrease in required SBD while providing the level of safety. Figure 27 below

shows these results in a graphical presentation illustrating the distances and probabilities

for the conventional and statistical cases.

Probability of overrun vs. SBD
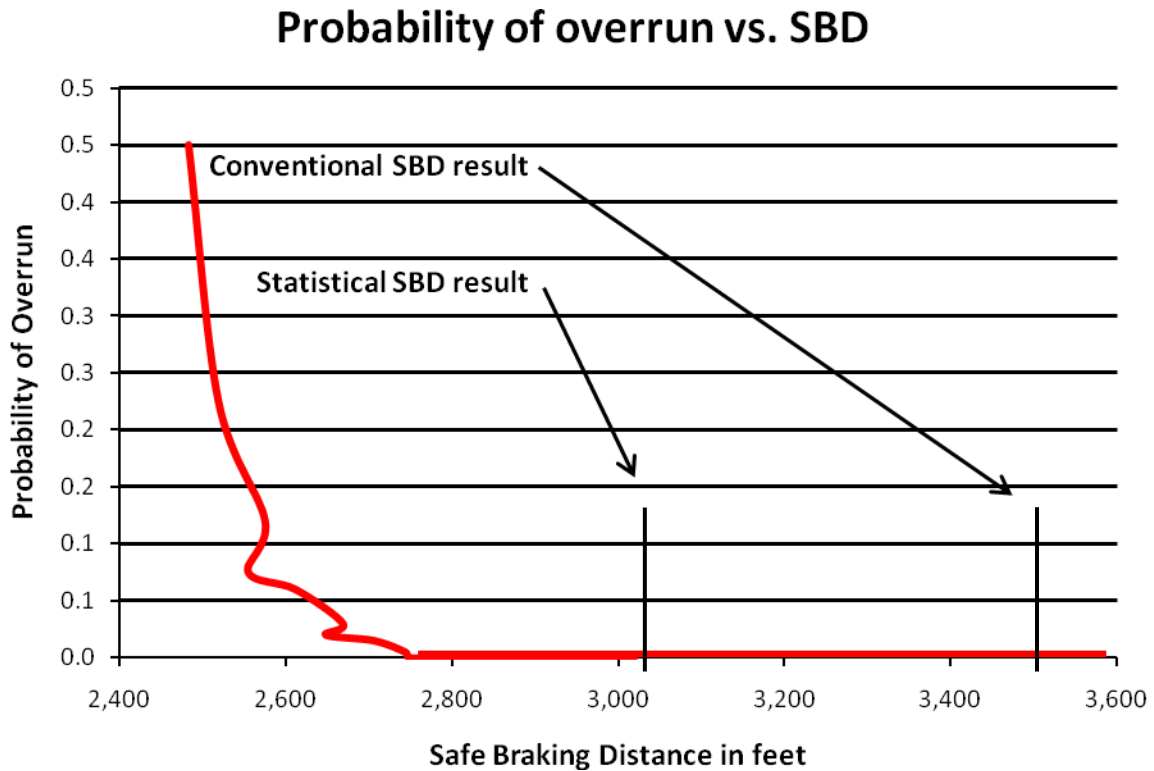
Figure 27, Graphical Results of the Statistical vs. Conventional SBD Calculation

The Figure clearly shows the while the statistical SBD result, which meets the

required level of safety of 5×10^{-10} from Equation 8, is significantly shorter that the SBD

from the conventional calculation using all worst case scenarios for each portion of the

IEEE model.

CHAPTER 6

6   ESTIMATED Approach for Braking Portion of SBD

6.1   Adhesion

The analysis from the previous chapter reduced the distances for the non braking

parameters A through G of the IEEE SBD model, but the remaining parameters that deal

with actual braking can also be reduced in terms of the systems approach. The IEEE

SBD model terms that have the largest impact on the required distance for any given

speed are Parts H and I. These terms represent the deceleration rate of the train once full

braking effect has been achieved. The maximum deceleration rate that a train can

generate from braking is limited to the adhesion between the wheel and rail.

Adhesion is part of a formula that relates vehicle weight with the force that is

applied to the wheel. This represents the highest level of force that can be applied before

wheel slip occurs [16].   As such, it is directly related to the coefficient of friction

between the wheel and rail. Wheel slip virtually eliminates the braking force applied to

the rail and significantly lengthens stopping distance from the difference in static and

dynamic friction forces[21]. Therefore, SBD calculations assume friction forces that are

low enough to not exceed the static values.

The model for adhesion is described as a function of the mass applied to each

wheel, and the prevailing coefficient of friction. Figure 28 shows the forces involved in

---

[21] Static friction is used for the case when both surfaces are traveling together. Dynamic friction is used
when the surfaces are in motion relative to each other such as when a wheel slips on the rail. The
coefficient of dynamic friction is always lower than that of static friction. SBD always is calculated in
terms of static friction as wheel slip creates several other affects that are undesirable for train operation.

this representation.   The braking force is that applied to the wheel through the braking system which is opposed by the friction forces between the wheel and the rail.
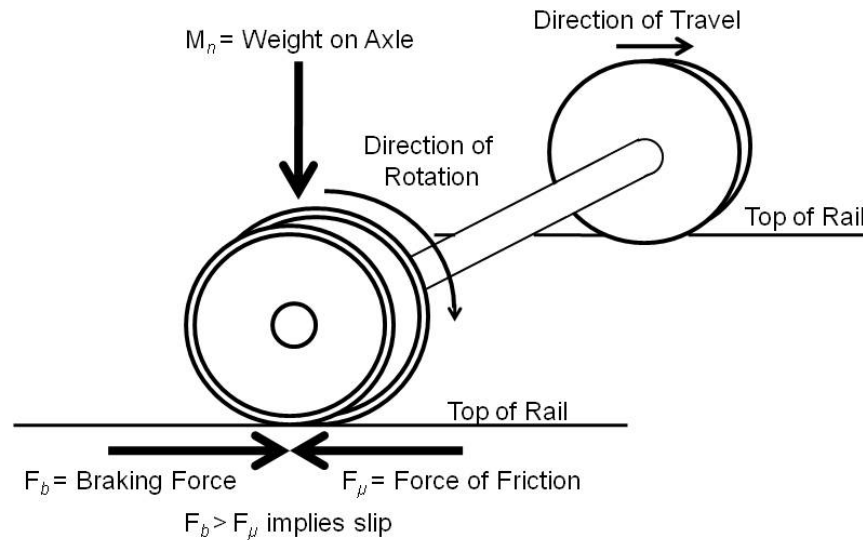
Figure 28, The Adhesion force Diagram

Padthe, Drincic, Oh, Rizos, Fassois, and Bernstein found that the adhesion model of a steel wheel on steel rail developed a hysteresis effect during successive traction/slip events [61], however for the purposes of SBD calculations, slip conditions are to be avoided to prevent long stopping distances and wheel damage. Train mass is time variant between stations due to passenger loadings, however when the train is operating this value does not change. Therefore the estimation of the coefficient of friction or adhesion is the only variable in stopping distance (part H and I of the IEEE model) that can change during train operation.

The next step is to derive equations to represent adhesion through parameters that are observed. The foundation of these equations is based on the laws of friction represented by:

$$F_b = \mu * M_n \qquad\qquad (9)$$

Where: F_b = Maximum braking force available in Pounds

μ = Adhesion Factor, and

M_n = Mass on each axle in Pounds

Therefore, the estimation of adhesion provides us with the maximum braking effort available to the train. This effort, typically expressed in Pounds of Force, can be found by using Train Performance Calculators[22] (TPCs) using train resistance formulas [16] to predict the distance traveled, time to reduce speed, and velocity of a decelerating train.

The adhesion estimation process in the proposed train control system is characterized by a real time calculation, assuming that the components of braking and adhesion (F_b and μ) vary as the train moves along the track. For the purposes of this research, train weight and available braking capacity are time invariant (that is, the brake system is uniformly capable of stopping the train).

Adhesion varies significantly from dry to wet to lubricated rail. Worst case scenarios for the design of SBD models cannot take into account the most severe conditions for fear of limiting system capacity to unacceptable levels for highly unlikely events. However, this risk does exist and represents times when rail conditions are extremely poor such as during the fall season where a thin film from crushed leaves is deposited on the top of the rail [44], [45], [46]. Another extreme condition would be

[22] Train Performance Calculators are simulation programs designed to predict train run times and reactions to changing conditions as the train moves on the track.

where trackside or vehicle mounted flange or Top of Rail (TOR) lubricators are

misadjusted [73]. These lubricators are used to extend the service life of the rail by

reducing friction forces that accelerate wear but can have detrimental effects for train

control system stopping distances, see Figure 29.

Figure 29, Typical rail lubrication in the field

Cocci, Presciani, Rindi and Volterrani [40] [41] extensively modeled the wheel

slip issue, but offered no solutions. Others have sprayed friction modifiers on the wheel

and rail in an attempt to raise adhesion with encouraging results [43]; however there are

practical limits to applying material to the rail continuously. High pressure detergent

solutions can be sprayed onto the railhead for short term relief from extreme conditions

where specific areas are known to present problems [44], [45], [46]. This technique is

costly and temporary in nature.

The data collected on various environmental conditions and the studies cited

indicate that contamination of the rail's running surface modifies adhesion. Quantifying

and measuring these contaminants provides a baseline for using contaminant levels alone as a way to determine the current adhesion level.

Despite these methods of adhesion control, variations continue to drive the traditional worst case approach to SBD to longer distances which lead to longer train spacing and lower system capacity. The proposed contaminant sensor, based on proven spectroscopic technology identifies known signatures of substances on the rail is shown below in Figure 30.
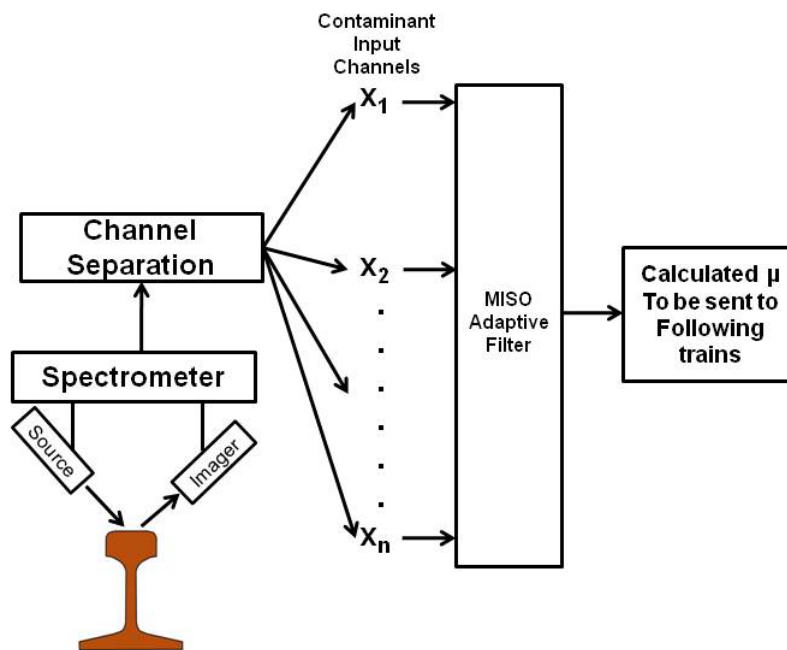
Figure 30, The proposed contaminant sensor layout

The signatures are isolated into separate channels that indicate the amount of contaminant present. Since each contaminant effects adhesion based in its level detected, each channel becomes an input to a Multiple Input Single Output (MISO) recursive least squares estimator (RLSE) that estimates the trains current adhesion.

The RLSE filter requires an observed output. This is found from the basic adhesion formula (Equation 9) using the direct measurement of train mass and the force applied at the wheel during high braking and acceleration levels as well as wheel slip events. This observed output is not continuous. However, the MISO filter produces it's own adaptive filter transfer function that is derived from the estimator. This new estimator can be used to bridge the gap between observations by estimating adhesion solely from the contaminant sample stream. Since train operation (particularly in Mass Transit) starts and stops in a frequent pattern, there are several opportunities to measure the adhesion under maximum braking and acceleration. Once the adhesion value is known on the train, this information is transmitted to following trains that combine this information about conditions ahead with the mass of the train to calculate the current stopping distance (parts H and I of the IEEE model). Combined with the calculated distances of parts A through G and J from chapter 5, a family of SBD calculations and probabilities representing stopping distance as a function of the probability of the train exceeding that distance is created. The minimum SBD required will have a probability that is less than that required for the desired level of safety.

The following sections describe the process and features of the adhesion estimation subsystem for the proposed train control system. The field conditions are described first, with a range and effect of differing adhesion. Sensor technology is then discussed, including experiments with conventional spectroscopic instruments. Finally, the RLSE is described in detail with simulated results using appropriate signals and additive noise.

6.2 Establishing Field Conditions

Previous field measurements used to analyze the non braking portion of the SBD model consisted of train data recorder output from actual in service train operation (chapter 5). Additional data channels on the same vehicles were used to evaluate the available adhesion. These additional channels included motor current (power and dynamic brake), Wheel Slip/slide, and Speed. In addition, weather data was either observed or obtained through weather services to correlate wheel slip patterns with wet (light to saturated conditions) rail as opposed to dry rail.

The data recorder provided a means to determine the braking and acceleration force applied to the wheel during station stops, wheel slip events and general train handling. From Equation 9, knowing the LRVs mass (which was assumed to be constant for this work, but could easily be measured in real time) [76] and this applied force yields the adhesion factor μ.

The data that creates this observed μ is available only when the train is in braking or accelerating. The proposed estimator is used to fill in these areas with adhesion values. This is why the proposed train control system requires contaminant based adhesion estimation.

The Figure 31 below illustrates a typical print out of the event recorder appropriate data channels turned on for the analysis. Underlying raw digital data values were also available that created the charts. Note the wheel slip exhibited in the highlighted area. Wheel slip occurs during both braking and acceleration, and both of

these conditions can be used to determine the available adhesion, along with braking and acceleration events throughout each run.

Data was collected from LRVs over several months. Additional archival event recorder downloads were available dating as far back as 2004.   All of the data was time stamped to allow for comparison to observed and historical weather data that was collected from the web at www.wunderground.com. There were sufficient areas of wheel slip on dry days to compare to wet days that showed how the lower adhesion affected operations.
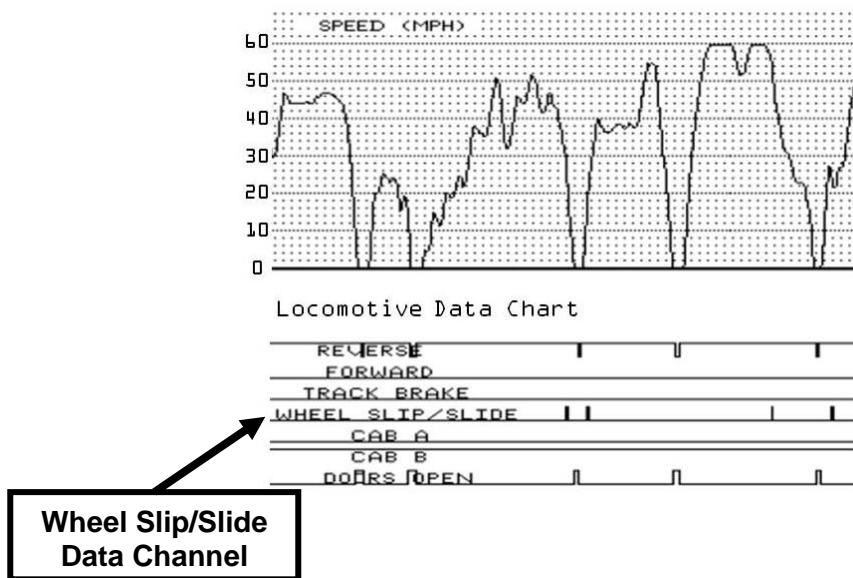
Figure 31, An example of wheel slip detected from event recorder data

Analysis of the data with full stop samples indicated that under dry rail conditions, trains decelerated to a stop at a rate of 2.2 mphps. However under wet rail conditions when there was a steady rain, the deceleration rate achieved without significant wheel slip dropped to 1.0 mphps. Although this was under a non-enforced condition (there was no enforcement in the train control), it reflects the desire of the

operator to operate the train without slipping. This has a significant impact on SBD for the Part H and I portion of the IEEE model. For example, stopping distance from 50 mph to stop with a 2.25 mphps rate is 815 feet, while the same train requires 1,833 feet to stop under the 1.0 mphps rate.

To show the dramatic effect this can have on SBD, for both dry and wet days, these rates of deceleration were used to calculate the distance for the IEEE model parts H and I.   Table 3 shows these values for three scenarios. The first row contains the values from the conventional worst case model. The second line represents the values from the statistical model of the IEEE parts A though G and SBD model and the stopping distance from the 1.0 mphps rate established for wet conditions on the rail. The third line incorporates all of the statistical data of the second row, but with the dry rail deceleration rate of 2.25 mphps. The table shows a dramatic difference in calculated SBD required under the different conditions.

Model Type		IEEE Model Component in feet									
	Deceleration Rate in mphps	A= Overspeed (entering Speed)	C= Free Running	D= Runaway	E= Propultion Removal	F= Dead Time	G= Brake Build Up	H+I= Overall Brake Rate	J= Overhang	Total SBD in Feet	Percent Improvement
Conventional Model	0.88	53	622	80	82	82	82	2567	15	3530	----
Model using wet deceleration	1	51	224	77	82	82	82	2138	15	2700	23.5%
Model with dry deceleration	2.25	51	224	77	82	82	82	950	15	1512	57.2%

Table 3, Typical SBD model comparison

6.3   Proposed Sensor Technology

The sensor technology applicable to help determine adhesion rates can be divided into two categories: Those that can detect adhesion limits after a wheel slip which are reactive sensors, and those that can detect adhesion limits before a wheel slip which are proactive sensors.

6.3.1   **Reactive Sensors**

Reactive sensors are in common use to control wheel slip on rail and transit vehicles. These sensor systems consist of axle or drive gear mounted optical tachometers that output a pulse stream whose frequency is proportional to train speed. Wheel slip occurs when the force applied to the wheel becomes greater that the static friction force between the wheel and rail. Therefore, at the moment wheel slip is detected by this system, the force applied at the wheel (motor current for acceleration or regenerative/dynamic braking or mechanical force applied to the wheel for deceleration) can be used to determine the maximum level of available adhesion from equation (9).

Axle tachometer devices can detect wheel slip by observing any quantum changes in the speed measurement. FFT techniques can also be applied to the signal can help determine speed changes that are simply too great for the available propulsion or braking system to achieve (implying wheel slip). Additional techniques for determining wheel slip include comparing wheel tachometer signals to other tachometers located on different axles, or to Doppler radar for an independent speed measurement.

Although these reactive sensors can provide invaluable data in determining areas of low adhesion, they are only effective in areas where braking or acceleration has occurred (areas that cause the reactive sensor to detect wheel slip). Therefore the information is incomplete and could miss areas of low adhesion that could impact the credibility of the SBD calculation. Such trains encountering these areas without prior knowledge operating under the assumption of normal or high adhesion would immediately be in a hazardous situation from operating with insufficient SBD. The

reduction in SBD distance of the IEEE model in part H and I would be inappropriate under these circumstances. However, these measurements can be very effective in confirming the proactive measurements described below as part of an adaptive filter.

6.3.2   Proactive Sensors

A proposed solution is to provide data on adhesion conditions utilizing a proactive sensor on each operating train along the entire route. The sensors would be train mounted on the wheel assembly known as a truck, and would be available to scan the top of rail continuously in time, in either direction, for contaminants that effect adhesion. The results are transmitted to all operating trains so they can calculate their SBD based on these parameters *before* the low adhesion conditions are encountered.

The contaminants present on the rail and wheel surface are either a substance applied to the rail, found along the right-of-way or surface oxidation of the rail steel [43], [77]. It is the substances rather than the oxidation being present on the rail or wheel that tends to decrease adhesion. By detecting these compounds on the rail or wheel surface, a better estimate of adhesion and maximum braking effort can be determined.

Surface contaminant detection methods not only find these contaminants, but they can determine their chemical makeup and concentration as well. For example, pharmaceutical facilities found that the Fourier Transform of reflective absorption from infrared spectroscopy found areas that contaminants could ruin production [50]. Liquid contaminants cause adhesion problems for rail operations as they act as lubricants between the rail and the wheel. These liquids can be found by similar methods to those described above [40].

There are several technologies available to use for the contaminant sensors. The research indicated that the most promising devices were standoff reflective spectrometers. These devices are becoming popular ensuring future availability, have been proven in harsh environments, and do not require direct contact with the sample to be effective. Fourier Transform Infrared (FTIR) is by far the most common in use. However, Ultraviolet spectrometers are also available [58].   In addition, these devices are used to detect improvised explosive devices in tests for the U.S. military [58], [78], [59] and [79]. In this application, the devices are mounted under military truck frames where they receive similar shock and vibration to that of a rail car.

Extensive work has been done to detect surface contaminants in military applications for chemical and biological weapons. These methods use a spectral analysis of Raman scatter from a reflected laser beam [53] [54].   Referred to as Laser Interrogation of Surface Agents (LISA), this technique employs properties useful in detecting rail surface qualities that effect adhesion and SBD. Raman spectroscopy utilizes laser light that interacts with the object with a corresponding change in energy that is reflected back. The scattering of the laser photons reveals several properties of the material the laser light is reflected from [80].

These devices not only detect the type of contaminant, but also the amount that is present [55], [79] and [81]. This feature can be used in sensing the amount of contaminants present for adhesion estimation. Level detection can be done in two ways. First, the sensitivity of the device can be adjusted to threshold levels that correlate a specific adhesion. Detection levels would be continuous over the range of expected

values of the containments. The second looks at the transmittance of the reflected laser source that is proportional to the level of contaminant present [56], [57].   The LISA work on Raman scatter spectroscopy mentioned above could be used in this approach. In fact, findings from research on field trials for these devices have provided accuracies approaching 7 mg/m^2 from a distance of one meter [78]. The sensor mounting on rail cars would be much closer, on the order of 8 or 9 inches. This allows the design of a sensor with much higher sensitivity. However, an actual experiment with these specific devices was beyond the means and scope of this research.

Scanning surfaces reveals concentrations of specific chemical molecule chains that provide unique signatures of various compounds. In the case of rail contamination, these compounds are known, and a library of these signatures can be generated to check against the data received from the sensors as the train runs along the track.

6.4   Spectroscopic Experiments

The theory of all spectrometer types has several basic commonalities. For example, they all use imagers that view reflected light from an illuminated area. To that end, it is possible to look at common laboratory spectrometers to test the ability of these devices to detect the more common contaminants that can affect adhesion. Conventional Fourier Transform Infrared (FTIR) spectroscopy was used in experiments to determine the quality and effectiveness of the technology on the contaminants.   For the purposes of experimenting with equipment capable of detecting the contaminants, this technology offers a low cost, accurate and proven method.

A steel angle was prepared as shown below in Figure 32 that was polished to simulate the top of rail in track. Preparation of the steel involved wire brushing the surface to remove all of the mill scale, then jewelers rouge and a high speed polishing tool was used to burnish the surface to a high gloss as would be found on the top of rail. The polishing compounds were then removed with a solvent wash. The surface was compared to laboratory samples of rail that was cut out of live track, and the two samples compared favorably in surface, color, and reflectivity. The experiment included analyzing the bare metal; along with contamination from known substances expected to be found on the rail head in the field.

Figure 32, Polished steel bar used in the initial experiments

In the experiment, polished steel (representing the head of a rail) is scanned to provide a baseline of dry rail. All scans were repeated and provided similar results as a check for repeatability. Subsequent measurements were made with the addition of contaminants found the field that included water (rain) and soy based grease used as a friction modifier from actual rail lubricators used in a transit system.

Figure 33, The laboratory FTIR set up to examine top of rail contaminants

A laboratory was established with a FTIR spectrophotometer, "rail" sample and instrumentation as shown in Figure 33. Each of these compounds was applied to a sample piece of steel in the laboratory to examine it with the spectrophotometer. This type of spectrometer uses a flat surface to contain the material to be tested with the light source and spectral sensor looking up from the bottom of the instrument. The steel sample that represented rail in the experiment was inverted and placed on the flat surface of the instrument. In the case where contaminants were introduced, the surface was coated and pressed against the flat surface. Thus, a thin, uniform film of contaminant was introduced.

Using spectrographic equipment involves comparing results of the output to a known library of material signatures. Elements and compounds absorb and reflect light in this process. The reflected spectrum indicates the chemical composition of the material under test.

Results from the tests comparing the baseline dry rail to various contaminated rail samples indicated that the spectrographs were able to easily detect these materials that can cause low adhesion. As shown in the Figures below, specific molecule chains of these contaminants indicate their presents in the experiment by the lower transmittance represented as dips in the output charts. The lower reading on the chart indicates the presents and the concentration of these compounds with specific signatures for the compounds of the samples. Lower readings (less transmittance in this case as the contaminant absorbs more light) from the spectrometer indicate higher concentrations of contaminant in the sample. The vertical scale was adjusted to better show the change in readings. These readings are directly related to the amount of contaminant and form the basis of the detection concentration scheme. This is how the LISA experiments referred to previously can determine concentrations of compounds and other materials associated with chemical and biological weapons. In the case if the military application, only very small amounts of material are detected to trigger alarms mounted on highway trucks [58], [59], and illustrates that the technology is rugged and robust enough to survive the rail car environment. Additionally, the equipment exhibited sampling time as low as 0.001 seconds which are sufficient as to prevent miss detection due to speed or vibration that could blur the image [59]. This is another important point in applying this technology to a rail car.

The first plot shown in Figure 34 is the spectrometer output for dry polished steel. It matches the results from having no sample in the FTIR instrument illustrating its highly reflective nature. This indicates that no contaminants are present, as expected.
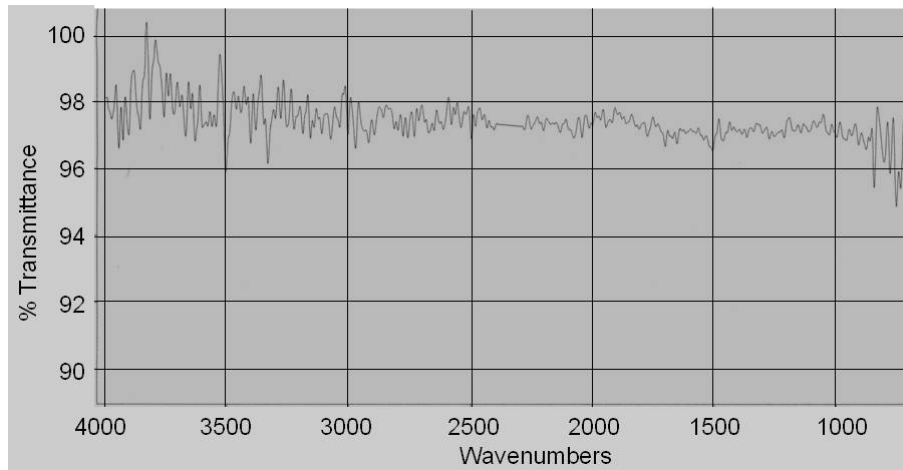
Figure 34, A spectrograph of a simulated polished rail surface.

The next step in the experiment was to perform the same analysis with

contaminated samples of the simulated rail.   First, water was used to wet the sample as it

was placed in the FTIR equipment. Water is expected to be the most common

contaminant due to rain and atmospheric moisture. As shown in the spectrograph below,

the water is clearly indicated as significant dips in the spectrum near the Oxygen-

Hydrogen resonance of Wavenumbers 3400 to 3200 and at 1600. The wavenumber in

spectroscopic parlance is the reciprocal of the received wavelength viewed by the CCD

imager in the spectrophotometer. Its units are in inverse nanometers.
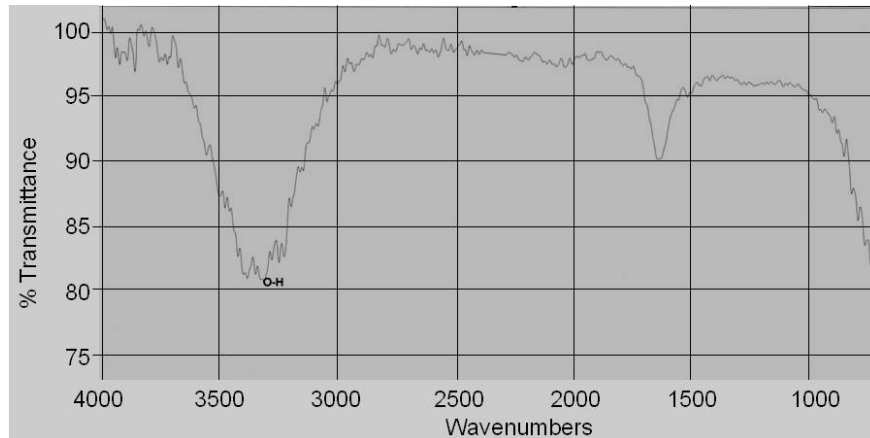
Figure 35, A spectrograph of the polished steel sample with water

A third test was similarly performed with the polished steel and grease. The grease was a soy based mixture that was an actual sample of rail lubricator grease used on an LRT operation. Rail lubricator grease can be used to prolong rail and wheel life as well as reduce noise associated with tight curves. As shown in the spectrograph of Figure 36 below, the soy based grease (soy based greases are becoming common because they are biodegradable) clearly shows as a significant dip in the spectrum near the resonance of the organic carbon chains characteristics of the soy at wavenumber 2923 and 1742. Other chains are evident as well that make up the signature for this compound, When introduces to the field, spectroscopic examination of the rail with correlation to this signature would indicate the presence and concentration of this compound.
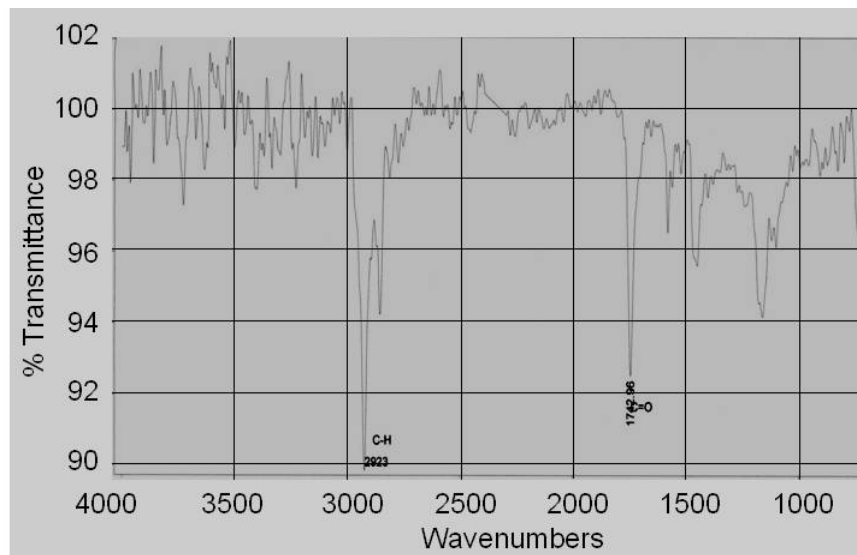
Figure 36, The spectrograph of the polished steel sample with grease

The results from the laboratory clearly showed that the contaminants could be easily found by commercial off-the-shelf equipment. It is also possible to measure the severity of the contamination from the spectrographs through the Bi-directional reflectance theories brought forth by Hapke and Clark and Roush [55], [56]. As the luminosity and distance to the area being examined are fixed (the rail near the wheel where the examination takes place is essentially stationary in the field of view of the spectrometer and lighting units provide constant illumination), the overall absorption of the each contaminant becomes a function of the amount of concentration on the rail. Thus it is possible to discriminate between levels up to saturation [82]. However, contaminant grain size plays a role in the reflective properties of the contaminant, and can cause errors using this method. This is particularly true of frost formation on the rail's surface.

For the specific case of a rail mounted sensor, the mean optical path of the reflected photos offers a solution to this problem. Clark and Roush found that comparing

the optical path provided consistent results in determining the abundance of surface contaminants for reflective spectroscopy. Their example utilized scatter from objects that were far greater that that proposed for the rail adhesion contaminant sensors, and proved that the mean optical path length was inversely proportional to the level of contamination. This is ideally suited to the proposed sensor as the conditions (length, illumination and optical quality) are all highly controlled.

Research conducted by the Transit Cooperative Research Program into ways to improve adhesion confirms that the presence and level of contaminants [75]. Their investigations into contaminants revealed a direct link in the level of contamination and the available adhesion level. Contaminants were examined in the laboratory with a Scanning Electron Microscope (SEM) and Fourier Transform Infrared Spectrometer. Concentrations of silica were found reflecting the use of sand to increase adhesion; however sand has abrasive qualities that increase wheel and rail wear by as much as 100 times the normal rate. This research also indicated that the adhesion levels deteriorated dramatically when moisture first appears on the rail head as it mixes with the other contaminants. Once the rail is cleaned from continued rain, the adhesion level rises to reflect the elimination of non water contaminants. Under these conditions, deceleration rates for transit vehicles were challenged to be greater than 1.86 mphps.

It was not be practical to install a spectrometer on a vehicle with the limited resources available; however this technology is adaptable for mounting on a railcar in a way similar to that shown in the Figure 37. This illustration shows a light source (the aluminum housing) with a CCD imager on a mounting rail attached to a rail vehicle truck

frame in use as a non contact rail wear and gage measurement system. This arrangement allows sensor mounting as close as eight inches above the rail, and survives the environmental conditions found under rail vehicles[23].
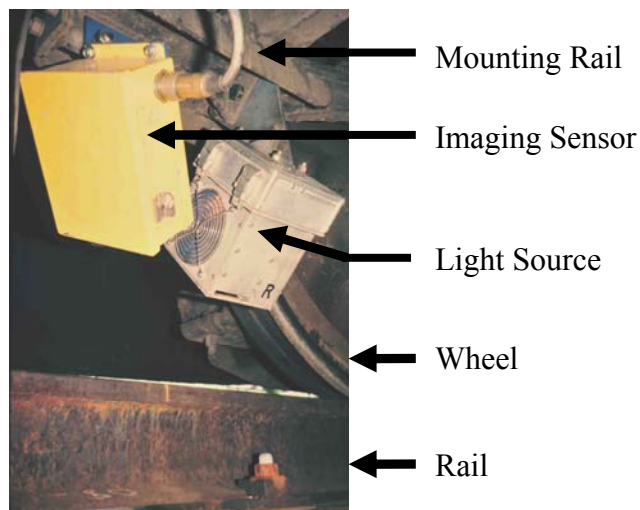
Figure 37, This illustrates a Typical mounting of Test Equipment on an Rail Vehicle

6.5   Estimation Methods for Adhesion

Each contaminant found contributes to the level of adhesion available to the train. The value is applied to inputs of the MISO filter. The calculation of adhesion based on various contaminant levels involves conditioning each contaminant input, and summing them. This allows the contaminant inputs to be arranged in a general equation shown below.

$$\mu = \sum_{j=1}^{k} c_j * x_j \qquad \qquad (10)$$

Where: μ = Estimated Adhesion

---

[23] The author experienced instrument mounting under rail cars while designing and installing non-contact track measuring systems on railroad track geometry inspection vehicles. Accelerations as high as 50 G can be seen here with a combination of rain and snow with temperature extremes from -40º F to +160º F.

c_j = calibrating coefficients,

x_j = conditioned contaminant strength, and

k = the number of contaminants

Contaminant levels would then be sampled as the train travels along the track. The coefficients can be established through empirical methods that compare a known level of adhesion to the level of contaminant found. Since the conditions over which these calculations are made can vary slowly with time from wheel wear, rail size and shape, and the cant/taper used[24], it is important to use a process that can adapt to these changes. The adhesion available to the train can be calculated from the force applied to the wheels immediately prior to incidents of wheel slip. However, slip does not occur at all times. This is the reason that an estimator is required to give a continuous adhesion result. Therefore the criteria for the estimator of adhesion includes the ability to operate on multiple inputs (the number of possible contaminants found on the rail), be computationally efficient so that it can be executed with limited processing available on board a train, and be able to operate on non continuous data.

Several models were considered for the estimation of adhesion, but a Multiple Input – Single Output (MISO) Adaptive filter was chosen as it meets all of the required criteria. The adaptive Recursive Least Squares Estimator (RLSE) filter is a real time algorithm that recalculates filter coefficients at every iteration [83]. RLSE filters are designed to minimize an underlying error correction equation that includes the error

---

[24] Rail is set in track with a specific "cant" or angle that is slightly rotated from level. Wheels have a "taper" to the tread to match rail cant to allow better ride quality and prevent wheels from hunting back and forth between the two rails [16].

signal from a variable filter and weighted previous results that are exponentially

decreased in effectiveness as subsequent data arrives in the input stream [84], [85], and

[86].
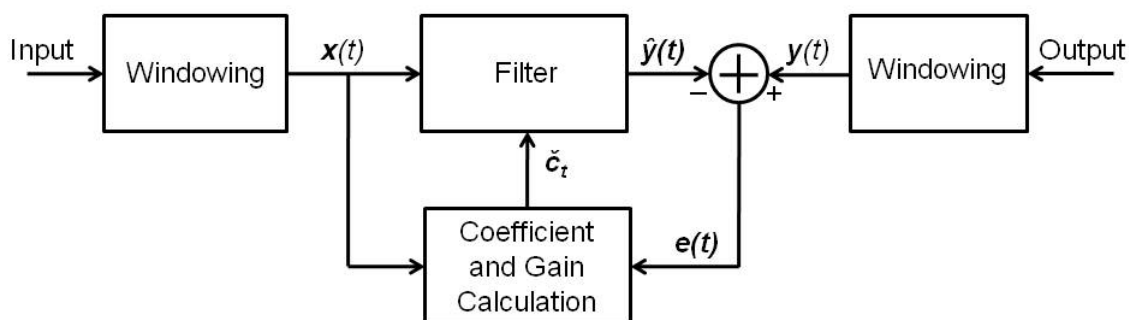
Figure 38, The Adaptive RLSE Filter Block Diagram

The basic block diagram of the adaptive RLSE filter is shown above in Figure 38.

It includes the unique feedback characteristic of this recursive process. For the proposed

RLSE filter, this represents one contaminant data stream. However, there will be

multiple contaminants included in the overall proposed adhesion estimator. The Multiple

Input Single Output (MISO) RSLE filter fits the requirements for the proposed system.

The model used to estimate adhesion is shown in Figure 39.
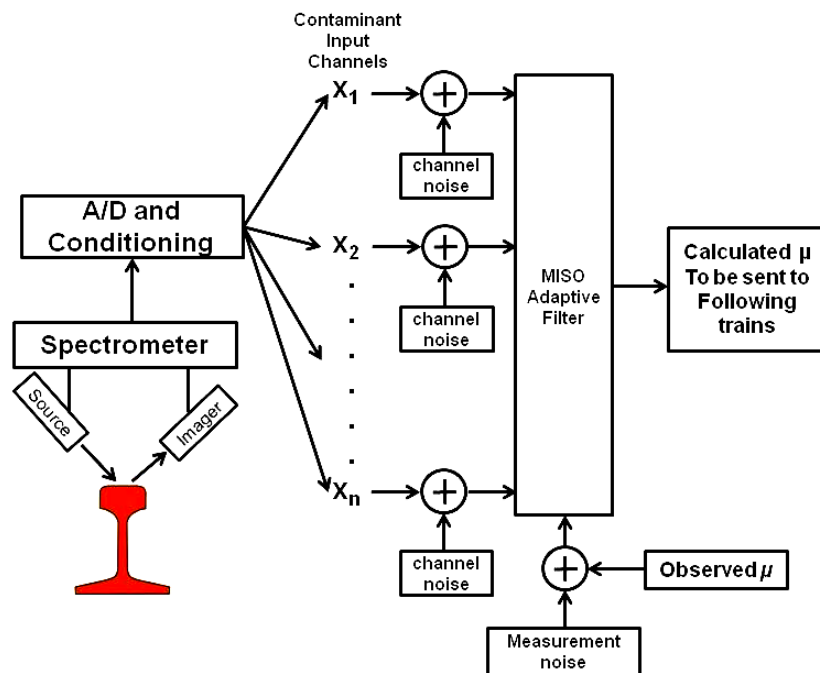
Figure 39, Adhesion System Model

The spectrometer is mounted on the unsprung portion of the rail vehicles' trucks so that it is within sight of the rail head at all times. Filtered output of the spectrometer is digitally converted and filtered to separate out each of the contaminant channels to be input into the MISO adaptive filter. The level is compared to known signatures of contaminants found.

To model the true response, each input channel is summed with additive noise that represents the spectral emission noise within the spectrometer as well as the quantization noise of the A/D converters. This is represented by values found in specification sheets and other references for spectrometers of this type [69], [70], [87], and [88]. Signal conditioning is also performed to prepare input channels for their contribution to the final adhesion output. This conditioning is actually the conversion of

raw channel values into a uniform scale from zero (no contaminant signature) to one (contaminant saturation).

The filter design equations for this example are represented as a vector whose elements are made up of the windowed sample stream as shown below;

$$e(t) = y(t) - \hat{y}(t) \tag{11}$$

$$\hat{y}(t) = c_1 x_1(t) + c_2 x_2(t) + \dots + c_n x_n(t) \tag{12}$$

Where; t = current time step,

$e(t)$ = error function,

$y(t)$ = measured output,

$\hat{y}(t)$ = filter output matrix,

c_n = coefficient vectors with n being the number of

contaminants, and

$x_n(t) = n^{th}$ sensor input at time t.

Therefore for the RLSE, the "cost" function Cost(C) to minimize is:

$$Cost(C) = \sum_{i=0}^{n-1} \lambda^i e^2(t - i) \tag{13}$$

Where:

λ = forgetting factor (a method of discounting older samples) and

$e^2(t\text{-}i)$ = Squared error function

Taking the derivative, and setting to zero to find the minimum:

$$\frac{\partial Cost(C)}{\partial C} = \sum_{i=0}^{n-1} \sum_{j=0}^{n-1} \lambda^i e(t - i) x_j(t - i) = 0 \tag{14}$$

Where n = The number of contaminants

Separating terms and substituting in Equation 11 provides:

$$\sum_{i=0}^{n-1} \lambda^i \left[y(t-i) - \hat{y}(t-i) \right] \sum_{j=0}^{k=1} x_j(t-i) = 0 \tag{15}$$

Further simplification yields:

$$\sum_{i=0}^{n-1} \lambda^i \sum_{j=0}^{k-1} x_j(t-1) \sum_{l=0}^{k-1} (t-i-l) x_j(t-i-l) = \sum_{i=0}^{n-1} \lambda^i y(t-i) \sum_{j=0}^{k-1} x_j(t-i) = 0 \tag{16}$$

This creates a set of equations for the RLSE to calculate the coefficients. For example, in the case of two sensor input streams ($i=0,1$) and three filter taps, the resulting field of equations can be shown as:

$$\lambda^0 \left[y_0(t)(c_0(t)x_0(t) + c_0(t-1)x_0(t-1) + c_0(t-2)x_0(t-2)) + \right.$$

$$\left. y_1(t)(c_1(t)x_1(t) + c_1(t-1)x_1(t-1) + c_1(t-2)x_1(t-2)) \right] +$$

$$\lambda^1 \left[y_0(t-1)(c_0(t-1)x_0(t-1) + c_0(t-2)x_0(t-2) + c_0(t-3)x_0(t-3)) + \right.$$

$$\left. y_1(t-1)(c_1(t-1)x_1(t-1) + c_1(t-2)x_1(t-2) + c_1(t-3)x_1(t-3)) \right] +$$

$$\lambda^2 \left[y_0(t-2)(c_0(t-2)x_0(t-2) + c_0(t-3)x_0(t-3) + c_0(t-4)x_0(t-4)) + \right.$$

$$\left. y_1(t-2)(c_1(t-2)x_1(t-2) + c_1(t-3)x_1(t-3) + c_1(t-4)x_1(t-4)) \right] + ... = 0 \tag{17}$$

The actual implementation of the MISO adaptive filter was carried out using Matlab®. The adaptive filters provided with the System Identification Toolbox from Matlab do not operate on MISO or MIMO models, but an alternate third party addition to that toolbox was found to be useful in modeling the adhesion system described above.

The University of Newcastle Identification Toolbox (UNIT) is such an add-on [66]. Developed at the University with supported from the Australian Research Council, this toolbox operates on both MISO and MIMO filters with a variety of algorithms. A

license was obtained and UNIT was used to analyze the adhesion model within the

Matlab environment. UNIT outputs can be plotted against input signals on a channel by

channel basis.

6.6   System Modeling with a MISO Adaptive Filter

Fabrication of the spectrometer, its associated hardware and field testing was not

possible with the limited resources available, so a MISO adaptive filter was tested using

real-life data and injected channel noise that simulates the inputs from these devices.

The adaptive filter requires an observed adhesion for which to construct the cost

model. This observed adhesion is actually the μ calculated from data on board the train.

The model used in this research used data from the same event recorder channels that was

used in the previous examples. The observed adhesion value was calculated from the

motor current used as a dynamic brake while the brake handle was in the 6th position or

higher[25] providing the force (F) acting on the train. The field data collected from the

LRV uses a "blended brake" to run the train. It is blended from the fact that the retarding

forces used for deceleration come from both the dynamic brake[26] and the traditional

friction brakes. All of the braking effort for deceleration at speeds above 15 mph is

derived from the dynamic brake, therefore monitoring this current effectively measures

the braking force applied to the LRV at these speeds. The conversion factor from Amps

---

[25] For the LRV used, the operating control used a single controller with 10 notches in motoring (acceleration) shown as P1 though P10 and 10 in braking shown as B1 to B10 with B10 the highest brake applied along with a Coast position.

[26] The dynamic brake reverses the traction motors geared to the axles and turns them into generators to resist motion whose load is dissipated into resistor banks. In electrified trains, current generated can be forced back into the traction power system to re-generate power into the system.

to Pounds of Force was calibrated with testing and acceptance of the LRV [89].

Conversely, current applied to the traction motors geared to the axles was also recorded

in the event recorder, and provides a measurement of the force applied to the wheel

during acceleration. Thus, adhesion can then be measured during both power and

braking modes on the LRV. Measurement noise that was within the range for

spectrographic devices was also added as in the model of figure 39 to simulate conditions

before being used by the adaptive filter. These values were the maximum value used

from instrument specification sheets. Measurement noise comes from two sources. The

first source is noise associated with the absorption of the emitted light on the rail. This

spectral noise is a function of the emitted wavelength (there is lower noise at higher

frequencies) and the angle of reflection [70], [88]. The other source is quantization

within the A/D converter of the device [69]. The modeled noise values were taken as

typical for the spectral devices and applied as shown in Figure 39.

There are two outputs of interest from the adaptive filter. The first is the

calculated adhesion coefficient. This is used in the cost function calculation and the

recursive algorithm to change the filter taps at each iteration of the filter. The second is a

transfer function for each input channel that can be used for calculating the adhesion

between observed samples. In essence, this creates an adhesion model that mimics the

adaptive filter. In between the direct observations of adhesion during braking and

acceleration, these transfer functions are used as the adhesion estimator acting on the

contaminant streams as shown in the Figure 40 below.
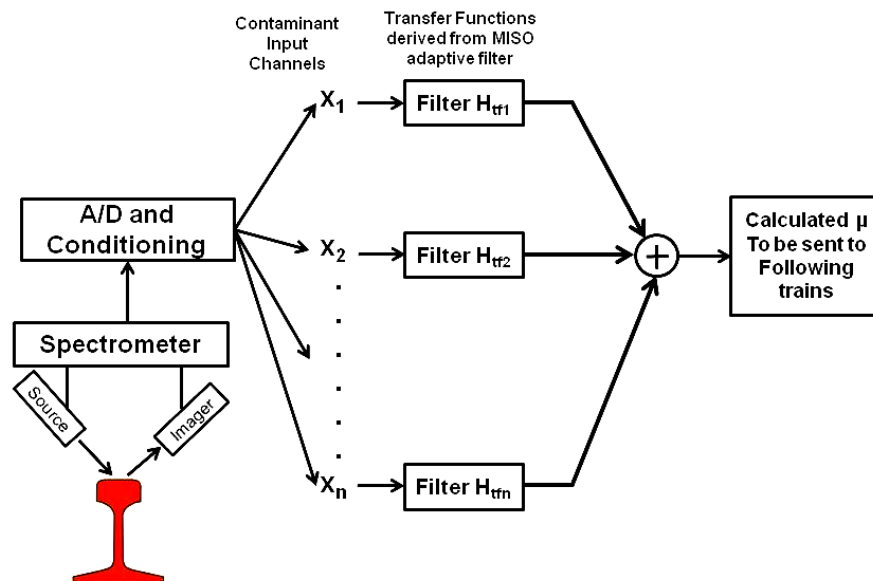
Figure 40, Adhesion Estimation from contaminant channels in between observations.

With the estimated solution of adhesion, the final step is the process of

determining the Part H and I braking from the equation of friction (9) in the beginning of

this chapter. Note that the adhesion used on board the train is actually the adhesion that

was transmitted from the train ahead, and is applied as in the proposed train control

system in Figure 17. The equation of friction is repeated here for convenience, and

includes adhesion, as well as the force applied to the train and it's mass.

$$F_b = \mu * M_n$$

    Where: F_b = Maximum braking force available

                      μ = Adhesion Factor, and

                      M_n = Mass associated with the axle

The mass of the train can be determined from either sensors on the suspension or

from known passenger loadings. For the example case of the LRT used in the baseline,

actual train weights were used to from the manufacturer to determine the amount of

optimization that occurred from the analysis [76] with the addition of a seated load representing a full train.   For the LRV used, the total weight was 22,455 pounds per axle. The data from the LRV event recorder was converted to force in pounds and these two values were used determine the observed adhesion from Equation (9) over several runs along the length of the line. The resultant force is the maximum available that can be applied in stopping the train before wheel slip occurs[27].

To provide for an optimized test, the averaged runs were grouped into two parts. The first part consisted of purely dry days where the rail was free from any water contaminants. The beginning of these runs also included a portion where flange lubricators were in use where the LRV alignment traveled through several sharp curves. The second part consisted of purely rainy days. This provided a saturated condition for the rail head where no additional water could be applied.   The two parts were spliced together to indicate an abrupt change in conditions as might be found when heavy rain would suddenly started.

The MISO adaptive filter was programmed in Matlab and all of the variables shown in Figure 39 including the random noise values for the contaminant streams and observed adhesion conditions. The contaminant stream consisted of values representative of sensor output under the grease, dry, and wet conditions; and the observed adhesion was derived from the LRV data described above.

---

[27] Wheel slip is to be avoided in SBD calculation for a number of reasons. First, the coefficient of dynamic friction is always less than that of static friction which results in longer stopping distances. Second is the fact that wheel slip implies sliding wheels along the rails. This causes slid flat spots on the wheels that are costly to eliminate and can cause severe impact stresses on the rail.

A Baseline Filter Output was created to filtered contaminant streams using filters designed to mimic the adaptive filter over the same range of input. It is a way of showing what is expected from the MISO filter in terms of the final output and helped in validating the overall system. The Matlab filter design tool was used to create simple low pass filters that were used in the baseline to compare the MISO output. The parameters were chosen based on a simple low pass filter as shown in Figure 41 below.
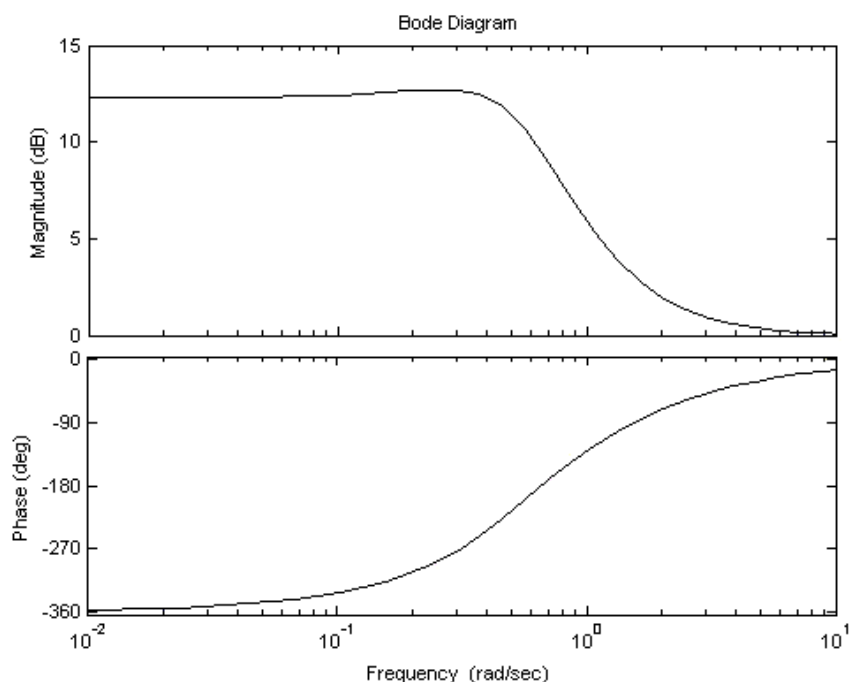
Figure 41, Comparison Filter Characteristics

The results of the MISO estimator are shown below in Figure 42 in terms of filter outputs. Shown in the figure are three plots superimposed onto the same axis. The Observed Adhesion (in blue) is the data input from the data recorder described above. The splice in the date can be clearly seen in the middle of the sample strings, and the dry adhesion values on the left are significantly greater that the wet values shown on the right. The extreme left reflects operation in city streets where rail contamination from

highway traffic and curve lubricators are used to prolong rail life in the presence of high
curvature of the track.

The Baseline Filter (in green) illustrates an output expectation based on fixed
filtering of the contaminant streams that also shows the changeover from differing
contaminant data.

The Estimated Filter Output (in red) consists of the same contaminant stream
filtered with the matrix transfer functions created by the MISO adaptive filter. This
output also tracks well with the observed adhesion and can be used as an effective
estimator in areas that do not have contiguous observations. The estimator used data
from the contaminant stream for the entire period. The MISO process actually had actual
observed data on average every 3,300 feet for which to use in the RLSE.
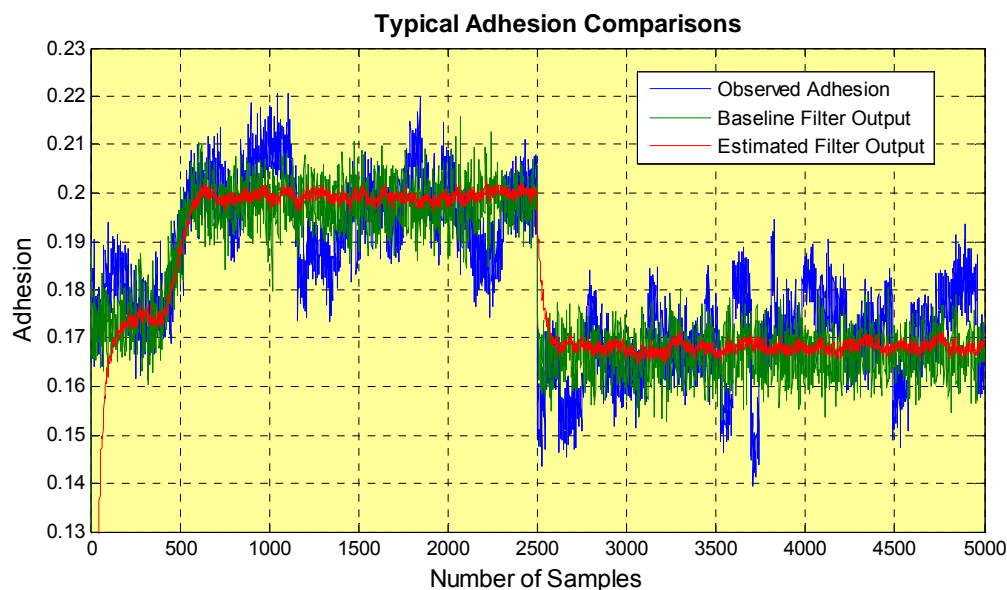
Figure 42, Adhesion value comparison of three methods.

The Estimated Filter Output represents the adhesion data that must be transmitted to following trains to be used in calculating their final SBD. The conversion to stopping distance for estimated adhesion is described next.

6.7   Adhesion and stopping distance results

The calculation of stopping distance with a known adhesion level involves two steps. The first is to convert the adhesion data received from the train ahead into a force that can be applied to reduce speed. This is the inverse of the process used on the train that originated the adhesion data, but with the mass of the following train.

With the force calculated adhesion data, this value is converted to stopping distance with the formula from Hay [16] derived from kinetic energy in classical mechanics (Force * Distance = ½ mass * velocity^2) as shown below.

$$Stopping_{dist} = \left(\frac{0.035 * M * V^2}{F_b} \right) \quad \text{(18)}$$

Where; M = Mass of the train in pounds,

V = Initial velocity in mph,

F_b = Maximum braking force available in pounds, and

0.035 = the conversion into working units

However, an important part of the process to determine stopping distance is to fully understand the underlying safety and expected accuracy of the calculation. In

addition, the sensitivity to input errors and noise needs to be modeled to determine the quality of the results. An analysis was performed to examine the expected ranges of error at the filter output with respect to the various noise levels. The source of these noise levels includes contributions from both the spectroscopic scatter and quantization noise from digitalization of the spectral signatures as noted previously [69], [70]. The noise was introduced into the system as random variable in the Matlab code.

The adhesion estimator provided over four thousand results to ensure a significant sampling of the outputs compared to the same process without noise. Each result that determined a stopping distance was entered into a table that listed the estimator result along with the result without noise. The next step was to utilize Equation 18 to determine the resulting stopping distance for each table entry. A constant LRV weight was used to provide uniform results throughout the test. For each entry of stopping distance, the additive noise created a difference in distance that the LRV would stop. This is the variation in stopping distance that is used to determine the likelihood of occurrence for each sample. The variations in stopping distances were collected into a histogram in the same way as the statistical analysis of parts a, c, and d of the IEEE SBD model discussed in section 5.2. As seen in Figure 43 below, the variation range largely from ±50 feet and are Gaussian with a mean of zero and a standard deviation of 20. This Gaussian curve is plotted over the histogram data for convenience in Figure 43.

Typical Stopping Distance Histogram
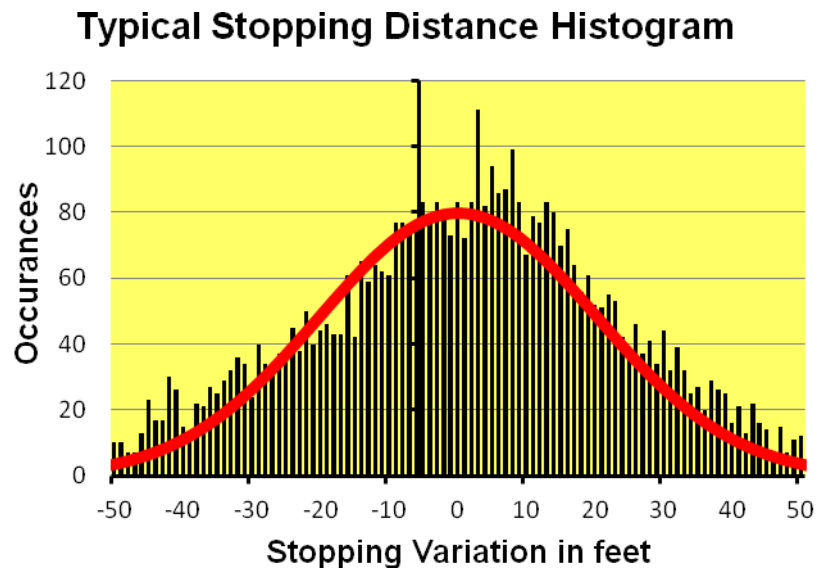
Figure 43, Stopping Distance variation with Gaussian distribution.

The histogram can be represented as a uniform series of uniformly spaced step

functions. This takes the form of a distribution of values that is described by each result

and its associated probability of occurrence. Shown below in Figure 44 is the

Cumulative Distribution Functions of stopping distance randomness.

$$F_x(x) = P(X(\xi) \le x) = \begin{cases} 1 & x \ge 50 \\ 0.833 & 25 \le x \le 50 \\ 0.5 & 0 \le x \le 25 \\ 0.166 & -25 \le x \le 0 \\ 0 & x < -25 \end{cases}$$
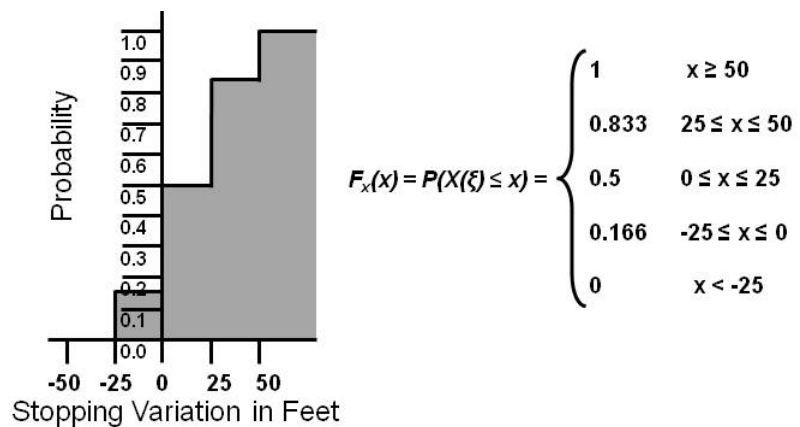
Figure 44, The CDF of stopping distances from the adhesion model

As in the statistical analysis from Chapter 5, the steps in the CDF are purposely

minimized to four steps so as to be handled within the limited processing power of the

train control processors on board the LRV.

Entry Speeds in mph	Probability $P(V_{H+1})$	Distance Offset in feet	Mean Stopping Distance in feet	Stopping Distance in feet
48	1.000	-25	408	383
48	0.833	0	408	408
48	0.500	25	408	433
48	0.166	50	408	458
49	1.000	-25	425	400
49	0.833	0	425	425
49	0.500	25	425	450
49	0.166	50	425	475
50	1.000	-25	443	418
50	0.833	0	443	443
50	0.500	25	443	468
50	0.166	50	443	493
51	1.000	-25	460	435
51	0.833	0	460	460
51	0.500	25	460	485
51	0.166	50	460	510
52	1.000	-25	479	454
52	0.833	0	479	479
52	0.500	25	479	504
52	0.166	50	479	529
53	1.000	-25	497	472
53	0.833	0	497	497
53	0.500	25	497	522
53	0.166	50	497	547

Table 4, Stopping distance results based on Adhesion estimation

Each stopping distance calculation carries with it a probability. These results are

shown above in Table 4, and are based on the values taken from the CDF. The different

entry speeds are the speeds encountered at the beginning of the SBD calculation from Table 2, the preliminary listing of calculated SBD values and their probabilities.

Table 4 also contains the range of actual stopping distances for the LRV once braking is established (parts Hand I of the IEEE SBD model). In chapter 5, all of the SBD model parts were analyzed for the LRT example except for parts H and I. H and I represent the actual stopping of the LRV once full braking is achieved. Table 4 fills in that portion of the model and allows for a complete statistical approach to SBD for every part and will be used to replace the fixed brake rate of 0.88 mphps and probability of 1 used in the preliminary results in Chapter 5 (the assumed guaranteed rate of deceleration along with the assurance that it will never be exceeded). Chapter 7 will describe the combined calculation that completes the analysis of the LRT example and illustrates the optimized SBD model.

CHAPTER 7

7   RESULTS AND CONCLUSIONS

7.1   Affects on Safe Braking Distance

The form of answer that was found for stopping distance based on adhesion levels is directly applicable to the previous analysis of the non braking portions of the SBD model. This allows a combination of both into a single list of SBD and associated probabilities that can be compared to the level of safety required that was calculated in Equation 8 of chapter 4.

The final listing of SBD distances with their associated probabilities is shown in the Table 5, below. Note that the SBD values have decreased significantly from their previous listing in table 2. This comes from the fact that in table 2, all of the stopping distances associated with part H and I were given the probability of 1 with an industry practice of 0.88 mphps constant value for distance. Table 5 modifies this by including the probability of stopping distances found from the adaptive filter that estimated the adhesion (and therefore optimized stopping distance). By utilizing the measured adhesion of a typical dry day, the adhesion available allows deceleration rates as high as 4.1 mphps. This value is well within the range of capability for transit vehicles, and allows for much shorter SBD calculations. As stated earlier, shorter SBD allows shorter headway between trains and more system capacity.

Parameters							Distance							
Overspeed		Reaction	Runaway Accel.	Brake Rate	Overhang	Combined Probability								
P(VA)	VA	P(VC)	P(VD-E-F-G)	P(VH+I)	J	P = (X(ξ) ≤ x)	DC	DD	DE	DF	DG	DH+I	DJ	DSBD
7.500E-01	49	6.000E-01	1.000E+00	1.000E+00	15	4.500E-01	215.5	71.9	71.9	71.9	71.1	365.00	15	882
7.500E-01	49	6.000E-01	1.000E+00	8.330E-01	15	3.748E-01	215.5	71.9	71.9	71.9	71.1	390.00	15	907
7.500E-01	49	3.000E-01	1.000E+00	1.000E+00	15	2.250E-01	251.4	71.9	71.9	71.9	71.1	365.00	15	918
7.500E-01	49	6.000E-01	1.000E+00	5.000E-01	15	2.250E-01	215.5	71.9	71.9	71.9	71.1	415.00	15	932
7.500E-01	49	3.000E-01	1.000E+00	8.330E-01	15	1.874E-01	251.4	71.9	71.9	71.9	71.1	390.00	15	943
2.000E-01	50	6.000E-01	1.000E+00	1.000E+00	15	1.200E-01	219.9	73.3	73.3	73.3	72.6	382.00	15	910
7.500E-01	49	3.000E-01	1.000E+00	5.000E-01	15	1.125E-01	251.4	71.9	71.9	71.9	71.1	415.00	15	968
2.000E-01	50	6.000E-01	1.000E+00	8.330E-01	15	9.996E-02	219.9	73.3	73.3	73.3	72.6	407.00	15	935
7.500E-01	49	1.000E-01	1.000E+00	1.000E+00	15	7.500E-02	287.3	71.9	71.9	71.9	71.1	365.00	15	954
7.500E-01	49	6.000E-01	1.000E+00	1.660E-01	15	7.470E-02	215.5	71.9	71.9	71.9	71.1	440.00	15	957
7.500E-01	49	1.000E-01	1.000E+00	8.330E-01	15	6.247E-02	287.3	71.9	71.9	71.9	71.1	390.00	15	979
2.000E-01	50	3.000E-01	1.000E+00	1.000E+00	15	6.000E-02	256.6	73.3	73.3	73.3	72.6	382.00	15	946
2.000E-01	50	6.000E-01	1.000E+00	5.000E-01	15	6.000E-02	219.9	73.3	73.3	73.3	72.6	432.00	15	960
2.000E-01	50	3.000E-01	1.000E+00	8.330E-01	15	4.998E-02	256.6	73.3	73.3	73.3	72.6	407.00	15	971
7.500E-01	49	1.000E-01	1.000E+00	5.000E-01	15	3.750E-02	287.3	71.9	71.9	71.9	71.1	415.00	15	1,004
7.500E-01	49	3.000E-01	1.000E+00	1.660E-01	15	3.735E-02	251.4	71.9	71.9	71.9	71.1	440.00	15	993
2.000E-01	50	3.000E-01	1.000E+00	5.000E-01	15	3.000E-02	256.6	73.3	73.3	73.3	72.6	432.00	15	996
5.000E-02	51	6.000E-01	1.000E+00	1.000E+00	15	3.000E-02	224.3	74.8	74.8	74.8	74.1	399.00	15	937
5.000E-02	51	6.000E-01	1.000E+00	8.330E-01	15	2.499E-02	224.3	74.8	74.8	74.8	74.1	424.00	15	962
2.000E-01	50	1.000E-01	1.000E+00	1.000E+00	15	2.000E-02	293.2	73.3	73.3	73.3	72.6	382.00	15	983
2.000E-01	50	6.000E-01	1.000E+00	1.660E-01	15	1.992E-02	219.9	73.3	73.3	73.3	72.6	457.00	15	985
2.000E-01	50	1.000E-01	1.000E+00	8.330E-01	15	1.666E-02	293.2	73.3	73.3	73.3	72.6	407.00	15	1,008
5.000E-02	51	3.000E-01	1.000E+00	1.000E+00	15	1.500E-02	261.7	74.8	74.8	74.8	74.1	399.00	15	974
5.000E-02	51	6.000E-01	1.000E+00	5.000E-01	15	1.500E-02	224.3	74.8	74.8	74.8	74.1	449.00	15	987
5.000E-02	51	3.000E-01	1.000E+00	8.330E-01	15	1.249E-02	261.7	74.8	74.8	74.8	74.1	424.00	15	999
7.500E-01	49	1.000E-01	1.000E+00	1.660E-01	15	1.245E-02	287.3	71.9	71.9	71.9	71.1	440.00	15	1,029
2.000E-01	50	1.000E-01	1.000E+00	5.000E-01	15	1.000E-02	293.2	73.3	73.3	73.3	72.6	432.00	15	1,033
2.000E-01	50	3.000E-01	1.000E+00	1.660E-01	15	9.960E-03	256.6	73.3	73.3	73.3	72.6	457.00	15	1,021
5.000E-02	51	3.000E-01	1.000E+00	5.000E-01	15	7.500E-03	261.7	74.8	74.8	74.8	74.1	449.00	15	1,024
5.000E-02	51	1.000E-01	1.000E+00	1.000E+00	15	5.000E-03	299.1	74.8	74.8	74.8	74.1	399.00	15	1,012
5.000E-02	51	6.000E-01	1.000E+00	1.660E-01	15	4.980E-03	224.3	74.8	74.8	74.8	74.1	474.00	15	1,012
5.000E-02	51	1.000E-01	1.000E+00	8.330E-01	15	4.165E-03	299.1	74.8	74.8	74.8	74.1	424.00	15	1,037
2.000E-01	50	1.000E-01	1.000E+00	1.660E-01	15	3.320E-03	293.2	73.3	73.3	73.3	72.6	457.00	15	1,058
5.000E-02	51	1.000E-01	1.000E+00	5.000E-01	15	2.500E-03	299.1	74.8	74.8	74.8	74.1	449.00	15	1,062
5.000E-02	51	3.000E-01	1.000E+00	1.660E-01	15	2.490E-03	261.7	74.8	74.8	74.8	74.1	474.00	15	1,049
5.000E-02	51	1.000E-01	1.000E+00	1.660E-01	15	8.300E-04	299.1	74.8	74.8	74.8	74.1	474.00	15	1,087
7.500E-01	49	6.000E-01	1.000E-07	1.000E+00	15	4.500E-08	215.5	73.3	77	76.3	75.5	416.00	15	949
7.500E-01	49	6.000E-01	1.000E-07	8.330E-01	15	3.749E-08	215.5	73.3	77	76.3	75.5	441.00	15	974
7.500E-01	49	3.000E-01	1.000E-07	1.000E+00	15	2.250E-08	251.4	73.3	77	76.3	75.5	416.00	15	985
7.500E-01	49	6.000E-01	1.000E-07	5.000E-01	15	2.250E-08	215.5	73.3	77	76.3	75.5	466.00	15	999
7.500E-01	49	3.000E-01	1.000E-07	8.330E-01	15	1.874E-08	251.4	73.3	77	76.3	75.5	441.00	15	1,010
2.000E-01	50	6.000E-01	1.000E-07	1.000E+00	15	1.200E-08	219.9	74.8	78.5	77.7	77	434.00	15	977
7.500E-01	49	3.000E-01	1.000E-07	5.000E-01	15	1.125E-08	251.4	73.3	77	76.3	75.5	466.00	15	1,035
2.000E-01	50	6.000E-01	1.000E-07	8.330E-01	15	9.996E-09	219.9	74.8	78.5	77.7	77	459.00	15	1,002
7.500E-01	49	1.000E-01	1.000E-07	1.000E+00	15	7.500E-09	287.3	73.3	77	76.3	75.5	416.00	15	1,020
7.500E-01	49	6.000E-01	1.000E-07	1.660E-01	15	7.470E-09	215.5	73.3	77	76.3	75.5	491.00	15	1,024
7.500E-01	49	1.000E-01	1.000E-07	8.330E-01	15	6.248E-09	287.3	73.3	77	76.3	75.5	441.00	15	1,045
2.000E-01	50	3.000E-01	1.000E-07	1.000E+00	15	6.000E-09	256.6	74.8	78.5	77.7	77	434.00	15	1,014
2.000E-01	50	6.000E-01	1.000E-07	5.000E-01	15	6.000E-09	219.9	74.8	78.5	77.7	77	484.00	15	1,027
2.000E-01	50	3.000E-01	1.000E-07	8.330E-01	15	4.998E-09	256.6	74.8	78.5	77.7	77	459.00	15	1,039
7.500E-01	49	1.000E-01	1.000E-07	5.000E-01	15	3.750E-09	287.3	73.3	77	76.3	75.5	466.00	15	1,070
7.500E-01	49	3.000E-01	1.000E-07	1.660E-01	15	3.735E-09	251.4	73.3	77	76.3	75.5	491.00	15	1,060
2.000E-01	50	3.000E-01	1.000E-07	5.000E-01	15	3.000E-09	256.6	74.8	78.5	77.7	77	484.00	15	1,064
5.000E-02	51	6.000E-01	1.000E-07	1.000E+00	15	3.000E-09	224.3	76.3	79.9	79.2	78.5	453.00	15	1,006
5.000E-02	51	6.000E-01	1.000E-07	8.330E-01	15	2.499E-09	224.3	76.3	79.9	79.2	78.5	478.00	15	1,031
2.000E-01	50	1.000E-01	1.000E-07	1.000E+00	15	2.000E-09	293.2	74.8	78.5	77.7	77	434.00	15	1,050
2.000E-01	50	6.000E-01	1.000E-07	1.660E-01	15	1.992E-09	219.9	74.8	78.5	77.7	77	509.00	15	1,052
2.000E-01	50	1.000E-01	1.000E-07	8.330E-01	15	1.666E-09	293.2	74.8	78.5	77.7	77	459.00	15	1,075
5.000E-02	51	3.000E-01	1.000E-07	1.000E+00	15	1.500E-09	261.7	76.3	79.9	79.2	78.5	453.00	15	1,044
5.000E-02	51	6.000E-01	1.000E-07	5.000E-01	15	1.500E-09	224.3	76.3	79.9	79.2	78.5	503.00	15	1,056
5.000E-02	51	3.000E-01	1.000E-07	8.330E-01	15	1.250E-09	261.7	76.3	79.9	79.2	78.5	478.00	15	1,069
7.500E-01	49	1.000E-01	1.000E-07	1.660E-01	15	1.245E-09	287.3	73.3	77	76.3	75.5	491.00	15	1,095
2.000E-01	50	1.000E-01	1.000E-07	5.000E-01	15	1.000E-09	293.2	74.8	78.5	77.7	77	484.00	15	1,100
2.000E-01	50	3.000E-01	1.000E-07	1.660E-01	15	9.960E-10	256.6	74.8	78.5	77.7	77	509.00	15	1,089
5.000E-02	51	3.000E-01	1.000E-07	5.000E-01	15	7.500E-10	261.7	76.3	79.9	79.2	78.5	503.00	15	1,094
5.000E-02	51	1.000E-01	1.000E-07	1.000E+00	15	5.000E-10	299.1	76.3	79.9	79.2	78.5	453.00	15	1,081
5.000E-02	51	6.000E-01	1.000E-07	1.660E-01	15	4.980E-10	224.3	76.3	79.9	79.2	78.5	528.00	15	1,081
5.000E-02	51	1.000E-01	1.000E-07	8.330E-01	15	4.165E-10	299.1	76.3	79.9	79.2	78.5	478.00	15	1,106
2.000E-01	50	1.000E-01	1.000E-07	1.660E-01	15	3.320E-10	293.2	74.8	78.5	77.7	77	509.00	15	1,125
5.000E-02	51	1.000E-01	1.000E-07	5.000E-01	15	2.500E-10	299.1	76.3	79.9	79.2	78.5	503.00	15	1,131
5.000E-02	**51**	**3.000E-01**	**1.000E-07**	**1.660E-01**	**15**	**2.490E-10**	**261.7**	**76.3**	**79.9**	**79.2**	**78.5**	**528.00**	**15**	**1,119**
5.000E-02	**51**	**1.000E-01**	**1.000E-07**	**1.660E-01**	**15**	**8.300E-11**	**299.1**	**76.3**	**79.9**	**79.2**	**78.5**	**528.00**	**15**	**1,156**

Table 5, listing of calculated stopping distances and their probabilities

Table 5 shows entries in red that provide the level of safety required in the LRT example with a significant decrease in distance needed to stop. Once known, this can be compared to traditional methods to understand the capacity increase that can result.

From the data shown above, the SBD that maintains the required level of safety of 5×10^{-10} is 1156'. This represents a reduction of 67% from the baseline example from chapter 3 with a corresponding increase in system capacity.

The SBD calculations used for both the base case and proposed approach clearly shows a decrease in distance required to provide the level of safety required. For the proposed methodology, there was improvement in both braking and non braking portions of the SBD calculation. In this analysis, the most significant contribution to savings was in the areas of runaway acceleration (part D) and stopping distance (parts H and I).

Each application of the method involves a review of issues concerning components and measurement of the parts involved. For the LRV case used in this analysis, specific failure modes were investigated to determine how these parts would interact. Included in this was that the probability of a runaway acceleration was very remote and would not significantly contribute to the SBD calculation. This differs greatly from the conventional worst case methods that would use all of the distance from a runaway acceleration incident with the maximum acceleration of the train at the exact time it would cause the greatest resulting stopping distance.

Reductions in part H and I of the model are possible only with advanced knowledge of the adhesion conditions. On board sensors alone cannot achieve this

decrease in SBD, and a complete systems approach of trains reporting adhesion conditions for use by following train movements is a unique way to fully optimize SBD and system capacity.

Precipitation is the most prevalent example of a contaminant. However the initial experiments showed that it is possible to differentiate between these contaminants and the level of contamination. This knowledge needs to be correlated to specific adhesion rates and specific train types for each application and property to be useful in SBD calculation.

7.2   Need for additional Research

The proposed train control system offers an optimization of SBD and capacity. Steps remaining in the in the process to fully realize these benefits require additional research and testing to include completing the field testing of portable spectroscopy equipment capable of being mounted on the train, as well as correlation to a complete library of contaminant signatures.

There are several other complimentary areas that can be investigated in the future that could enhance the results and provide useful data for a range of vehicle modes outside the traditional railroad applications. This is particularly true of the statistical approach detailed here.   The examples used in the analysis utilized a LRT operation that was in close proximity to the research. The techniques used to quantify performance improvements can easily be applied to a range of fixed guideway systems and railroad operations that should provide similar improvements. As seen in the examples of the IEEE 1698, each mode requires a unique perspective in terms of data acquisition and the type of train control applied.

Another step in optimizing SBD includes real time data to further qualify SBD model performance. For example, it is possible to measure the actual time and distance parameters for all of the parts of the IEEE SBD model. Replacing the modeled distance with the actual distance consumed by the train once it is known, allows updates to SBD eliminating the conservative nature of that model part. Any decrease in SBD can be used to provide additional safety for the system, or the applied brake rate in model parts I and H can be adjusted to provide a more precise stopping location for better ride quality. This feedback loop can be applied effectively in mass transit applications where precision stopping is required for station stops with platform screen doors, or limited platform length.

Optimizing system capacity is an important part of providing cost effective and convenient service on a rail line. It also promotes sustainability by increasing the effectiveness of rail and mass transit. The results of this research provide indications as to how optimized SBD can meet the goals of modern train control.

REFERENCES CITED

[1]   Richard Saunders, Jr., *Main Lines – Rebirth of the North American Railroads, 1970-2002*, DeKalb, Illinois: Northern Illinois University Press, 2003, ch 5 and 6, pp153-219.

[2]   AAR Railroad data books, 1930 thru 2010, available at http://pubs.aar.org/pubstores/

[3]   American Public Transit Association, Transit Ridership Reports by Quarter, 1996 through 2010. [Online}: available at www.apta.com.

[4]   David Thurston, *"Signaling and Capacity Through Computer Modeling"*, International Conference on Computer Modeling for Rail Operations, Delray Beach, Florida, February 26, 2004.

[5]   David Thurston, *"Capacity as a Driver for Selecting CBTC/PTC Train Control"*, Presented at the Sixth International Conference on Communications Based Train Control, Washington, D.C., 2005.

[6]   David Thurston, "*Analyzing a Modern Train Control System for SEPTA's Green Line"*, APTA Rapid Transit Conference, Atlanta, Georgia, 1996.

[7]   Everett Edgar King, Railway Signaling, New York, NY, McGraw-Hill, 1921.

[8]   Kendrick Bisset, Tony Rowbotham, David Thurston, Rob Burkhardt, Jeff Power, and Jim Hoelscher, *An Introduction to North American Railway Signaling*, Omaha, Nebraska: Simmons-Boardman, 2008.

[9]   Susanta Patra, "Worst-Case Software Safety Level for Braking Distance Algorithm of a Train", Silver Software, UK, IEEE Xplore web library.

[10]   Transport: Railways, "Tractive Effort, acceleration and braking", The Mathematical Association, 2004

[11]   *IEEE Guide for the Calculation of Braking Distances for Rail Transit Vehicles*, IEEE STD. 1698-2009, November, 2009.

[12]   Code of Federal Regulation, Part 49 232.103 Subpart e, no train shall move w/o 85% operative brakes.

[13]   Northeast Operating Rules Advisory Committee (NORAC) rules for the operation of trains on several railroads in the Northeast portion of the Unites States, Ninth Edition, April6, 2008.

[14]   General Code of Operating Rules (GCOR) rules for the operation of trains on virtually every railroad west of the Mississippi River, Sixth Edition, April 7, 2010.

[15]   Amtrak Braking Distance Standard Plan S-603 "Braking Distance Calculations", October 9, 1989, pp 4 – 7.

[16]   William W. Hay, Railroad Engineering, 2nd ed. New York: John Wiley and Sons, 1982, ch. 6, 9, 10, 11, 12, pp. 69-88, 140-147, 156-198.

[17]   Mick McDonald, "More Return on Investment – Capitalizing on under-utilized capabilities of Modern Equipment", *American Public Transit Association - Rail Conference*, San Francisco, CA, June 2, 2008

[18]   Pasi T. Lautala, "From Classroom to Rail Industry - A Rail Engineer in the Making", Proceedings of the American Railway Engineering and Maintenance of Way (AREMA) 2007 Annual Conference, Chicago, IL, September, 2007.

[19]   Code of Federal Regulation, Part 49 236.563 Subpart E – Automatic Train Stop, Train Control and Cab Signal Systems Standards, "Delay Time"

[20]   Mark Halinaty, Firth Whitwam, P.L. Chiu, Challenges of Implementing CBTC on an Existing Railway, *IRSE Technical Convention*, Singapore, 2005.

[21]   *IEEE Standard for Communications-Based Train Control Performance and Functional Requirements*, IEEE STD. 1474.1-2004

[22]   Bramen Adams and Rodney Hitt, *The Railroad Dictionary*, New York, NY, Railroad Age Gazette, 1907.

[23]   Steven McEvoy, *A Classic Railway Signal Tower*, West Chester: Instantpublisher, 2007, ch. 2 thru 5, pp. 29-60.

[24]   *IEEE Recommended Practice for the Determination of Safe Braking Distance in Fixed Guideway Land Transportation Systems*, P679.1/D1 (unpublished).

[25]   Jim Hall, Safety Recommendation from the National Transportation Safety Board
         concerning the NYCT accident on the Williamsburg Bridge – Reference R-96-22
         through -25 (and NTSB/RAR-96/03), NTSB, Washington, D.C., 1996.

[26]   B. Vincze, G. Tarnai, 2006, *"Development and Analysis of Train Brake Curve
         Calculation Methods with Complex Simulation"*, [Online], available:
         http://web.axelero.hu/egzo/doc/2006_elektro_brake_curve.pdf.

[27]   *Australian Rail Track Corporation Ltd Engineering Standard for Braking
         Distance*, ARTC Standard SDS-03, March 2005.

[28]   Xiangtao Zhuan, "Optimal Handling and Fault-Tolerant Speed Regulation of
         Heavy Haul Trains", PhD. Dissertation, Department of Built Environment and
         Information Technology, University of Pretoria, Pretoria, South Africa, October,
         2006.

[29]   Gintautas Bureika and Sarunas Mikaliunas, "Research on the Compatibility of the
         Calculation Methods of Rolling Stock Brakes", Transport 2008, 23(4), accepted
         October 2008, pp 351- 355.

[30]   Roger Short, "The Use and Misuse of SIL", *IRSE News*, Issue 142, pp 2-7,
         February, 2009.

[31]   R. J. Adduci, W. T. Hathaway, L. J. Meadow, "Hazard Analysis Guidelines for
         Transit Projects", U.S Dept. of Transportation, Research and Special Programs
         Administration, Cambridge, MA, DOT-VNTSC-FTA-00-01, January, 2000.

[32]   J. North, A. Fazio, and N. Shashidhara, "Probabilistic Approach to a Safe Braking
         Model for Light Rail", *3rd International Conference on Computer Modeling for
         Rail Operations*, Philadelphia, Pennsylvania, 2008.

[33]   Al Fazio, "Application of Cab Signals/ATC to LRT", Unpublished.

[34]   Al Fazio, *"Hudson Bergen Light Rail – A Review of Speed and Capacity
         Improvements at Hoboken Terminal"*, unpublished.

[35]   Ken Rodriguez, Vincent Ho, and Harry Burt, "Safe Braking of Light Rail
         Vehicles", *American Public Transit Association Rapid Transit Conference*,
         Proceedings Volume 2 – Rolling Stock, Washington, D.C., 1997.

[36]   Monica Malvezzi, Alain Bonnet, Cliff Cork, Robert Karbstein, Paolo Presciani,
         November, 2006, *A Numerical Model for the Probabilistic Analysis of Braking
         Performance in Railways,* [online]. Avalable:
         http://www.grrt.fr/html/travaux/download.php?filename=214malvezzi.pdf.

[37]   David Barney, David Haley and George Nikandros, Calculating Train Braking Distance, 6th Australian Workshop on Safety Critical Systems and Software (SCS'01) – Conferences in Research and Practice in Information Technology, Vol 3. P. Lindsay, Ed., Brisbane, Australia, 2001.

[38]   David Thurston, Parsons Corporation and Temple University, "Beyond Adaptive Braking", 2010 Joint Rail Conference (IEEE, ASME, ASCE), Urbana, Illinois, April 29, 2010.

[39]   Bill Moore Ede, Scientist, Alan Polivka, Assistant Vice-President, Joe Brosseau, Senior Engineer, Communications & Train Control, TTCI, Yan Tse, Program Manager Federal Railroad Administration, Al Reinschmidt, Vice-President – Commercial Programs, TTCI, "Improving Enforcement Algorithms for Communications-Based Train Control using Adaptive Methods", 9th International Heavy Haul Conference, Shanghai, China, June 22 - 24, 2009.

[40]   M. Malvezzi, B. Allotta, and A. Rindi, "Simulation of Degraded Adhesion Conditions on a Full Scale Locomotive Roller Rig", *12th IFToMM World Congress*, Besancon, France, June 18-21, 2007.

[41]   G. Cocci, P. Presciani, A. Rindi, and G.P.J. Volterrani, "Railway Wagon Model with Anti-Slip Braking System", *16th European MDI User Conference*, Berchtesgaden, Germany, November 14-15, 2001.

[42]   Brian Armstrong and Qunyi Chen, *"The Z-Properties Chart"*, IEEE Control Systems Magazine, October 2008.

[43]   G. Vasic, F. J. Franklin, A. Kapoor, "New Rail Materials and Coatings", The Railway Safety Standards Board (University of Sheffield, UK), Report Number RRUK/A2/1, July, 2003.

[44]   Autumn Leaves Provide Tricks but no Treats for Metro-North, Metro-North Railroad press release, October 11, 2007.

[45]   F. W. Lipfert, Engineering proposal titled: "Proposal for a Study of Reduced Wheel/Rail Adhesion on the MTA/Metro-North Railroad, December, 2003.

[46]   SEPTA Leaf Grief, Southeastern Pennsylvania Transportation Authority press release, October 19, 2006.

[47]   J. J. Kalker, "On Rolling Contact of Two Elastic Bodies in the Presence of Dry Friction". PhD Dissertation, Laboratory of Engineering Mechanics, Department of Mechanical Engineering, Delft University of Technology, The Netherlands, August, 1973.

[48]   J. Yu, T.X. Mei, D.A. Wilson, 2006, *Re-adhesion control based on wheel Set dynamics in railway traction system, UKACC Control 2006*

[49]   Sung Hwan Park, Jong Shik Kim, Jeong Ju Choi, and Hiro-O Yamazaki, *"Modeling and Control of Adhesion Force in Railway Rolling Stocks"*, IEEE Control Systems Magazine, October 2008.

[50]   Michelle Hamilton, "Application of grazing-angle reflection absorption Fourier transform infrared spectroscopy to the analysis of surface contamination", PhD dissertation, Chemistry Dept., University of Canterbury, Christchurch, New Zealand, 2007.

[51]   Roland Harig, Rene Braun, Chris Dyer, Chris Howle, Benjamin Truscott, "Short Range Remote Detection of Liquid Surface Contamination by Active Imaging Fourier Transform Spectrometry", *Optics Express*, vol. 16, no. 8, April 14, 2008.

[52]   Michael W. P. Petryk, "Promising Spectroscopic Techniques for the Portable Detection of Condensed-Phase Contaminants on Surfaces", Applied Spectroscopy Reviews, Vol. 42, pages 287-343, February, 2007.

[53]   T. H. Chyba, N. S. Higdon, W. T. Armstrong, C. T. Lobb, D. A. Richer, P. L. Ponsardin, B. P. Kelly, Q. Bui, R. Babnick, W. Marsh, "LASER Interrogation of Surface Agenta (LISA) for Standoff Sensing of Chemical Agents", 21st International Laser Radar Conference (ILRC), Quebec,, Canada, November, 2002.

[54]   Aurthur J. Sedlacek, III, Mark D. Ray, "Short-range, Non-contact Detection of Surface Contamination Using Raman Lidar", SPIE vol. 4577, Boston, Massachusetts, November, 2001.

[55]   Roger N. Clark and Ted L. Roush,"Reflective Spectroscopy: Quantitative Analysis Techniques for Remote Sensing Applications", Journal of Geophysical Research, Vol. 89, No. B7, pages 6329-6340, July, 10, 1984.

[56]   B. Hapke, Bidirectional Reflectance Spectroscopy, 1: Theory, Journal of Geophysical Resources, Volume 86, pp 3039-3054, 1981

[57]   B. Hapke and E. Wells, Reflectance Spectroscopy, 2: Experiments and observations, Journal of Geophysical Resources Volume 86, pp 3055-3060, 1981.

[58]   Steven Christesen, Kristina Gonser, J. Michael Lochner, Arthur Sedlaecek, Thomas Chyba, Daniel Sink, Jay Pendell Jones, Bennett Corrado, and Andrew Slaterbeck, "UV Raman Detection of Chemical Agents", Proceedings for the Army Science Conference (24th), Orlando, FL, December, 2005.

[59]   Thomas Chyba, N. Scott Higdon, Wayne T. Armstrong, C. Ted Lobb, Patrick L. Ponsardin, Dale A. Richter, Brian T. Kelly, Quang Bui, Robert Babnick, Marc Boysworth, Arthur Sedlacek, and Steven D. Christesen, "Field Tests of the LASER Interrogation of Surface Agents (LISA) System for On-The-Move Standoff Sensing of Chemical Agents", AMD001523, July 1, 2003.

[60]   Jorge Nocedal and Stephen Wright, Numerical Optimization. New York, Springer, 1999.

[61]   Ashwani Padthe, Bojana Drincic, Jinhyoung Oh, Demosthenis Rizos, Spilios Fassois, and Dennis Bernstein, *"Duhem Modeling of Friction-Induced Hysteresis"*, IEEE Control Systems Magazine, October 2008.

[62]   HyunWppk Lee, Corina Sandu, and Carvel Holton, Railway Technology Laboratory – Center for Vehicle System Safety, Virginia Polytechnic Institute and State University at Blacksburg, VA., "Wheel-Rail Dynamic Model and Stocastic Analysis of the Friction in the Contact Patch", 2010 Joint Rail Conference (IEEE, ASME, ASCE), Urbana, Illinois, April 29, 2010.

[63]   Lili Han, Jie Sheng, Feng Ding and Yang Shi, "Recursive Least Squares Identification for Multirate Multi-Input Single-Output Systems, 2009 American Control Conference, St. Louis, MO, USA, June 10-12, 2009.

[64]   Xi Chen, "Recursive Least-Squares Method with Membership Functions, Proceedings of the Third International Conference on Machine Learning and Cybernetics, Shanghai, China, August 2004.

[65]   Erkan Kaplanoğlu, Koray K. Şafak, H. Selçuk Varol, "Real-Time Parameter Estimation of a MIMO System", Proceedings of the International MultiConference of Engineers and Computer Scientists 2008 Vol. II, IMECS 2008, Hong Kong, 19-21 March, 2008.

[66]   Adrian Wills, Brett Ninness, Stuart Gibson, "An Identification Toolbox for Profiling Novel Techniques", Published by the University of New Castle, Australia and supported by the Australian Research Council. http://www.ee.newcastle.edu.au/reports/EE06029.pdf.

[67]   Dr. Sudhir Kumar, Principal Investigator, "Improved Methods for Increasing Wheel/Rail Adhesion in the Presence of Natural Contaminants", Transportation Research Board of the National Academies of Science Research Results Digest, No. 17, May, 1997.

[68]   Ryan M. Flaherty, "A Comparison of Spectrometers: StellarNet, Inc vs. the Competition", Extreme Spectroscopy Solutions, Tampa, FL, http://www.stellarnet-inc.com/public/download/StellarNetFeatures.pdf.

[69]   Anthony Kearsey, Richard Barnard, Yutheeka Gadhyan, Youzuo Lin, Lin Tong, Jiaping Wang, Guangjin Zhong, "Modeling the Background Noise in a Mass Spectrometer for Denoising Applications", http://ima.umn.edu/2007-2008/MM8.6-15.08/activities/Kearsley-Anthony/master.pdf

[70]   ChunMin Zhang, BaoChang Zhao, ZhiLin Yuan, and Weioian Huang, "Analysis of Signal-to-Noise Ratio of an Ultra-Compact Static Polarization Interference Imaging Spectrometer", Journal of Optics A:Pure and Applied Optics, May 8, 2009.

[71]   Peter Wigger and Rüdiger vom Hövel, Safety Assessment – Application of CENELEC Standards – Experience and Outlook, *Copenhagen Metro Inauguration Seminar*, Copenhagen, Denmark, November 21-22, 2002.

[72]   Office of Technology Assessment and the Urban Mass Transit Advisory Panel, Automatic Train Control in Rail Rapid Transit, Washington, D.C., NTIS order #PB-254738, May, 1976.

[73]   Robert J. Kosinski, A Literature Review on Reaction Time, Clemson University, Clemson, S.C., September, 2010 (http://biae.clemson.edu/bpc/bp/Lab/110/reaction.htm).

[74]   W. Ian Hamilton and Teresa Clarke, "Driver Performance Modeling and its Practical Application to Railway Safety", Elsevier: Applied Ergonomics, July 7, 2005.

[75]   Richard P. Reiff, Nicholas Ruud, and Semih F. Kalay, Transportation Test Center, Inc., TCRB Report 71, Track Related Research – "Friction Control Methods Used by the Transit Industry", Washington, D.C., 2005.

[76]   Stadler Rail AG vehicle information for GTW 2/6 Low Floor articulated Diesel Multiple Unit information cut sheet available at: http://www.stadlerrail.com/media/uploads/factsheets/GTW_SNJ_en.pdf

[77]   Scott Gage, Association of American Railroads - Transportation Test Center, "Metrolink Loss of Shunt", Unpublished Letter Report to Metrolink on rail contaminants, April, 1995.

[78]   Aurthur J. Sedlacek III, Mark D. Ray, N. S. Higdon, and D. A. Richer, "Short-Range, Non Contact Detection of Surface Contamination Using Raman Lidar", Proceedings of SPIE, 4577, 95-104, 2001.

[79]   Emily Meyer, and Benjamin Ervin, "Standoff Detection of Persistent Chemical Agents on Surfaces, Chemical and Biological Defense Science and Technology Conference, November 18, 2010.

[80]   P. Vandenabeele and L. Moens, Department of Analytical Chemistry, Ghent University, Proefluinstraat 86, 9000 Ghent, Belgium, "Introducing Students to Raman Spectroscopy", Published on line via Springer-Verlag, March 2, 2006.

[81]   Application Note from Evans Analytical Group, AN 363 TXRF and SURFACESIMS.XP The Total Solution for Surface Contamination Measurements, V.3, May 7, 2007.

[82]   Ming Wu, Mark Ray, K. Hang Fung, Mark W. Ruckman, David Harder, and Arthur J. Sedlacek , Applied Spectroscopy, Vol. 54, Issue 6, pp. 800-806 (2000)

[83]   Dimitris Manolakis, Vinay Ingle, and Stephen Kogen, Statistical and Adaptive Signal Processing, Boston: McGraw Hill, 2000, ch. 8and 10, pp. 395-438, 548-560.

[84]   Sanjit Mitra, Digital Signal Processing – a Computer Based Approach, 3rd ed., Boston: McGraw Hill, 2006, pp. 514-515.

[85]   Bernard Widrow, Eugene Walach, Senior Editors, Adaptive Inverse Control: A Signal Processing Approach, Reissue Edition, The Institute of Electrical and Electronic Engineers, 2008.

[86]   Bernard Widrow and Eugene Walach, Adaptive Inverse Control, Reissue Edition, Piscataway, NJ,: IEEE Press, 2008, ch. 10, pp. 270-302.

[87]   Peter Werle and Franz Slemr, "Signal-to-Noise Ratio Analysis in Laser Absorption Spectrometers Uing Optical Multipass Cells", Applied Optices, Vol 30 No. 4, February 1, 1991.

[88]   Engineering Note – "Spectrometer Signal-to-Noise and Dynamic Range Comparison", Ocean Optics, Inc., Number 211-00000-000-04-1206, December 4, 2006.

[89]   Quantum Engineering Drawing C1088 Revision F, "SNJLRT Recorder Installation", October 18, 1999.

SELECTED BIBLIOGRAPHY

AAR Railroad data books, 1930 thru 2005, available at http://pubs.aar.org/pubstores/

Adams, Bramen and Hitt, Rodney, *The Railroad Dictionary*, New York, NY, Railroad Age Gazette, 1907.

Adduci, R. J.; Hathaway, W. T.; Meadow, L. J., "Hazard Analysis Guidelines for Transit Projects", U.S Dept. of Transportation, Research and Special Programs Administration, Cambridge, MA, DOT-VNTSC-FTA-00-01, January, 2000.

American Public Transit Association, Transit Ridership Reports by Quarter, 1996 through 2008. [Online}: available at www.apta.com.

Amtrak Braking Distance Standard Plan S-603 "Braking Distance Calculations", October 9, 1989, pp 4 – 7.

Armstrong, Brian and Chen, Qunyi, *"The Z-Properties Chart"*, IEEE Control Systems Magazine, October 2008.

Australian Rail Track Corporation Ltd Engineering Standard for Braking Distance, ARTC Standard SDS-03, March 2005.

Autumn Leaves Provide Tricks but no Treats for Metro-North, Metro-North Railroad press release, October 11, 2007.

Barney, David; Hanley, David and Nikandros George, Calculating Train Braking Distance, 6th Australian Workshop on Safety Critical Systems and Software (SCS'01) – Conferences in Research and Practice in Information Technology, Vol 3. P. Lindsay, Ed., Brisbane, Australia, 2001.

Bisset, Kendrick; Rowbotham, Tony; Thurston, David; Burkhardt, Rob; Power, Jeff; and Hoelscher, Jim, *An Introduction to North American Railway Signaling*, Omaha, Nebraska: Simmons-Boardman, 2008.

Christesen, Steven; Goner, Kristina; Lochner, J. Michael; Sedlaecek, Arthur; Chyba, Thomas; Sink,Daniel; Pendell, Jay; Bennet, Jones;, and Slaterbeck, Andrew; "UV Raman Detection of Chemical Agents", Proceedings for the Army Science Conference (24th), Orlando, FL, December, 2005.

Chyba, Thomas; Higdon, N. Scott; Armstrong,Wayne T.; C.; Lobb, Ted; Ponsardin, Patrick L.; Richter, Dale A.; Kelly, Brian T.; Bui, Quang; Babnick, Robert; Boysworth,

Marc; Sedlacek, Arthur and Christesen, Steven D.; "Field Tests of the LASER Interrogation of Surface Agents (LISA) System for On-The-Move Standoff Sensing of Chemical Agents", AMD001523, July 1, 2003.

Clark, Roger N. and Roush, Ted L., "Reflective Spectroscopy: Quantitative Analysis Techniques for Remote Sensing Applications", Journal of Geophysical Research, Vol. 89, No. B7, pages 6329-6340, July, 10, 1984.

Cocci, G.; Presciani, P.; Rindi, A.; and Volterrani, P.J., "Railway Wagon Model with Anti-Slip Braking System", *16th European MDI User Conference*, Berchtesgaden, Germany, November 14-15, 2001.

Code of Federal Regulation, Part 49 236.563 Subpart E – Automatic Train Stop, Train Control and Cab Signal Systems Standards, "Delay Time"

Code of Federal Regulation, Part 49 232.103 Subpart e, no train shall move w/o 85% operative brakes.

Chen, Xi, "Recursive Least-Squares Method with Membership Functions, Proceedings of the Third International Conference on Machine Learning and Cybernetics, Shanghai, China, August 2004.

Chyba, T. H.; Higdon, N. S.; Armstrong, W. T.; Lobb, C. T.; Richer, D. A.; Ponsardin, P. L.; Kelly, B. P.; Babnick, Q. Bui, R.; and March, W., "LASER Interrogation of Surface Agenta (LISA) for Standoff Sensing of Chemical Agents", 21st International Laser Radar Conference (ILRC), Quebec,, Canada, November, 2002.

Ede, Bill Moore , Scientist; Polivka, Alan, Assistant Vice-President; Brosseau, Joe, Senior Engineer, Communications & Train Control, TTCI; Tse, Yan, Program Manager Federal Railroad Administration; and Reinschmidt, Al, Vice-President – Commercial Programs, TTCI, "Improving Enforcement Algorithms for Communications-Based Train Control using Adaptive Methods", 9th International Heavy Haul Conference, Shanghai, China, June 22 - 24, 2009.

Engineering Note – "Spectrometer Signal-to-Noise and Dynamic Range Comparison", Ocean Optics, Inc., Number 211-00000-000-04-1206, December 4, 2006.

Fazio, Al, "Application of Cab Signals/ATC to LRT", Unpublished.

Fazio, Al, *"Hudson Bergen Light Rail – A Review of Speed and Capacity Improvements at Hoboken Terminal"*, unpublished.

Flaherty, Ryan M., "A Comparison of Spectrometers: StellarNet, Inc vs. the Competition", Extreme Spectroscopy Solutions, Tampa, FL, http://www.stellarnet-inc.com/public/download/StellarNetFeatures.pdf.

General Code of Operating Rules (GCOR) rules for the operation of trains on virtually every railroad west of the Mississippi River, Sixth Edition, April 7, 2010.

Gintautas Bureika and Sarunas Mikaliunas, "Research on the Compatibility of the Calculation Methods of Rolling Stock Brakes", Transport 2008, 23(4), accepted October 2008, pp 351- 355.

Halinaty, Mark; Whitman, Firth and Chiu, P.L., Challenges of Implementing CBTC on an Existing Railway, *IRSE Technical Convention*, Singapore, 2005.

Hall, Jim, Safety Recommendation from the National Transportation Safety Board concerning the NYCT accident on the Williamsburg Bridge – Reference R-96-22 through -25 (and NTSB/RAR-96/03), NTSB, Washington, D.C., 1996.

Han, Lili; Sheng, Jie; Ding, Feng; and Shi, Yang, "Recursive Least Squares Identification for Multirate Multi-Input Single-Output Systems, 2009 American Control Conference, St. Louis, MO, USA, June 10-12, 2009.

Hamilton, Michelle, "Application of grazing-angle reflection absorption Fourier transform infrared spectroscopy to the analysis of surface contamination", PhD dissertation, Chemistry Dept., University of Canterbury, Christchurch, New Zealand, 2007.

Hamilton, W. Ian and Clarke, Teresa, "Driver Performance Modeling and its Practical Application to Railway Safety", Elsevier: Applied Ergonomics, July 7, 2005.

Hapke, B., "Bidirectional Reflectance Spectroscopy, 1: Theory", Journal of Geophysical Resources, Volume 86, pp 3039-3054, 1981

Hapke, B. and Wells, E., "Bidirectional Reflectance Spectroscopy, 2: Experiments and observations", Journal of Geophysical Resources, Volume 86, pp 3055-3060, 1981.

Harig, Roland; Braun, Rene; Dyer, Chris; Howle, Chris; and Truscott, Benjamin, "Short Range Remote Detection of Liquid Surface Contamination by Active Imaging Fourier Transform Spectrometry", *Optics Express*, vol. 16, no. 8, April 14, 2008.

Hay, William W., Railroad Engineering, 2nd ed. New York: John Wiley and Sons, 1982, ch. 6, 9, 10, 11, 12, pp. 69-88, 140-147, 156-198.

IEEE Recommended Practice for the Determination of Safe Braking Distance in Fixed Guideway Land Transportation Systems, P679.1/D1 (unpublished).

IEEE Guide for the Calculation of Braking Distances for Rail Transit Vehicles, IEEE STD. 1698-2009, November, 2009.

IEEE Standard for Communications-Based Train Control Performance and Functional Requirements, IEEE STD. 1474.1-2004

Kalker, J. J., "On Rolling Contact of Two Elastic Bodies in the Presence of Dry Friction". PhD Dissertation, Laboratory of Engineering Mechanics, Department of Mechanical Engineering, Delft University of Technology, The Netherlands, August, 1973.

Kaplanoğlu, Erkan; Şafak, Koray K.; Varol, H. Selçuk, "Real-Time Parameter Estimation of a MIMO System", Proceedings of the International MultiConference of Engineers and Computer Scientists 2008 Vol. II, IMECS 2008, Hong Kong, 19-21 March, 2008.

Kearsey, Anthony; Barnard, Richard; Gadhyan, Yutheeka; Lin, Youzuo; Tong, Lin; Wang, Jiaping; Zhong, Guangjin, "Modeling the Background Noise in a Mass Spectrometer for Denoising Applications", http://ima.umn.edu/2007-2008/MM8.6-15.08/activities/Kearsley-Anthony/master.pdf

King, Everett Edgar, Railway Signaling, New York, NY, McGraw-Hill, 1921.

Kosinski, Robert J., A Literature Review on Reaction Time, Clemson University, Clemson, S.C., September, 2010 (http://biae.clemson.edu/bpc/bp/Lab/110/reaction.htm).

Kumar, Dr. Sudhir, Principal Investigator, "Improved Methods for Increasing Wheel/Rail Adhesion in the Presence of Natural Contaminants", Transportation Research Board of the National Academies of Science Research Results Digest, No. 17, May, 1997.

Lee, Hyun Wppk; Sandu, Corina; and Holton, Carvel, Railway Technology Laboratory – Center for Vehicle System Safety, Virginia Polytechnic Institute and State University at Blacksburg, VA., "Wheel-Rail Dynamic Model and Stocastic Analysis of the Friction in the Contact Patch", 2010 Joint Rail Conference (IEEE, ASME, ASCE), Urbana, Illinois, April 29, 2010.

Lautala, Pasi T., "From Classroom to Rail Industry - A Rail Engineer in the Making", Proceedings of the American Railway Engineering and Maintenance of Way (AREMA) 2007 Annual Conference, Chicago, IL, September, 2007.

Lipfert, F. W., Engineering proposal titled: "Proposal for a Study of Reduced Wheel/Rail Adhesion on the MTA/Metro-North Railroad, December, 2003.

Malvezzi, M.; Allotta, B.; and Rindi, A., "Simulation of Degraded Adhesion Conditions on a Full Scale Locomotive Roller Rig", *12th IFToMM World Congress*, Besancon, France, June 18-21, 2007.

Malvezzi, Monica; Bonnet, Alain; Cork, Cliff; Karbstein, Robert; Presciani, Paolo, November, 2006, *A Numerical Model for the Probabilistic Analysis of Braking Performance in Railways,* [online]. Avaialble: http://www.grrt.fr/html/travaux/download.php?filename=214malvezzi.pdf. (Groupement Regional Nord - Pas de Calais pout la Recherche dans les Transports.

Manolakis, Dimitris; Ingle, Vinay; and Kogen, Stephen, Statistical and Adaptive Signal Processing, Boston: McGraw Hill, 2000, ch. 8and 10, pp. 395-438, 548-560.

McEvoy, Steven, *A Classic Railway Signal Tower*, West Chester: Instantpublisher, 2007, ch. 2 thru 5, pp. 29-60.

McDonald, Mick, "More Return on Investment – Capitalizing on under-utilized capabilities of Modern Equipment", *American Public Transit Association - Rail Conference*, San Francisco, CA, June 2, 2008

Mitra, Sanjit, Digital Signal Processing – a Computer Based Approach, 3rd ed., Boston: McGraw Hill, 2006, pp. 514-515.

Meyer, Emily and Ervin, Benjamin; "Standoff Detection of Persistent Chemical Agents on Surfaces, Chemical and Biological Defense Science and Technology Conference, November 18, 2010.

Nocedal, Jorge; Wright, Stephen, Numerical Optimization. New York, Springer, 1999.

North, J.; Fazio, A. and N. Shashidhara, "Probabilistic Approach to a Safe Braking Model for Light Rail", *3rd International Conference on Computer Modeling for Rail Operations*, Philadelphia, Pennsylvania, 2008.

Northeast Operating Rules Advisory Committee (NORAC) rules for the operation of trains on several railroads in the Northeast portion of the Unites States, Ninth Edition, April6, 2008.

Office of Technology Assessment and the Urban Mass Transit Advisory Panel, Automatic Train Control in Rail Rapid Transit, Washington, D.C., NTIS order #PB-254738, May, 1976.

Padthe, Ashwani; Drincic, Bojana; Oh, Jinhyoung; Rizos, Demosthenis; Fassois, Spilios; and Bernstein, Dennis, *"Duhem Modeling of Friction-Induced Hysteresis"*, IEEE Control Systems Magazine, October 2008.

Park,Sung Hwan; Kim, Jong Shik; Choi, Jeong Ju; and Yamazaki, Hiro-O, *"Modeling and Control of Adhesion Force in Railway Rolling Stocks"*, IEEE Control Systems Magazine, October 2008.

Petryk, Michael W. P., "Promising Spectroscopic Techniques for the Portable Detection of Condensed-Phase Contaminants on Surfaces", Applied Spectroscopy Reviews, Vol. 42, pages 287-343, February, 2007.

Reiff, Richard P.; Ruud, Nicholas, and Kalay, Semih F., Transportation Test Center, Inc., TCRB Report 71, Track Related Research – "Friction Control Methods Used by the Transit Industry", Washington, D.C., 2005.

Rodriquez, Ken; Ho, Vincent and Burt, Harry, "Safe Braking of Light Rail Vehicles", *American Public Transit Association Rapid Transit Conference*, Proceedings Volume 2 – Rolling Stock, Washington, D.C., 1997.

Saunders, Richard Jr., *Main Lines – Rebirth of the North American Railroads, 1970-2002*, DeKalb, Illinois: Northern Illinois University Press, 2003, ch 5 and 6, pp153-219.

Sedlacek, Aurthur J. III and Ray, Mark D., "Short-range, Non-contact Detection of Surface Contamination Using Raman Lidar", SPIE vol. 4577, Boston, Massachusetts, November, 2001.

Sedlacek III, Aurthur J.; Ray, Mark D.; Higdon, N. S.; and Richer, D. A.;, "Short-Range, Non Contact Detection of Surface Contamination Using Raman Lidar", Proceedings of SPIE, 4577, 95-104, 2001.

SEPTA Leaf Grief, Southeastern Pennsylvania Transportation Authority press release, October 19, 2006.

Short, Roger, "The Use and Misuse of SIL", *IRSE News*, Issue 142, pp 2-7, February, 2009.

Stadler Rail AG vehicle information for GTW 2/6 Low Floor articulated Diesel Multiple Unit information cut sheet available at: http://www.stadlerrail.com/media/uploads/factsheets/GTW_SNJ_en.pdf

Susanta Patra, "Worst-Case Software Safety Level for Braking Distance Algorithm of a Train", Silver Software, UK, IEEE Xplore web library.

Thurston, David, "*Analyzing a Modern Train Control System for SEPTA's Green Line"*, APTA Rapid Transit Conference, Atlanta, Georgia, 1996.

Thurston, David, *"Capacity as a Driver for Selecting CBTC/PTC Train Control"*, Presented at the Sixth International Conference on Communications Based Train Control, Washington, D.C., 2005.

Thurston, David, *"Signaling and Capacity Through Computer Modeling"*, International Conference on Computer Modeling for Rail Operations, Delray Beach, Florida, February 26, 2004.

Thurston, David, Parsons Corporation and Temple University, "Beyond Adaptive Braking", 2010 Joint Rail Conference (IEEE, ASME, ASCE), Urbana, Illinois, April 29, 2010.

Transport: Railways, "Tractive Effort, acceleration and braking", The Mathematical Association, 2004

Vandenabeele, P. and Moens, L., Department of Analytical Chemistry, Ghent University, Proefluinstraat 86, 9000 Ghent, Belgium, "Introducing Students to Raman Spectroscopy", Published on line via Springer-Verlag, March 2, 2006.

Vasic, G.; Franklin, F. J.; Kapoor, A., "New Rail Materials and Coatings", The Railway Safety Standards Board (University of Sheffield, UK), Report Number RRUK/A2/1, July, 2003.

Vincze, B.; Tarnai, G., 2006, *"Development and Analysis of Train Brake Curve Calculation Methods with Complex Simulation"*, [Online], available: http://web.axelero.hu/egzo/doc/2006_elektro_brake_curve.pdf.

Werle, Peter and Slemr, Franz, "Signal-to-Noise Ratio Analysis in Laser Absorption Spectrometers Uing Optical Multipass Cells", Applied Optices, Vol 30 No. 4, February 1, 1991.

Widron, Bernard; Walach, Eugene; Senior Editors, Adaptive Inverse Control: A Signal Processing Approach, Reissue Edition, The Institute of Electrical and Electronic Engineers, 2008.

Widrow, Bernard and Walach, Eugene, Adaptive Inverse Control, Reissue Edition, Piscataway, NJ,: IEEE Press, 2008, ch. 10, pp. 270-302.

Wigger, Peter and Hövel, Rüdiger vom, Safety Assessment – Application of CENELEC Standards – Experience and Outlook, *Copenhagen Metro Inauguration Seminar*, Copenhagen, Denmark, November 21-22, 2002.

Wills, Adrian; Ninnes, Brett; Gibson, Stuart, "An Identification Toolbox for Profiling Novel Techniques", Published by the University of New Castle, Australia and supported

by the Australian Research Council.
http://www.ee.newcastle.edu.au/reports/EE06029.pdf.

Yu J., Mei T.X., and Wilson D.A., 2006, *Re-adhesion control based on wheel Set dynamics in railway traction system*, UKACC Control 2006

Zhang, ChunMin; Zhao, BaoChang; Yuan, ZhiLin; and Huang, Weioian, "Analysis of Signal-to-Noise Ratio of an Ultra-Compact Static Polarization Interference Imaging Spectrometer", Journal of Optics A:Pure and Applied Optics, May 8, 2009.

Zhuan, Xiangtao, "Optimal Handling and Fault-Tolerant Speed Regulation of Heavy Haul Trains", PhD. Dissertation, Department of Built Environment and Information Technology, University of Pretoria, Pretoria, South Africa, October, 2006.

APPENDIX A: DERIVATION OF GRADE COMPENSATION

Calculating stopping distance involves not only the characteristics of the train, but the physical alignment as well. While the effect of curvature is often ignored (the train resistance in a curve always caused trains to stop in shorter distances and is not significant), the effect of grade on SBD can be significant. It is typically viewed from the perspective of "equated distance". Equated distance takes the actual physical distance and converts it to a distance equivalent to that on tangent, level track. Hence the term "equated". Once converted, the design of signal spacing (or Block Layout) is easily performed with simple charts showing braking distance on level track.   Stated simply, "equated distance" for the "actual distance" of track alignment with grades is the equivalent length on which a train can reduce speed or stop.

In the LRT example used in the analysis having a stopping rate of 0.88 mphps (parts H and I of the IEEE model) requires 3,000 feet to stop from 60 MPH. Therefore, this train also required 3000 feet of equated distance to stop on track that is not level and tangent.

The "(4+G)/4" equated distance factor is commonly used within the industry to "equate" distances to design signal spacing, however it is actually only applicable to trains having a constant 0.88 mphps brake rate. The following is a derivation of this formula, and how it is applied.

By using a force diagram that represents a train on a specific grade (as shown in the figure below), it can be seen that the acceleration due to the grade is a function of the grade itself.
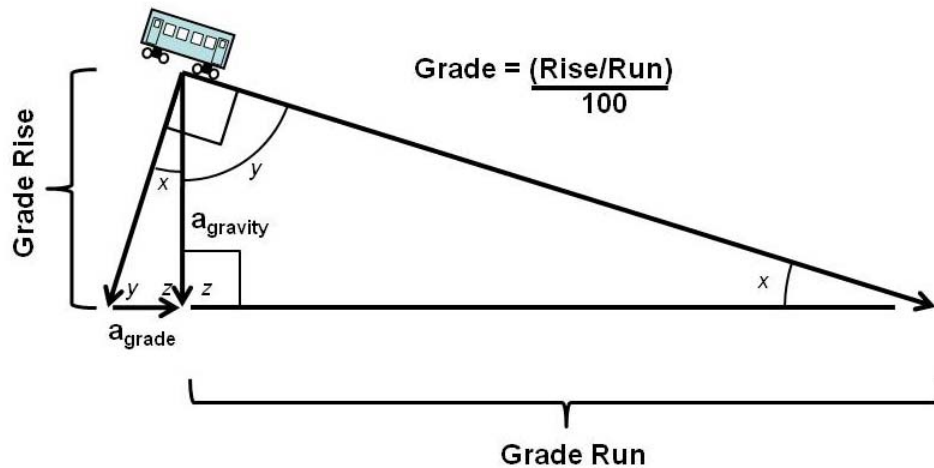

Figure 45, The Force Diagram for Grade Compensation

From the diagram it can be seen that x + y = 90 degrees, tan (z) = rise/run (or grade x 100), for small angles tan (x) ≈sin (x), and $a_{grade} = a_{gravity} * \sin x$. This can be represented in a table of potential values to represent the range of grades that would be normally encountered along a railroad.

Grade Run	Grade Rise	% Grade	x angle	Sin (x)	Feet/second^2 $a_{grade} = a_{gravity}*\sin (x)$	a_{grade} in mphps
100	1	1%	0.57297	0.01	0.322	0.22
100	2	2%	1.14599	0.02	0.644	0.44
100	3	3%	1.71913	0.03	0.966	0.66
100	4	4%	2.29244	0.04	1.288	0.88

Table 6, Various Accelerations due to Grade

Referring to the above diagram and table, the acceleration due to gravity down a 1% grade (a_{grade} (1%)) is:

$$a_{grade}(1\%) = a_{gravity} * \sin(x) = a_{gravity} * 0.01 * \left(\frac{3600}{5280}\right) = 0.22 mphps \qquad \textbf{(1)}$$

Stopping distance is assumed to be constant over the entire length of the braking action on level track, and is represented by:

$$Stopping\_Dist_{Level} = \frac{V_i^2}{2a} \qquad \textbf{(2)}$$

Where:

V_i = initial speed, and

a = the deceleration rate.

When the train is on a grade, the total acceleration (or deceleration) is actually a function of the sum of the braking effort and the acceleration due to the grade as shown below.

$$Stoping\_Dist_{Grade} = \frac{V_i^2}{2(a_{braking} + a_{grade})}$$

(3)

Where:

V_i = initial speed,

a_{brake} = deceleration rate of the train on level tangent track

a_{grade} = deceleration rate caused by the grade

(a_{grade} is positive upgrade and negative downgrade).

If we multiplying the numerator and denominator by the stopping distance on level track we get:

$$Stopping\_Dist_{grade} = \frac{V_i^2 * Stopping\_Dist_{Level}}{2(a_{brake} + a_{grade}) * Stopping\_Dist_{Level}} \qquad \textbf{(4)}$$

Combining equations (2) and (4):

$$Stopping\_Dist_{grade} = \frac{V_i^2 * \boldsymbol{Stopping\_Dist_{Level}}}{2(a_{brake} + a_{grade}) * (V_i^2/2a_{brake})} \qquad \textbf{(5)}$$

Reducing this equation further yield:

$$Stopping\_Dist_{grade} = \frac{\boldsymbol{Stopping\_Dist_{level}} * 2 * a_{brake}}{2(a_{brake} + a_{grade})}, \text{ and}$$

$$Stopping\_Dist_{grade} = \frac{\boldsymbol{Stopping\_Dist_{level}}}{1 + (a_{grade}/a_{brake})} = \frac{Stopping\_Dist_{level}}{1 + \left(\dfrac{0.22G}{a_{brake}}\right)} \qquad \textbf{(6)}$$

Where G = grade in percent

The deceleration rate (a_{brake}) used in the examples for level tangent track was 0.88 mphps. This is a value in common use within the railroad industry for commuter rail and some Light Rail Transit operations, and it is the basis for the equated distance equation (see equation (1)) in general use on railways in North America. Note that for this 0.88 value that:

$$Stoping\_Dist_{grade} = \frac{Stopping\_Dist_{level}}{1 + \left(\dfrac{0.22G}{0.88}\right)} = \frac{\boldsymbol{Stopping\_Dist_{level}}}{1 + (G/4)} = \frac{4 * Stopping\_Dist_{level}}{4 + G}, \text{ or}$$

$$Stopping\_Dist_{grade} = \left(\frac{4}{4 + G}\right) * Stopping\_Dist_{levle}$$

A positive G (upgrade) reduces $Stopping\_Dist_{grade}$, and negative G (downgrade) increases $Stopping\_Dist_{grade}$. In addition, the reciprocal equation yields the conversion for equated distance.

$$Stopping\_Dist_{level} = \frac{4 + \boldsymbol{G}}{4} * Stopping\_Dist_{grade}$$

Therefore, the final equation for equated distance is:

$$Equated\_Dist = \frac{4+\boldsymbol{G}}{4} * Actual\_Dist \qquad\qquad \textbf{(7)}$$

# APPENDIX B: TPC SOFTWARE DESCRIPTION

The Train Performance Calculator used to evaluate the overall effect of SBD on capacity is called *TrackMaster*[©] Simulation. The software was developed by Parsons Corporation several years ago, and has been used on several operational analysis projects throughout the United States. It consists of a Microsoft Excel file with several macro programs linked to it. Portions of documentation from the program are reproduced here as information.

<div align="center">

TrackMaster[©] Simulation
Train Acceleration and Braking Models
</div>

Acceleration

Vehicle Acceleration

Transit and Light Rail (LRV) equipment performance is usually presented as an acceleration potential "curve" over the range of operating speeds of the vehicle. This acceleration capability is usually stated as "Miles per hour per second" (mphps) acceleration at a given speed.
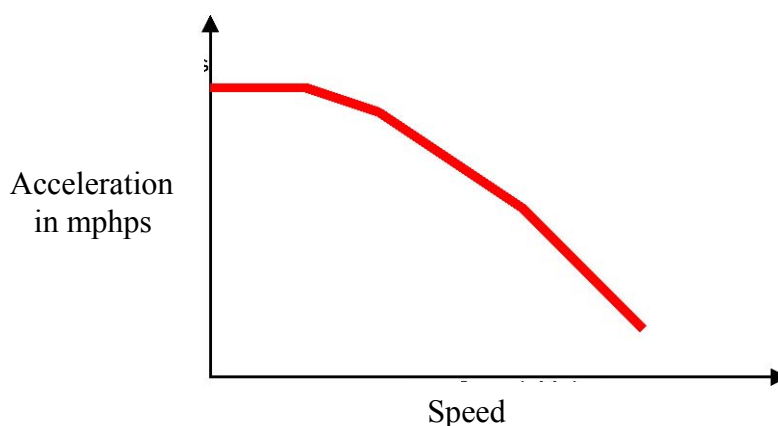
This shape of the acceleration curve reflects the interaction of the vehicle's fixed power output (tractive effort) and the increasing resistance with speed due to wheel flange and air resistance. For homogenous train consists of self-powered equipment like LRVs or MU commuter equipment, the acceleration curve is an elegant way to represent the power performance of the train set.

Grade and Curve Effects

Rail equipment is highly sensitive to the effect of gravity on performance, as represented by the grade "percent" (1 foot rise per 100 feet = 1% grade) under the vehicle. As the grade increases or decreases, the accelerative force of gravity either accelerates the train (down hill) or decelerates it (up hill) proportional to the grade percent—1% gradient transfers 1% of each ton's weight (2000*.01= 20 lbs) into accelerative force. This same proportional relationship can be applied to the acceleration rate of gravity—the classic gravity acceleration constant of 32.1933 *feet per second per second* can be converted to the equivalent mphps acceleration:

$$(32.1933/5280)(60*60) = 21.95 \text{ MPHPS}$$

Each 1% of grade provides 21.95*.01= .2195 mphps of acceleration or deceleration. This positive acceleration (downhill) or deceleration (uphill) is additive to the powered acceleration of the vehicle. Equipment capable of accelerating at 1.0 mphps at 20 mph will be able to accelerate at 1.2195 mphps down a 1% grade, or at .7805 mphps up the same gradient.

Curves add a modest amount of flange resistance that increases linearly with the tightness of the curve, generally states in rail industry units of "degrees of curvature" (per 100 foot of arc). The empirically accepted relationship is that 1° of curvature is the equivalent of 0.04% grade, so typically curves are converted into the grade equivalent percentage (always positive) and use to produce an "adjusted grade" percentage for further calculation.

TrackMaster Acceleration Method

TrackMaster computes vehicle performance for acceleration and braking by looking at the train's status in fixed 1-second time increments. This works nicely with the mphps acceleration tables, which are built in 1 mph increments. The following table shows the acceleration of a vehicle over a 10-second period from 10 mph to 20.32 mph.

Time	Seconds	Speed Mph	Acceleration MphPs	Speed Mph	Avg Mph	Distance feet
1	+1	10.00	1.22	11.22	10.61	15.56
2	+1	11.22	1.22	12.44	11.83	17.35
3	+1	12.44	1.18	13.62	13.03	19.11
4	+1	13.62	1.16	14.78	14.20	20.83
5	+1	14.78	1.15	15.93	15.36	22.52
6	+1	15.93	1.14	17.07	16.50	24.20
7	+1	17.07	1.12	18.19	17.63	25.86
8	+1	18.19	1.09	19.28	18.74	27.48
9	+1	19.28	1.04	20.32	19.80	29.04
10	+1	20.32	1.04	21.36	20.84	30.57
						232.51

Vehicle acceleration is computed in fixed 1-second intervals until the required distance was reached. In the Example above, if the distance to be computed was 225 feet (instead of 232.51), then the performance of the final "second" would be prorated to produce the speed at the remaining distance into the final second:

						201.95 feet
9.7587	0.7587	20.32	1.04	21.11	20.71	23.05 feet
						225.00

The train would cover 225 feet in 9.7587 seconds and reach a final velocity of 21.11 mph. This is the standard train acceleration "model" for *TrackMaster*, with the available acceleration at any speed reflecting the vehicle acceleration table values, plus the net effects of grade (and curve) acceleration. For single vehicles or small transit—type consists, the train can be considered a "point mass", meaning that the train is computed as if its entire mass was at the head end, and that the (adjusted) grade at that point is the only grade considered.

To reflect operator practices, a maximum net acceleration can be imposed, typically less than 2 mphps, for passenger comfort. The net acceleration of the vehicle is so limited, although the extra power can be used when starting on uphill heavy adverse gradients (another common LRV line characteristic). Downhill "comfort" acceleration may be provided in part by gravity, while the operator applied only a minimum of power to accelerate the train.

TPC Acceleration

When *TrackMaster* applications move into the world of longer and heavier freight and passenger trains, locomotive powered, with varying consists, the simple and elegant "acceleration model" is no longer applicable. Since we no longer have homogenous, self-powered consists, the "acceleration model" must be de-composed into its elements of tractive effort and rolling resistance, and re-computed to produce the acceleration characteristics of each unique train consist of powered locomotives and trailing cars.

The first component, tractive effort, is by industry standard, represented in a table of pounds of tractive effort produced by a locomotive. At low speeds, the tractive effort will reflect the locomotive's *weight* (in pounds) *on drivers* (powered axles) times the *coefficient of friction*, basically "leaning" the locomotive's weight into pulling the train behind it. While the locomotive weight is an easily known value, the coefficient of friction is a much more speculative number:

  • **0.25** (25% of weight) is the common planning standard for railroad locomotives;
  • **0.18** is the value often used by railroads when assigning power to trains;
  • **0.40**+ values can be reached by new high-adhesion or AC-motor units.

This suggests that a 200 ton locomotive can have a starting tractive effort ranging between 72,000 and 160,000 pounds, depending upon rail conditions, wheel anti-slip controls, and other factors. Beyond 5-10 mph, the standard tractive effort "curve" provided by the locomotive manufacturer is used. Tractive Effort used in the TPC reflect the standard coefficient of friction for the types of units—0.25 for most diesel units, 0.42 for AC freight motors, etc. These coefficients can be overridden with run-specific values, when desired. The tractive effort of the unit declines exponentially as speed increases, while the resistance of the train to acceleration increases with speed. The sum of the two forces (in pounds) is the net force available to accelerate the train.

The resistance of a train consist to acceleration is another complex value that has been empirically modeled to develop equations describing the rolling resistance of rail equipment. A number of such equations have been fitted, but *TrackMaster* uses two of the industry standards.

The Davis equation and its variants for streamlined trains are generally accepted for high-speed, light weight (passenger) trains, but the AAR equation provides much more accurate resistance for the heavy freight cars and trains.

$$R = W(1.5 + 72.5/W + 0.15V + .055V^2/W)$$
R= Resistance in lbs
W= Weight in tons
V= velocity in mph

AAR Electrical Section Equation

$$R = W(1.3 + 29/W + BV + CAV^2/W)$$
R= Resistance in lbs
W= Weight in tons
V= velocity in mph
A= cross-sectional area in feet
B= flange coefficient,
    0.0300 for lead unit
    0.0045 for trailing cars
C= air resistance coefficient
    0.0024 for lead unit
    0.0034 for trailing cars

Davis Equation

The net force available for acceleration adds the combined tractive effort (in pounds) of the locomotives to the combined resistance (in pounds) of the entire consist (locomotives and cars). Note the subtle difference between locomotive "tractive effort" and the older measure called "drawbar pull", which was the net force produced by the locomotives (typically a steam engine) after accounting for the resistance of the locomotive itself—the pounds of force available at the drawbar (behind the locomotive, but not the tender).

TrackMaster combines the tractive effort of each train's locomotives and the resistance of it's consist into a net accelerative force, and then converts it to the equivalent of the acceleration curve. To match the acceleration curve table values, *TrackMaster* needs to compute the mphps increase in speed possible as speed (V_1) increases in 1-second time intervals. The following set of equations is used to derive the acceleration equivalent from the net tractive force in pounds:

T= time, set equal to 1-second
W= weight in tons
V_1 = starting speed mph
V_2 = ending speed mph
F_a = net acceleration force, TE less Resistance in lbs,
    available at V_1

$$T= 95.6W\ (V_2\text{-}V_1)/F_a \qquad\qquad 1= 95.6W\ (V_2\text{-}V_1)/F_a$$
$$F_a = 95.6W\ (V_2\text{-}V_1)$$
$$F_a/95.6W = (V_2\text{-}V_1) = \text{speed increase (from } V_1) \text{ in 1 second}$$

Acceleration Curve Computation

As train speed increases, locomotive tractive effort declines, train resistance increases, and the acceleration of the train tapers off to the point where the locomotive and train reach an equilibrium point where resistance and tractive effort balance and no further acceleration is possible. If the MAS is lower than the equilibrium speed, then the engineer must reduce power (and tractive effort) to maintain the equilibrium speed at the speed limit. By computing a train-specific acceleration table in this manner, *TrackMaster* can then utilize the same computational method for variable train consists as it uses for the simple homogenous self-powered trains. The effects of grade and curvature must still be considered in producing the train's performance. Where small commuter trains and LRVs can be modeled acceptably as a "point mass" at the head end location, longer trains, and especially freight trains that can reach 5-9,000 feet in length, must take a more considered look at the gradient under the train. At each head-end location on the train's route, *TrackMaster* looks back along the consist and computes the "average" grade under the train. If half the train is on a +0.50% grade and half on a -0.50% grade, the net grade force on the train will be the same as for a 0% grade; if ¾ of the train is on the 0.5% grade, then the grade effect will be the same as if the entire train were on a 0.25% grade (=.75*0.50 + .25*-0.50). As the train moves forward, the equivalent grade profile under the train is recalculated, and but no consideration of the distribution of weight within the train consist is made—the train's weight is assumed to be distributed uniformly from nose to tail.

Braking

Vehicle Braking

The physics of braking are a mirror image of acceleration, only applying a negative force to reduce speed instead of a positive force to increase speed. Transit and LRV cars come equipped with a variety of braking systems designed to provide smooth, safe speed reductions. For *TrackMaster* simulation purposes we are interested in a "service braking" rate that would normally be provided in revenue service. This stands in contrast to other braking rates: "emergency braking", "civil design" braking that are used for emergency stopping or signal designs. Modern transit and LRV equipment are engineered to provide a constant service braking deceleration rate across their whole range of operating speeds. While *TrackMaster* provides the ability to "step" braking rates in 1 Mph increments (like acceleration), typically, the braking rate is the same for all speeds.

The computational method for braking is identical to that used for acceleration, but is computed "back" in time and distance from a speed reduction point. The available braking deceleration rate (mphps) adds the deceleration (or acceleration) from grades to the vehicle's braking rate. As with acceleration, a "comfort" braking rate can be imposed, so that trains apply less brake force uphill, use gravity to assist the stop, and maintain a net braking rate at the service braking rate.

Downhill, gravity works against the braking, and the stopping distance will be increased as the net braking rate is reduced.

While *TrackMaster* computes acceleration "forward" in to see how fast a train may be moving at a given point along its route, the simulation computes braking "backward" from a speed reduction or stopping point. The same 1-second interval method is used, but calculating backwards from the lowest speed (or stop) to the current train speed to determine how far away the train must begin its braking in order to "hit" the stopping point or be at the new speed limit when enter the next piece of track. Note that this method is different than classical computational method for "stopping/braking distance" that add time (and distance) for recognition and application of brakes before the actual braking can begin. That time (and distance) is assumed to have occurred in advance of the *TrackMaster* braking calculations, which then reflect the actual braking action.

In order to replicate the range of braking technologies available on modern freight, passenger, commuter, and LRV equipment, *TrackMaster* provides three methods of modeling train braking: air brakes, "comfort" braking, and "custom" braking.

Comfort Braking

Comfort braking is the simplest form, imposing a controlled maximum service braking rate (in mphps) that ensures passenger comfort; it is typically used for high-speed passenger, Amtrak corridor equipment, modern commuter equipment, and even for LRVs, although the LRV idea of "comfort braking" may mean deceleration rates of up to 3.0 mphps, or twice that acceptable to rail passenger operators, where braking systems deliver deceleration rates of 1.5-1.6 mphps for service braking.

Custom Braking

Custom braking is an extension of the comfort braking concept that provides an externally defined braking rate in either mphps or pounds of brake force available at a given speed. This information is typically part of the equipment manufacturer's specifications and requires homogeneous train sets to be properly applied. If a custom brake force curve is required, then it is used in place of the air *Brake Force* computation discussed below.

Air Brakes

While transit equipment and modern, high-speed passenger equipment all come equipment with multiple computerized braking systems that can easily be described by a simple deceleration curve, heavy freight trains and old passenger equipment continue to rely on the traditional air brake technology to slow and stop trains. Even when locomotive dynamic braking is used to reduce the stress on the air brake equipment, speed reduction in lower speed ranges and stops still require the use of air brakes. Current enhancements to freight train braking like EPB (electro-pneumatic braking) address the propagation speed and control of the air brake system rather than the fundamental braking physics of the air brake, which are now over a century old.

$$T = \text{time, set equal to 1-second}$$
$$W = \text{weight in tons}$$
$$V_1 = \text{starting speed mph}$$
$$V_2 = \text{ending speed mph}$$
$$F_b = \text{net deceleration force, Braking force plus Resistance in lbs, available at } V_1$$
$$F_b = \textit{Brake Force} + R_e + R_g + R_c$$

$$T = 95.6W\,(V_1 - V_2)/F_a$$
$$1 = 95.6W\,(V_1 - V_2)/F_a$$
$$F_b = 95.6W\,(V_1 - V_2)$$
$$F_b/95.6W = (V_1 - V_2) = \text{speed decrease (from } V_2\text{) in 1 second}$$

Deceleration Curve Computation

The physics of (braking) deceleration are identical with acceleration, with the exception that the resistance forces on the train from rolling (R_e) resistance and wind, (R_g) grade, (R_c) curves, etc., are added to the braking force applied to the train in order to reduce speed.

Air brakes are a complex mechanism that can exert braking power at different levels, based on the reduction in air pressure in the train's brake line. Reductions can be characterized as:

> • *Light* – for speed control
> • *Service* – typical stopping application
> • *Emergency* – one-time stop (at all costs)

For *TrackMaster* simulation purposes, the service application is used, reflecting the normal technique to reduce train speed or maintain train speed on a downgrade.

The computation of Brake Force for air brake equipment uses another empirically derived formula that is a railroad industry standard:

Brake Force= $\sum pRwef/x$

• **p = ratio, brake cylinder pressure to brake pipe pressure,** typical value = 0.45
• **R = braking ratio,** typical value = 0.55
• **w = weight of each car**
• **e = efficiency of brake rigging system**
• **f = coefficient of friction of brake shoe on wheel**
• **x = car factor (1= for locomotives, =2 for cars)**

Air Brake force Calculation (lbs)

The combined **ef** factors for typical freight equipment using cast iron brake shoes on steel wheels have been found to decline in efficiency with speed:

> **ef = .25 – (Vmph)/300)** for speeds below 39 mph;
> **ef = 0.12** for speeds 39 mph and greater

This formulation is used to compute the cumulative *Brake Force* available to decelerate the train. For variable consists and long trains using standard air brake equipment, it is still the industry standard for computing stopping distances. Modern heavy freight trains

rely extensively on dynamic braking applications by locomotives, often to reduce the wear and tear on brake equipment, but air brakes remain the industry standard for train handling, and TrackMaster uses this braking model for freight train braking.

APPENDIX C: TPC RUN – SBD VS. PERFORMANCE

A Train Performance Calculator used to determine the capacity loss attributed to the difference in operating trains at normal performance as opposed to a full SBD model. A TPC run was set up with parameters typically associated with a SBD model with run times and distance listed in the following output. Then the same train characteristics were used but with performance criteria input into the model. The outputs are included in this appendix. A capacity calculation was also run as shown in the table below using the formulas as shown below.

First, the train length is assumed to be 800 feet. This is added to the braking distance used in either SBD mode or performance mode. This is divided by the initial velocity at the start of the block which results in the time in minutes it takes the train to travel this distance ($D_t + D_b$).

$$T = (D_t + D_b)/(V_i * 1.4666)$$

Where T = Time to traverse the distance

D_t = Train length,

D_b = Braking Distance, and

V_i = Initial Velocity

T is converted to the number of Trains per Hour and plotted over speeds from 10 to 60 mph.

Capacity Gap - SBD vs Performance

SBD Computations (Table 1)

[A]	0.0	Overspeed Mph
[C]	2.0	Reaction Time, seconds
[D]	0.0	PER1	Runaway Acceleration Time, seconds
[E]	1.0	Propulsion Removal Time, seconds
[F]	1.0	Dead Time, seconds
[G]	1.0	Brake Build-up time, seconds
[H]	0.8800	Brake Rate	MPH
[J]	15.00	Location uncertainty, ft
[X]	0.00	Grade%

MpH/FpS factor 1.467 Gravity 32.174 FpS²

Calculate Table

Speed			Reaction Time [C]		Runaway Acceleration [D]		Propulsion Removal [E]		Dead Time [F]		Brake Build-up Time [G]		Braking [H]		Location Uncertainty [J]		Keep
Time Seconds	Distance Feet	Speed Mph	Distance	Time	Distance	Time	Distance	Time	Distance	Time	Distance	Time	Distance	Time	Distance	Time	√
15.90	164	10	29.3333	2.0000	0.0000	0.0000	14.6667	1.0000	14.6667	1.0000	14.4182	1.0000	75.4626	10.9000	15.0000	0.0000	
21.50	300	15	44.0000	2.0000	0.0000	0.0000	22.0000	1.0000	22.0000	1.0000	21.7515	1.0000	175.5955	16.5000	15.0000	0.0000	
27.20	479	20	58.6667	2.0000	0.0000	0.0000	29.3333	1.0000	29.3333	1.0000	29.0849	1.0000	317.3963	22.2000	15.0000	0.0000	
32.90	699	25	73.3333	2.0000	0.0000	0.0000	36.6667	1.0000	36.6667	1.0000	36.4182	1.0000	500.8834	27.9000	15.0000	0.0000	
38.60	961	30	88.0000	2.0000	0.0000	0.0000	44.0000	1.0000	44.0000	1.0000	43.7515	1.0000	725.9968	33.6000	15.0000	0.0000	
44.30	1,264	35	102.6667	2.0000	0.0000	0.0000	51.3333	1.0000	51.3333	1.0000	51.0849	1.0000	992.7963	39.3000	15.0000	0.0000	
50.00	1,609	40	117.3333	2.0000	0.0000	0.0000	58.6667	1.0000	58.6667	1.0000	58.4182	1.0000	1301.2622	45.0000	15.0000	0.0000	
55.60	1,996	45	132.0000	2.0000	0.0000	0.0000	66.0000	1.0000	66.0000	1.0000	65.7515	1.0000	1651.3960	50.6000	15.0000	0.0000	
61.30	2,425	50	146.6667	2.0000	0.0000	0.0000	73.3333	1.0000	73.3333	1.0000	73.0849	1.0000	2043.1966	56.3000	15.0000	0.0000	
67.00	2,895	55	161.3333	2.0000	0.0000	0.0000	80.6667	1.0000	80.6667	1.0000	80.4182	1.0000	2476.6635	62.0000	15.0000	0.0000	
72.70	3,407	60	176.0000	2.0000	0.0000	0.0000	88.0000	1.0000	88.0000	1.0000	87.7515	1.0000	2951.7966	67.7000	15.0000	0.0000	
78.40	3,960	65	190.6667	2.0000	0.0000	0.0000	95.3333	1.0000	95.3333	1.0000	95.0849	1.0000	3468.5960	73.4000	15.0000	0.0000	
84.00	4,555	70	205.3333	2.0000	0.0000	0.0000	102.6667	1.0000	102.6667	1.0000	102.4182	1.0000	4027.0622	79.0000	15.0000	0.0000	
89.70	5,192	75	220.0000	2.0000	0.0000	0.0000	110.0000	1.0000	110.0000	1.0000	109.7515	1.0000	4627.1963	84.7000	15.0000	0.0000	
95.40	5,870	80	234.6667	2.0000	0.0000	0.0000	117.3333	1.0000	117.3333	1.0000	117.0849	1.0000	5268.9968	90.4000	15.0000	0.0000	
101.10	6,591	85	249.3333	2.0000	0.0000	0.0000	124.6667	1.0000	124.6667	1.0000	124.4182	1.0000	5952.4634	96.1000	15.0000	0.0000	
106.80	7,352	90	264.0000	2.0000	0.0000	0.0000	132.0000	1.0000	132.0000	1.0000	131.7515	1.0000	6677.5963	101.8000	15.0000	0.0000	
112.50	8,156	95	278.6667	2.0000	0.0000	0.0000	139.3333	1.0000	139.3333	1.0000	139.0849	1.0000	7444.3955	107.5000	15.0000	0.0000	
118.10	9,001	100	293.3333	2.0000	0.0000	0.0000	146.6667	1.0000	146.6667	1.0000	146.4182	1.0000	8252.8626	113.1000	15.0000	0.0000	
123.80	9,888	105	308.0000	2.0000	0.0000	0.0000	154.0000	1.0000	154.0000	1.0000	153.7515	1.0000	9102.9966	118.8000	15.0000	0.0000	
129.50	10,816	110	322.6667	2.0000	0.0000	0.0000	161.3333	1.0000	161.3333	1.0000	161.0849	1.0000	9994.7968	124.5000	15.0000	0.0000	
135.20	11,786	115	337.3333	2.0000	0.0000	0.0000	168.6667	1.0000	168.6667	1.0000	168.4182	1.0000	10928.2633	130.2000	15.0000	0.0000	
140.90	12,798	120	352.0000	2.0000	0.0000	0.0000	176.0000	1.0000	176.0000	1.0000	175.7515	1.0000	11903.3960	135.9000	15.0000	0.0000	

SBD Computations (Table 2)

[A]	0.0	Overspeed Mph
[C]	2.0	Reaction Time, seconds
[D]	0.0	PER1	Runaway Acceleration Time, seconds
[E]	1.0	Propulsion Removal Time, seconds
[F]	1.0	Dead Time, seconds
[G]	1.0	Brake Build-up time, seconds
[H]	0.8800	Brake Rate	MPH
[J]	15.00	Location uncertainty, ft
[X]	0.00	Grade%

MpH/FpS factor 1.467 Gravity 32.174 FpS²

Calculate Table

Speed			Reaction Time [C]		Runaway Acceleration [D]		Propulsion Removal [E]		Dead Time [F]		Brake Build-up Time [G]		Braking [H]		Location Uncertainty [J]		Keep
Time Seconds	Distance Feet	Speed Mph	Distance	Time	Distance	Time	Distance	Time	Distance	Time	Distance	Time	Distance	Time	Distance	Time	√
15.90	164	10	29.3333	2.0000	0.0000	0.0000	14.6667	1.0000	14.6667	1.0000	14.4182	1.0000	75.4626	10.9000	15.0000	0.0000	
21.50	300	15	44.0000	2.0000	0.0000	0.0000	22.0000	1.0000	22.0000	1.0000	21.7515	1.0000	175.5955	16.5000	15.0000	0.0000	
27.20	479	20	58.6667	2.0000	0.0000	0.0000	29.3333	1.0000	29.3333	1.0000	29.0849	1.0000	317.3963	22.2000	15.0000	0.0000	
32.90	699	25	73.3333	2.0000	0.0000	0.0000	36.6667	1.0000	36.6667	1.0000	36.4182	1.0000	500.8834	27.9000	15.0000	0.0000	
38.60	961	30	88.0000	2.0000	0.0000	0.0000	44.0000	1.0000	44.0000	1.0000	43.7515	1.0000	725.9968	33.6000	15.0000	0.0000	
44.30	1,264	35	102.6667	2.0000	0.0000	0.0000	51.3333	1.0000	51.3333	1.0000	51.0849	1.0000	992.7963	39.3000	15.0000	0.0000	
50.00	1,609	40	117.3333	2.0000	0.0000	0.0000	58.6667	1.0000	58.6667	1.0000	58.4182	1.0000	1301.2622	45.0000	15.0000	0.0000	
55.60	1,996	45	132.0000	2.0000	0.0000	0.0000	66.0000	1.0000	66.0000	1.0000	65.7515	1.0000	1651.3960	50.6000	15.0000	0.0000	
61.30	2,425	50	146.6667	2.0000	0.0000	0.0000	73.3333	1.0000	73.3333	1.0000	73.0849	1.0000	2043.1966	56.3000	15.0000	0.0000	
67.00	2,895	55	161.3333	2.0000	0.0000	0.0000	80.6667	1.0000	80.6667	1.0000	80.4182	1.0000	2476.6635	62.0000	15.0000	0.0000	
72.70	3,407	60	176.0000	2.0000	0.0000	0.0000	88.0000	1.0000	88.0000	1.0000	87.7515	1.0000	2951.7966	67.7000	15.0000	0.0000	
78.40	3,960	65	190.6667	2.0000	0.0000	0.0000	95.3333	1.0000	95.3333	1.0000	95.0849	1.0000	3468.5960	73.4000	15.0000	0.0000	
84.00	4,555	70	205.3333	2.0000	0.0000	0.0000	102.6667	1.0000	102.6667	1.0000	102.4182	1.0000	4027.0622	79.0000	15.0000	0.0000	
89.70	5,192	75	220.0000	2.0000	0.0000	0.0000	110.0000	1.0000	110.0000	1.0000	109.7515	1.0000	4627.1963	84.7000	15.0000	0.0000	
95.40	5,870	80	234.6667	2.0000	0.0000	0.0000	117.3333	1.0000	117.3333	1.0000	117.0849	1.0000	5268.9968	90.4000	15.0000	0.0000	
101.10	6,591	85	249.3333	2.0000	0.0000	0.0000	124.6667	1.0000	124.6667	1.0000	124.4182	1.0000	5952.4634	96.1000	15.0000	0.0000	
106.80	7,352	90	264.0000	2.0000	0.0000	0.0000	132.0000	1.0000	132.0000	1.0000	131.7515	1.0000	6677.5963	101.8000	15.0000	0.0000	
112.50	8,156	95	278.6667	2.0000	0.0000	0.0000	139.3333	1.0000	139.3333	1.0000	139.0849	1.0000	7444.3955	107.5000	15.0000	0.0000	
118.10	9,001	100	293.3333	2.0000	0.0000	0.0000	146.6667	1.0000	146.6667	1.0000	146.4182	1.0000	8252.8626	113.1000	15.0000	0.0000	
123.80	9,888	105	308.0000	2.0000	0.0000	0.0000	154.0000	1.0000	154.0000	1.0000	153.7515	1.0000	9102.9966	118.8000	15.0000	0.0000	
129.50	10,816	110	322.6667	2.0000	0.0000	0.0000	161.3333	1.0000	161.3333	1.0000	161.0849	1.0000	9994.7968	124.5000	15.0000	0.0000	
135.20	11,786	115	337.3333	2.0000	0.0000	0.0000	168.6667	1.0000	168.6667	1.0000	168.4182	1.0000	10928.2633	130.2000	15.0000	0.0000	
140.90	12,798	120	352.0000	2.0000	0.0000	0.0000	176.0000	1.0000	176.0000	1.0000	175.7515	1.0000	11903.3960	135.9000	15.0000	0.0000	